

Iron electrocoagulation and H₂O₂ dosing to promote arsenic removal in groundwater (bio)filters

Roy, M.

DOI

[10.4233/uuid:ab8963a7-f628-45a4-a352-91fd096782e3](https://doi.org/10.4233/uuid:ab8963a7-f628-45a4-a352-91fd096782e3)

Publication date

2024

Document Version

Final published version

Citation (APA)

Roy, M. (2024). *Iron electrocoagulation and H₂O₂ dosing to promote arsenic removal in groundwater (bio)filters*. [Dissertation (TU Delft), Delft University of Technology]. <https://doi.org/10.4233/uuid:ab8963a7-f628-45a4-a352-91fd096782e3>

Important note

To cite this publication, please use the final published version (if applicable). Please check the document version above.

Copyright

Other than for strictly personal use, it is not permitted to download, forward or distribute the text or part of it, without the consent of the author(s) and/or copyright holder(s), unless the work is under an open content license such as Creative Commons.

Takedown policy

Please contact us and provide details if you believe this document breaches copyrights. We will remove access to the work immediately and investigate your claim.

**Iron electrocoagulation and H₂O₂
dosing to promote arsenic removal
in groundwater (bio)filters**

Mrinal Roy

Iron electrocoagulation and H₂O₂ dosing to promote arsenic removal in groundwater (bio)filters

Dissertation

for the purpose of obtaining the degree of doctor

at Delft University of Technology

by the authority of the Rector Magnificus, Prof. dr. ir. T.H.J.J. van der Hagen,

Chair of the Board for Doctorates

to be defended publicly on

Thursday 20 June 2024 at 10:00 o'clock

by

Mrinal ROY

Master of Science in Civil Engineering, Delft University

of Technology, The Netherlands

born in Silchar, India

The dissertation has been approved by the promotor.

Composition of the doctoral committee:

| | |
|------------------------------|--|
| Rector Magnificus | Chairperson |
| Prof. dr. ir. D. van Halem | Delft University of Technology, promotor |
| Prof. dr. ir. L. C. Rietveld | Delft University of Technology, promotor |

Independent members:

| | |
|------------------------------|--|
| Dr. A. Mink | TNO, The Netherlands |
| Prof. dr. K. M. U. Ahmed | Dhaka University, Bangladesh |
| Prof. dr. P. Osseweijer | AS, Delft University of Technology |
| Prof. dr. M. D. Kennedy | IHE Delft/Delft University of Technology |
| Prof. dr. ir. J. B. van Lier | Delft University of Technology (<i>reserve member</i>) |

Other member:

| | |
|-------------------------|---------------|
| Dr. C. M. van Genuchten | GEUS, Denmark |
|-------------------------|---------------|

This research study was supported by TKI Watertechnology, Top Sector Water and TU Delft Global Initiative.

Printed by: Proefschrift-AIO.nl

Layout: Proefschrift-AIO.nl | Annelies Lips

Cover Design: Proefschrift-AIO.nl | Guntra Laivacuma

Copyright © 2024 by M. Roy

All rights reserved. No part of the material protected by the copyright may be reproduced or utilised in any form or by any means, electronic or mechanical, including photocopying, recording, or by any information storage and retrieval system, without the written permission from the copyright owner.

An electronic version of this dissertation is made available at TU Delft Repository

To my foremothers, forefathers, and the people of Assam.

Table of contents

| | |
|---|-----------|
| Acknowledgements | 9 |
| Abbreviations | 11 |
| Summary | 12 |
| Samenvatting | 15 |
| Chapter 1 Introduction | 19 |
| 1.1 Arsenic in groundwater | 20 |
| 1.2 Treatment technologies for arsenic removal from groundwater | 22 |
| 1.3 Biological As(III) oxidation in sand filters | 24 |
| 1.4 Iron Electrocoagulation | 25 |
| 1.5 Fe(II) oxidation with hydrogen peroxide | 26 |
| 1.6 Knowledge gaps: Coupling iron electrocoagulation and hydrogen peroxide dosing to groundwater biofilters | 27 |
| 1.7 Research objective and questions | 29 |
| 1.8 Structure of the thesis | 29 |
| References | 31 |
| Chapter 2 Integrating biological As(III) oxidation with Fe(0) electrocoagulation for As removal from groundwater | 39 |
| Abstract | 40 |
| 2.1 Introduction | 41 |
| 2.2 Materials and methods | 42 |
| 2.2.1 Chemicals | 42 |
| 2.2.2 Experimental setup | 42 |
| 2.2.3 Chemical analysis | 46 |
| 2.2.4 X-ray absorption spectroscopy | 46 |
| 2.2.5 Microbial characterisation | 47 |
| 2.3 Results and discussion | 48 |
| 2.3.1 As removal in FeEC batch experiments | 48 |
| 2.3.3 As(III) removal by bio-FeEC | 51 |
| 2.3.4 Characterisation of As-laden Fe(III)-precipitates | 53 |
| 2.3.5 Benefits and challenges of bio-FeEC | 56 |
| 2.4 Conclusions | 59 |
| References | 60 |
| Appendix | 65 |
| S2.1 X-ray absorption spectroscopy | 65 |

| | |
|---|-----------|
| Chapter 3 Embedding Fe(0) electrocoagulation in a biologically active As(III) oxidising filter bed | 71 |
| 3.1 Introduction | 73 |
| 3.2 Materials and methods | 75 |
| 3.2.1 Experimental setup | 75 |
| 3.2.2 Overview of column experiments | 77 |
| 3.2.3 Energy consumption | 79 |
| 3.2.4 Used water, chemicals, sampling and analytical methods | 79 |
| 3.3 Results and discussion | 80 |
| 3.3.1 Ripening of biotic columns | 80 |
| 3.3.2 Fe and As depth profile in biotic embedded-FeEC and supernatant-FeEC columns | 81 |
| 3.3.3 Effect of As oxidation state on removal in embedded-FeEC | 83 |
| 3.3.4 Enhancing deep-bed infiltration of Fe in embedded-FeEC filter beds | 84 |
| 3.3.6 Benefits and challenges of embedded-FeEC systems | 88 |
| 3.4 Conclusions | 90 |
| References | 91 |
| Appendix | 94 |
| S3.1 Batch FeEC reactor | 94 |
| S3.2 As removal in batch FeEC | 95 |
| S3.3 Electrode characteristics | 96 |

| | |
|---|-----------|
| Chapter 4 Groundwater native-Fe(II) oxidation prior to aeration with H₂O₂ to enhance As(III) removal | 99 |
| Abstract | 100 |
| 4.1 Introduction | 101 |
| 4.2 Materials and methods | 103 |
| 4.2.1 Chemicals | 103 |
| 4.2.2 Experimental setup and procedure | 103 |
| 4.2.3 Experimental conditions | 104 |
| 4.2.4 Chemical analysis | 104 |
| 4.2.5 X-ray absorption spectroscopy | 104 |
| 4.3 Results and discussion | 106 |
| 4.3.1 Solid-phase Fe structure and its relation to Fe(II) oxidation kinetics | 106 |
| 4.3.2 As(III) removal by Fe(III)-precipitates | 108 |
| 4.3.3 Under- and over-dosage of H ₂ O ₂ | 110 |
| 4.3.4 Application to raw anaerobic groundwater | 112 |
| 4.3.5 Implications for groundwater treatment | 113 |
| 4.4 Conclusions | 115 |

| | |
|------------------------------------|-----|
| References | 116 |
| Appendix | 119 |
| S4.1 X-ray absorption spectroscopy | 119 |

Chapter 5 Coupling H₂O₂ dosing and Fe(0) electrocoagulation to enhance As(III) removal in groundwater – A field study in Assam (India) **123**

| | |
|--|-----|
| Abstract | 124 |
| 5.2 Materials and methods | 127 |
| 5.2.1 Experimental setup and procedure | 127 |
| 5.2.2 Chemicals, sampling, and analytical methods | 128 |
| 5.3 Results and discussion | 130 |
| 5.3.1 Impact of Fe(II) oxidant type on As(III) removal | 130 |
| 5.3.2 Impact of Fe/As ratio on As(III) co-removal | 131 |
| 5.3.3 Impact of pH on As/Fe uptake ratio | 133 |
| 5.3.4 Co-removal of other contaminants with As | 134 |
| 5.3.5 Implications for groundwater treatment | 136 |
| 5.4 Conclusions | 137 |
| Appendix | 138 |
| References | 140 |

Chapter 6 | Conclusions and outlook **145**

| | |
|--|-----|
| 6.1 Conclusions | 146 |
| 6.1.1 Overall conclusion | 146 |
| 6.1.2 Mechanisms for enhanced As(III) removal with anaerobic Fe(II) oxidation by H ₂ O ₂ | 147 |
| 6.1.3 Technological sequence of the As removal technologies | 149 |
| 6.2 Outlook | 150 |
| 6.2.1 Future research | 150 |
| References | 152 |

Curriculum vitae **156**

List of publications **157**

Acknowledgements

This dissertation represents a journey spanning several years, filled with immersive learning experiences and dedicated research efforts. Yet, words seem insufficient to capture the depth of this undertaking or adequately express the gratitude I feel toward the numerous individuals who have played a pivotal role in shaping this work. In the vast sea of gratitude, these acknowledgments are but a glimpse of the interconnected web of support that has sustained me. To everyone who has contributed, knowingly or unknowingly, to the realization of this work, my heartfelt thanks.

My foremost acknowledgments extend to my promotors and supervisors, who bestowed their confidence and granted me the opportunity to embark on this challenging academic pursuit. Prof. Doris van Halem and Prof. Luuk Rietveld, your unwavering support, invaluable guidance, project-management, and relentless commitment throughout the entirety of my doctoral journey have been instrumental in completing this thesis. I am indebted to you for illuminating my path with your profound knowledge, fostering curiosity, and guiding me through uncharted territories. Your passion for research and dedication to excellence have been a constant source of inspiration, and I am deeply thankful for your steadfast support in shaping both my academic and professional trajectory. Special gratitude is reserved for Dr. Case van Genuchten, whose insights and expertise have been instrumental in shaping the direction of this research and significantly enriching my knowledge of iron chemistry, X-ray absorption spectroscopy, and the quality of this work. Thanks to you, I now understand the importance of distinguishing between poorly-ordered Fe solids and amorphous Fe solids. I would also like to express my gratitude to the TU Delft Global Initiative for awarding me a grant to conduct a field study in India. Furthermore, I want to thank Prof. Ajay Kalamdhad and his WMRG group for all the local assistance I needed during my field study in Assam, India.

I am indebted to TU Delft for creating a conducive academic environment and providing the essential resources that were instrumental in the successful completion of this research. The unwavering support from the Water Lab staff, including Armand, Jane, and Patricia, played a pivotal role during the experimental phase. I extend my heartfelt appreciation to Jane and Patricia for their invaluable contributions to analysing thousands of samples using the ICP-MS; their dedication was integral to the success of this research project.

I would like to express my heartfelt gratitude to my colleagues and friends: Shreya, Dhavissen, Erik, Steef, Rogelio, Arash, Silvy, Guss, Sara, Mona, Bruno, Kajol,

Devanita, Emiel, Roos, Simon, Antonella, Job, Pooja, Magnolia, Francesc, Nessia. Your unwavering support and inspiration throughout this journey have been invaluable. The camaraderie, insightful discussions, PSOR fun times, and consistent encouragement you provided played a crucial role in shaping my research and enriching my academic experience. I feel truly fortunate to have shared this intellectual adventure with such a talented and dedicated group. The lasting friendships forged during our time together are deeply cherished. Special thanks go to Erik, Emiel, Devanita, and Roos for their assistance with proofreading and Dutch translation. Mariska and Rielle, I am grateful for your efforts in organising important meetings. I also extend my sincere gratitude to a dedicated and talented group of students I have supervised: Sejal, Erik, Maitry, and Akhilesh. Your hard work, enthusiasm, and intellectual curiosity significantly contributed to the success of my PhD thesis. I appreciate the collaborative spirit you brought to our academic journey, and I am confident that your contributions will have a lasting impact on the field.

Finally, I am profoundly grateful for the unwavering support and love that my parents have bestowed upon me throughout my life. Their sacrifices, guidance, and encouragement have shaped the person I am today, and I owe them an immeasurable debt of gratitude. Additionally, I am fortunate to have Apoorva as my life partner who has been my constant source of strength, understanding, and companionship. Her love has been a source of joy and comfort, enriching my journey in ways words cannot adequately express. To my parents and my partner, I extend my deepest appreciation for being the pillars of my life, and I am truly blessed to have such incredible individuals by my side.

Abbreviations

- WHO = World Health Organization
- As = Arsenic
- As(III) = Arsenite
- As(V) = Arsenate
- Fe = Iron
- H₂O₂ = Hydrogen peroxide
- DO = Dissolved oxygen
- FeEC = Iron electrocoagulation
- DC = Direct current
- XAS = X-ray absorption spectroscopy
- LCFs = Linear combination fits
- CN = Coordination number
- Lp = Lepidocrocite
- 2LFh = 2-line ferrihydrite
- Oxy-HFO = Oxyanion-rich hydrous ferric oxide
- AsOB = Arsenic oxidising bacteria
- HTS = High-throughput sequencing
- OTUs = Operational Taxonomic Units
- RA = Relative abundance
- CD = Charge dosage
- CDR = Charge dosage rate
- ROS = Reactive oxygen species
- ICP-MS = Inductively coupled plasma mass spectrometry
- DOC = Dissolved organic carbon
- NOM = Natural organic matter
- TOC = Total organic carbon

Summary

Groundwater is typically a safe source of drinking water due to its stable and good microbial quality. However, the presence of geogenic arsenic (As) in groundwater, poses a serious health concern, impacting hundreds of millions of people worldwide. Prolonged groundwater consumption with elevated As levels can lead to chronic diseases, including cancer. According to the World Health Organization (WHO), As levels in drinking water should be less than 10 µg/L to minimise potential health risks. Consequently, As-contaminated groundwater should be treated before consumption.

Numerous advanced technologies can be applied to remove As from groundwater, including chemical oxidation with strong oxidants (e.g., KMnO_4 , NaOCl), chemical precipitation using metal coagulants (e.g., FeCl_3), adsorption, ion exchange, and membrane filtration. Nevertheless, the widespread use of such technologies is often constrained by the need for chemicals, high energy consumption, complex design and operation, the necessity of skilled personnel, and the associated costs of investment, maintenance, and operation. Aeration-filtration is a less advanced and cost-effective alternative for As removal from groundwater. Aeration-filtration is typically applied in untreated anaerobic groundwater to remove native-iron (Fe(II)), manganese (Mn(II)), methane (CH_4), hydrogen sulfide (H_2S), and ammonium (NH_4^+), however, it also has the potential to serve as a (partial) As barrier. In this process, native-Fe(II) in groundwater is oxidised and hydrolysed to Fe(III)-precipitates through dissolved oxygen (DO) inserted during aeration, which potentially adsorb dissolved As. Subsequently, the water is filtered through rapid sand filtration to remove the As-laden Fe(III)-precipitates. However, the efficacy of As removal through aeration-filtration can vary, with previous studies reporting removal ranging from 8 to 50%. This variability can be attributed to factors such as the oxidation state of As, the ratio of Fe to As, and groundwater pH. In raw anaerobic groundwater, As exists primarily as arsenite (As(III)), and has a much lower sorption affinity to Fe(III)-precipitates than the oxidised form, arsenate (As(V)). Although As(III) oxidation during aeration is thermodynamically feasible, the oxidation rate is often slow and incomplete hampering the full removal potential. Also, the Fe to As ratio in the groundwater is typically insufficient to form sufficient Fe(III)-precipitates to remove the desired amount of As. Furthermore, groundwater pH rises during aeration (due to CO_2 degassing), which results in less As(V) adsorption onto the Fe(III)-precipitates. To address these challenges, chemical oxidants and coagulants, such as $\text{KMnO}_4/\text{NaOCl}$ and FeCl_3 , could be added to enhance As(III) removal during aeration-filtration. However, this approach has limitations associated with chemical handling and storage. Therefore, this thesis highlights the application of novel technologies that offer advantages over the established, advanced technologies, and

which can be integrated in the conventional aeration-filtration technology to enhance the co-removal of As(III) from groundwater.

In Chapter 2, a novel continuous-flow As removal system is presented, that leverages the biological oxidation of As(III) in combination with iron electrocoagulation (FeEC), an electrochemical Fe dosage technology. Laboratory-scale rapid sand filter columns were used, which were transformed into As(III) oxidising biofilters by ripening the filter beds with chlorine-free Dutch tap water spiked with 150 µg/L As(III). In the biofilters >95% of the influent 150 µg/L As(III) oxidised to As(V) in the filtrate at 49 day of ripening. Microbial characterisation of the oxidising biomass through 16S rRNA analysis revealed the presence of bacteria belonging to *Comamonadaceae*, *Rhodobacteraceae*, and *Acidovorax*, known for their capability to oxidise As(III). Subsequently, the biologically oxidised As(V) in the biofilter filtrate was removed through FeEC to below the WHO guideline of 10 µg/L, applied in a continuous-flow mode. This was accomplished with a tenfold lower iron dosage as well as energy requirement compared to FeEC applied in the biofilter supernatant before biological oxidation.

In Chapter 3, a continuous flow rapid sand filter column system was demonstrated, which incorporated three distinct functions within a single reactor system: biological As(III) oxidation in biofilters, Fe dosing through FeEC to eliminate biologically oxidised As(V), and filtration of As-laden Fe(III)-precipitates. To accomplish this, FeEC was embedded and operated inside an As(III) oxidising biofilter, designed for treating chlorine-free Dutch tap water spiked with 150 µg/L As(III). The FeEC system was horizontally embedded at a depth of 50 cm from the top of the biofilter bed. At this depth, more than 85% of the influent 150 µg/L As(III) was oxidised to As(V). Subsequently, the embedded FeEC released Fe to adsorb the biologically oxidised As(V) (dissolved), and the bed layer below the FeEC system (height = 70 cm) filtered out the As-laden Fe(III)-precipitates. Operating FeEC within the biofilter resulted in the removal of 81% of the influent 150 µg/L As(III), as opposed to 67% removal when FeEC was operated in the supernatant (i.e., FeEC before biological oxidation). However, energy consumption was higher when FeEC was operated within the filter bed (sand matrix) at 14 Wh/m³, compared to FeEC operation in the supernatant (water matrix), which consumed 7 Wh/m³. The efficacy of As removal and energy consumption in the embedded-FeEC systems was further optimised by achieving deeper penetration of Fe(III)-precipitates inside the bed. This optimisation was accomplished by adjusting operational variables such as flow rate and pH levels.

In Chapter 4, an innovative approach to oxidise Fe(II) was introduced, dosing hydrogen peroxide (H_2O_2), distinct from the conventional method using DO through aeration. Experiments were conducted to simultaneously oxidise Fe(II) and As(III) adding either H_2O_2 under anaerobic conditions or DO by aeration. The results demonstrated that the complete anaerobic oxidation of $100\ \mu\text{M}$ Fe(II) with $100\ \mu\text{M}$ H_2O_2 led to the simultaneous removal of 95% of $7\ \mu\text{M}$ As(III), in contrast to only 44% removal when using DO. Additionally, it was discovered that when using $100\ \mu\text{M}$ Fe(II), the initial Fe(II)/ H_2O_2 ratio was crucial in decreasing the concentration of $7\ \mu\text{M}$ As(III) to levels below the WHO guideline of $10\ \mu\text{g/L}$. The enhanced As(III) co-removal, while adding the oxidant H_2O_2 is due to a greater stoichiometric yield of reactive oxygen species through Fenton reactions, which rapidly oxidises As(III). Additionally, an X-ray absorption spectroscopy analysis indicated that the reduction in crystallinity of the generated Fe(III)-precipitates from moderately crystalline lepidocrocite in the Fe(II)+DO system to poorly-ordered precipitates in the Fe(II)+ H_2O_2 considerably improved As(III) removal. These poorly-ordered precipitates have a higher specific surface area, resulting in a higher adsorption capacity compared to moderately crystalline precipitates.

Finally, in Chapter 5, H_2O_2 in combination with FeEC was applied to remediate As-contaminated groundwater in Assam (India). This study focused on the influence of oxidising native-Fe(II) in groundwater and Fe(II) generated by FeEC with H_2O_2 (prior to aeration), compared to DO inserted through aeration, while the effect on the co-removal of As(III) under varying groundwater compositions were also evaluated. Experiments, conducted at various locations, demonstrated that employing H_2O_2 as an oxidant for Fe(II) provided advantages in As(III) co-removal under real-world groundwater conditions. Across all locations, oxidising both the native-Fe(II) in the groundwater and the Fe(II) released by FeEC with H_2O_2 consistently achieved an overall As(III) removal efficacy ranging from 82 to 99%, while the addition of DO resulted in a removal efficacy between 48 to 72%. The field study also revealed that the highest As uptake by native-Fe(II) in groundwater (As/Fe uptake ratio) occurred at pH 6.5 to 6.8, which is substantially lower than the pH commonly observed after aeration due to CO_2 degassing (pH 7.0 to 8.0).

In conclusion, the introduction of FeEC and H_2O_2 dosing, integrated into a conventional aeration-(bio)filtration system, considerably increasing the efficacy of As(III) removal from anaerobic groundwater.

Samenvatting

Grondwater is doorgaans een veilige bron voor de productie van drinkwater vanwege de stabiele en goede microbiële kwaliteit. Het van nature aanwezige arsen (As) in grondwater vormt echter een ernstig gezondheidsrisico en treft wereldwijd miljoenen mensen. Langdurige consumptie van grondwater met verhoogde As concentraties kan leiden tot chronische ziekten, waaronder kanker. Volgens de World Health Organization (WHO) moeten As concentraties in drinkwater lager dan 10 µg/L zijn om mogelijke gezondheidsrisico's te minimaliseren. Om deze reden moet grondwater dat verontreinigd is met As worden gezuiverd voor consumptie.

Verskillende geavanceerde technologieën kunnen worden toegepast om As uit grondwater te verwijderen, waaronder chemische oxidatie met sterke oxidanten (bijv. KMnO_4 , NaOCl), chemische neerslag met metaal coagulanten (bijv. FeCl_3), adsorptie, ionenuitwisseling, en membraanfiltratie. Wijdverbreide toepassing van dergelijke technologieën wordt echter vaak beperkt door de beschikbaarheid van chemicaliën, een hoog energieverbruik, complexe ontwerp- en bedieningsvereisten, de noodzaak van gekwalificeerd personeel, en de bijbehorende kosten van investering, onderhoud, en bediening. Beluchting-filtratie is een minder geavanceerd en kosteneffectief alternatief voor het verwijderen van As uit grondwater. Beluchting-filtratie wordt doorgaans toegepast op onbehandeld anaeroob grondwater om van nature aanwezig ijzer (Fe(II)), mangaan (Mn(II)), methaan (CH_4), waterstofsulfide (H_2S), en ammonium (NH_4^+) te verwijderen. Daarnaast heeft deze techniek ook de potentie om een (gedeeltelijke) barrière tegen As te vormen. Tijdens beluchting wordt zuurstof in het grondwater geïntroduceerd, waardoor het van nature aanwezige Fe(II) wordt geoxideerd en gehydrolyseerd tot Fe(III)-vlokken, die opgelost As adsorberen. Vervolgens wordt het water gefilterd door snelfiltratie om de Fe(III)-vlokken met geadsorbeerd As te verwijderen. Het rendement van As-verwijdering door beluchting-filtratie kan echter variëren, met gerapporteerde verwijderingen tussen de 8 tot 50%. Deze variatie kan veroorzaakt worden door factoren zoals de oxidatievorm van As, de verhouding van Fe tot As, en de pH van het grondwater. In ruw anaeroob grondwater komt As voornamelijk voor als arseniet (As(III)), wat een veel lagere adsorptie affiniteit voor Fe(III)-vlokken heeft dan de geoxideerde vorm, arsenaat (As(V)). Hoewel As(III)-oxidatie tijdens beluchting thermodynamisch mogelijk is, is de oxidatiesnelheid vaak traag en onvolledig, wat het verwijderingsrendement belemmert. Ook is de verhouding Fe tot As in het grondwater vaak onvoldoende om de gewenste As-verwijdering te realiseren. Bovendien stijgt de pH van het grondwater tijdens beluchting (door CO_2 ontgassing), wat resulteert in verlaagde As(V)-adsorptie op de aanwezige Fe(III)-vlokken. Een mogelijke oplossing voor deze uitdagingen is om chemische oxidanten en coagulanten, zoals $\text{KMnO}_4/\text{NaOCl}$ en FeCl_3 , toe te voegen om As(III)-verwijdering

tijdens beluchting-filtratie te verhogen. Deze benadering heeft echter nadelen, zoals chemische behandeling en opslag. Daarom belicht dit proefschrift de toepassing van nieuwe technologieën die voordelen bieden ten opzichte van gangbare geavanceerde technologieën en geïmplementeerd kunnen worden in de conventionele beluchting-filtratietechnologie om de verwijdering van As(III) uit grondwater te verbeteren.

In hoofdstuk 2, wordt een innovatief, continu bedreven As-verwijderingssysteem gepresenteerd dat gebruikmaakt van de biologische oxidatie van As(III) in combinatie met ijzer elektrocoagulatie (FeEC), een elektrochemische technologie om Fe te doseren. In een lab opstelling werden zandfilterkolommen gerijpt tot As(III)-oxiderende biofilters met chloorvrij kraanwater, waaraan 150 µg/L As(III) was toegevoegd. Na een rijping van 49 dagen, oxideerden de biofilters meer dan 95% van het ingaande 150 µg/L As(III) tot As(V). Microbiële karakterisering van de oxiderende biomassa, door 16S rRNA-analyse, toonde de aanwezigheid van bacteriën behorende tot *Comamonadaceae*, *Rhodobacteraceae*, en *Acidovorax* aan, bekend om hun vermogen om As(III) te oxideren. Vervolgens werd het biologisch geoxideerde As(V) in het filtraat van de biofilter verwijderd door FeEC tot onder de WHO-richtlijn van 10 µg/L. Dit werd bereikt met een tienvoudig lagere ijzerdosering en energiebehoefte in vergelijking met FeEC toegepast in het bovenwater van het filter vóór biologische oxidatie.

In hoofdstuk 3, wordt een systeem met snelle zandfilter kolommen gedemonstreerd. Drie afzonderlijke functies werden geïntegreerd in één reactor: biologische As(III)-oxidatie in biofilters, Fe-dosering via FeEC om biologisch geoxideerde As(V) te verwijderen, en filtratie van As-beladen Fe(III)-vlokken. Om dit te bereiken, werd FeEC geïmplementeerd in een As(III)-oxiderende biofilter, voor de behandeling van chloorvrij leidingwater met toevoeging van 150 µg/L As(III). Het FeEC-systeem werd horizontaal geplaatst op een diepte van 50 cm vanaf de bovenkant van het biofilter bed. Op deze diepte werd meer dan 85% van het inkomende 150 µg/L As(III) geoxideerd tot As(V). Vervolgens gaf het geïmplementeerde FeEC Fe vrij om het biologisch geoxideerde, opgeloste As(V) te adsorberen. Vervolgens, filtreerde het filterbed onder het FeEC-systeem (hoogte = 70 cm) de As-beladen Fe(III)-vlokken uit het water. De uitvoering van FeEC in het biofilter resulteerde in de verwijdering van 81% van het inkomende 150 µg/L As(III), in tegenstelling tot 67% verwijdering wanneer FeEC werd toegepast in het bovenwater (d.w.z., FeEC vóór biologische oxidatie). Echter, het energieverbruik was hoger wanneer FeEC in het filterbed (zandmatrix) werd geplaatst (14 Wh/m³), vergeleken met de plaatsing in het bovenwater (watermatrix), wat 7 Wh/m³ verbruikte. De efficiëntie van As-verwijdering en het energieverbruik werd verder geoptimaliseerd door een diepere indringing van Fe(III)-vlokken in het filterbed te bereiken door operationele variabelen zoals filtratiesnelheid en pH te variëren.

In hoofdstuk 4, wordt een innovatieve benadering geïntroduceerd om Fe(II) te oxideren, waarbij waterstofperoxide (H_2O_2) werd gedoseerd, in plaats van de conventionele methode met opgelost zuurstof (DO) via beluchting. Experimenten werden uitgevoerd om Fe(II) en As(III) door toevoeging van H_2O_2 onder anaerobe omstandigheden of door DO gelijktijdig te oxideren. De resultaten toonden aan dat de volledige anaerobe oxidatie van $100 \mu\text{M}$ Fe(II) met $100 \mu\text{M}$ H_2O_2 leidde tot een gelijktijdige verwijdering van 95% van de $7 \mu\text{M}$ As(III), in tegenstelling tot slechts 44% verwijdering bij gebruik van DO. Bovendien werd ontdekt dat bij gebruik van $100 \mu\text{M}$ Fe(II) de initiële Fe(II): H_2O_2 verhouding cruciaal was om de concentratie van $7 \mu\text{M}$ As(III) te verlagen tot niveaus onder de WHO richtlijn van $10 \mu\text{g/L}$. De verbeterde As(III) co-verwijdering bij het toevoegen van de oxidant H_2O_2 komt door een hogere stoichiometrische opbrengst van reactieve zuurstofsoorten via Fenton-reacties, die As(III) snel oxideren. Bovendien liet een analyse met X-ray absorption spectroscopy zien dat de afname in kristalliniteit van de gegeneerde Fe(III)-vlokken, van het matig kristallijne lepidocrociet in het Fe(II)+DO systeem tot amorfe vlokken in het Fe(II)+ H_2O_2 systeem, de verwijdering van As(III) aanzienlijk verbeterde. Deze amorfe vlokken hebben een groter specifiek oppervlak, wat resulteert in een hogere adsorptiecapaciteit in vergelijking met matig kristallijne vlokken.

Tot slot wordt in hoofdstuk 5 de combinatie van H_2O_2 met FeEC toegepast om As-verontreinigd grondwater in Assam (India) te zuiveren. De invloed van het oxideren van het van nature aanwezige Fe(II) in grondwater, en Fe(II) gegeneerd door FeEC, door H_2O_2 (voor beluchting) werd hierbij vergeleken met DO ingebracht door beluchting, waarbij tevens de effecten ervan op de co-verwijdering van As(III) in variërende grondwatercomposities werd geëvalueerd. Experimenten, uitgevoerd op verschillende locaties, toonden aan dat het gebruik van H_2O_2 als Fe(II) oxidant voordelen bood bij de co-verwijdering van As(III). Op alle locaties bereikte het oxideren met H_2O_2 van zowel het van nature aanwezige Fe(II) in het grondwater als het Fe(II) vrijgegeven door FeEC, een As(III)-verwijderingsefficiëntie variërend van 82 tot 99%, terwijl in het geval van het inbrengen van DO in een verwijderingspercentage van slechts 48 tot 72% resulteerde. De veldstudie toonde ook aan dat de hoogste opname van As door het van nature aanwezig Fe(II) in grondwater (As/Fe opname verhouding) plaatsvond bij pH 6.5 tot 6.8. Deze optimale pH is aanzienlijk lager dan de pH die vaak wordt waargenomen na beluchting, als gevolg van CO_2 ontgassing (pH 7.0 tot 8.0).

In het proefschrift wordt dus aangetoond dat FeEC en H_2O_2 dosering, geïmplementeerd in een conventioneel beluchting-(bio)filtratiesysteem, de effectiviteit van het verwijderen van As(III) uit anaeroob grondwater aanzienlijk verhoogt.



Chapter 1

Introduction

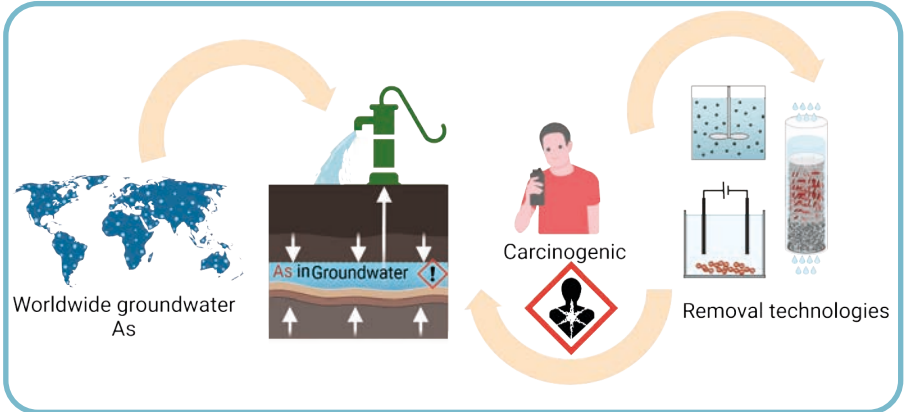


Image created in Biorender

1.1 Arsenic in groundwater

It is estimated that one third of the earth's population uses groundwater as their source for drinking water supply (International Association of Hydrogeologists, 2020). Groundwater is more reliable than surface water, with a stable quality, and typically free from anthropogenic contaminants, such as pathogenic microorganisms and organic micropollutants (Schmoll et al., 2006). Therefore, it is considered a relatively safe drinking water source and in many regions worldwide it is directly consumed with little or no treatment (Carrard et al., 2019; Guppy et al., 2018).

Despite natural groundwater having a good microbial quality, the presence of other natural contaminants in groundwater can be of concern. Depending on the geochemical and hydrochemical conditions, iron, ammonium, methane, hydrogen sulfide, manganese and even fluoride can be found in groundwater sources (Goody & Darling, 2005; Liang et al., 2022; Podgorski & Berg, 2022; Podgorski et al., 2022). However, the natural groundwater contaminant of most global concern, due to its widespread presence in nature as well as its high toxicity at low intake levels, is arsenic (As) (Shaji et al., 2021; Shankar et al., 2014). Drinking As-contaminated water has even been found to be the most dominant pathway for human exposure to As (Chung et al., 2014). Following the United Nations Synthesis report, As toxicity from drinking water ranks second to its hazardous effects on human health (Johnston et al., 2001). It has been estimated that around 94 to 220 million people worldwide have been exposed to groundwater with toxic As concentrations, with the majority (94%) being in Asian countries (Podgorski & Berg, 2020). Long-term consumption of As-contaminated water at toxic levels may lead to chronic diseases such as skin, bladder, kidney and lung cancers, reproductive disorders, and neurodevelopmental diseases in children (Kapaj et al., 2006; Tseng, 1977). As a result, in 1993, the World Health Organization (WHO) set a provisional guideline of $<10 \mu\text{g/L}$ As in drinking water (WHO, 1993). Therefore, groundwater contaminated with As above this level should be treated before drinking.

The presence of As in natural groundwater is geogenic and associated with geochemical and geomicrobial processes (Ravenscroft et al., 2009; Smedley & Kinniburgh, 2002). The four main mechanisms causing As contamination of groundwater are reductive dissolution, oxidation of As-bearing sulfide minerals, geothermally influenced groundwater, and alkali desorption. In reducing aquifers under anaerobic conditions, As is released in the groundwater due to the reductive dissolution of As-bearing iron(III) minerals in the aquifer sediments (Bhattacharya et al., 1997; Nickson et al., 2000). This mechanism is the primary cause of As contamination e.g., in the groundwater of the Bengal Delta Plain (Bangladesh, West Bengal (India)) (Bhattacharya et al.,

2004), the Mekong Delta Plain (Vietnam, Cambodia) (Berg et al., 2007), and China, where As concentration as high as 1800 $\mu\text{g/L}$ have been measured (Smedley et al., 2003). As contamination from As-bearing sulfide minerals is most common in mining areas where sulfide minerals (FeS_2 and FeAsS) oxidation causes As desorption into groundwater (Ravenscroft et al., 2009; Smedley & Kinniburgh, 2002). As mobilisation in geothermally influenced groundwater's is typically linked to higher temperatures and higher chloride concentrations (Smedley & Kinniburgh, 2002; Welch et al., 1988; Wilkie and Hering, 1998). Groundwater in the USA and Nicaragua has been observed to be contaminated due to geothermal activity (Gonzalez et al., 2019; Welch et al., 1988). As release via alkali desorption involves interaction of naturally occurring minerals, predominantly iron and manganese oxides, with As-bearing sediments in aquifers. Under alkaline conditions the pH rises, causing changes in mineral surface charges. This alteration prompts the desorption of adsorbed As species from mineral surfaces (Bhattacharya et al., 1997; Ravenscroft et al., 2009; Smedley & Kinniburgh, 2002).

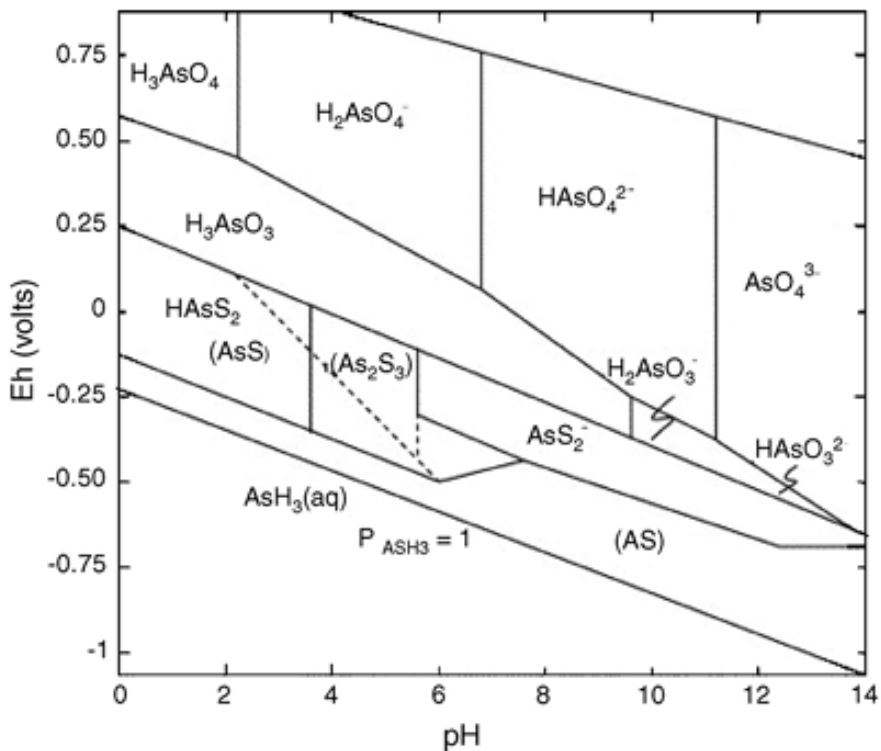


Fig. 1.1. The Eh-pH diagram for arsenic at 25°C and 101.3 kPa (Mohan & Pittman, 2007).

In the aqueous environment, As is mainly present in two oxidation states: trivalent oxyanion As (arsenite (+3) or As(III)) and pentavalent oxyanion As (arsenate (+5) or As(V)). The redox potential and pH of the water controls the As oxidation state and its speciation (Fig. 1.1). Under reducing conditions and $\text{pH} < 9.2$, As(III) is the thermodynamically stable form and present as H_3AsO_3 , whereas under oxidising conditions, As(V) is the predominant form, mainly present as HAsO_4^{2-} ($\text{pH} > 6.9$) or H_2AsO_4^- ($\text{pH} < 6.9$) (Katsoyiannis & Zouboulis, 2004; Mohan & Pittman, 2007; Smedley & Kinniburgh, 2002).

1.2 Treatment technologies for arsenic removal from groundwater

As removal from groundwater can be achieved through various technologies, including coagulation (chemical precipitation) and floc removal, adsorption, ion exchange, and membrane filtration (Alka et al., 2021; Chiavola et al., 2019; Chiavola et al., 2015; George et al., 2006; Neisan et al., 2023; Sancha, 2006; Wickramasinghe et al., 2004). Coagulation involves adding a coagulant, such as iron or aluminium salts, to form flocs that trap As, allowing for subsequent removal through sedimentation and/or filtration (Hesami et al., 2012; Khan et al., 2002; Lakshmanan et al., 2008). Adsorption utilises adsorbents, such as iron oxide-based sorbents, and zero-valent iron, and other metal oxide-coated sand, to attract and bind As ions, effectively reducing their concentration in water (Gonzalez-Pech et al., 2022; Kanel et al., 2005; L. Kim et al., 2022). Ion exchange involves the substitution of As ions in water with harmless ions, such as chloride, through the use of ion exchange resins (Alka et al., 2021; Mohanty, 2017). Lastly, membrane filtration relies on membranes with pore sizes small enough to physically block the passage of As oxyanions, enabling the production of clean drinking water (Algieri et al., 2022; Rajendran et al., 2021). All these methods offer effective As removal solutions, and their selection depends on factors such as As concentration, water matrix quality, and treatment system requirements. However, each approach has its limitations. Coagulation suffers from dosing chemical coagulants and formation of As-containing sludge, necessitating additional disposal measures (Mohanty, 2017; Yadav et al., 2021). Adsorption techniques require replacement or regeneration of the adsorbent material, leading to operational costs and/or waste generation (Mohan & Pittman, 2007). Ion exchange can be limited by competing ions in the water and the As oxidation state, reducing its efficiency and requiring periodic resin regeneration or replacement (Yadav et al., 2021). Membrane filtration requires relatively high installation and operating costs, as well as expertise to operate the system, can be prone to high energy consumption and fouling, leading to decreased flux and increased maintenance, and generation of a highly toxic concentrate (Algieri et al., 2022; Yadav et al., 2021).

Conventional aeration-filtration applied to raw anaerobic groundwater can be a suitable alternative to treat As-contaminated groundwater (Gude et al., 2016; Hug & Leupin, 2003; Roberts et al., 2004). Compared to the more advanced technologies discussed above, As removal through aeration-filtration is cost-effective due to a low capital investment and operational costs, energy efficient, a low chemical demand, relatively simple to design, install, and operate, and that it can be constructed with locally available materials (e.g. sand) (Annaduzzaman et al., 2021; Gude et al., 2017). However, the process requires periodic backwashing of the clogged filters (Wolthoorn, 2003), generating As-containing backwash water and sludge, which demands safe disposal. Aeration-filtration is commonly designed to remove native-iron (Fe(II)), manganese (Mn(II)), methane (CH₄), hydrogen sulfide (H₂S), and ammonium (NH₄⁺) from groundwater, and can thus also act as an As barrier, co-removing it with the native-Fe(II) (Annaduzzaman et al., 2021; Han et al., 2013; Katsoyiannis et al., 2008; Vries et al., 2017). The process involves oxidation of native-Fe(II) in the anaerobic groundwater by dissolved oxygen (DO) inserted through aeration to generate Fe(III) (oxyhydr)oxides (further referred to as Fe(III)-precipitates/Fe solids) that can bind the As, followed by the removal of the As-laden Fe(III)-precipitates by sand filtration (Bora et al., 2016; Gude et al., 2016).

The aeration-filtration technology represents a sustainable alternative to other advanced arsenic (As) removal technologies; however, in most cases, the As removal is often ineffective. The co-removal of As with the groundwater native-Fe(II) through aeration-filtration can vary from 8 to 50% (Holm & Wilson, 2006; Li et al., 2016; van Genuchten & Ahmad, 2020), depending on various factors, such as As oxidation state, groundwater pH, and Fe(II) concentration. In raw anaerobic groundwater, As exists as neutrally charged As(III), which has a lower affinity to Fe(III)-precipitates, compared to the oxidised form, As(V), a negatively charged oxyanion at neutral pH (H₂AsO₄⁻/HASO₄²⁻) (Bissen & Frimmel, 2003; Gude et al., 2017; Roberts et al., 2004). As an example, Annaduzzaman et al. (2022) reported that the As removal capacity by Fe(III)-precipitates, generated via aeration, was 76 µg As/mg Fe for As(V), compared to 38 µg As/mg Fe for As(III). Although As(III) oxidation through aeration (i.e., oxidation by DO) is thermodynamically possible, the oxidation rate is too slow, having a half-life of days, to convert As(III) into As(V) (Hug & Leupin, 2003; Kim & Nriagu, 2000). As a consequence, most of the unoxidised As(III) does not adsorb and remains in the dissolved phase, leading to break through of As. In such cases, strong chemical oxidants, such as sodium hypochlorite (NaOCl), potassium permanganate (KMnO₄), and ozone (O₃) are commonly dosed during or after aeration, rapidly oxidising As(III) (Kim & Nriagu, 2000; Sorlini & Gialdini, 2010). These chemical oxidants can be expensive, require proper handling and storage, and proper supply chains (Jackman & Hughes, 2010; Katsoyiannis & Zouboulis,

2004). Moreover, these chemicals result in the generation of unwanted by-products or residuals that can be toxic and require further treatment. For example, hypochlorite can react with the organic matter present in water to generate disinfection by-products such as trihalomethanes, which are carcinogenic (Fang et al., 2021; Richardson & Plewa, 2020). In bromide-rich waters, ozone can result in the formation of bromate, which is also toxic (Morrison et al., 2023).

In other cases, the initial Fe(II)/As(III) ratio in groundwater can also limit As removal during aeration–filtration. Gude et al. (2016) and Ahmad et al. (2018) reported an Fe/As ratio of 141.3–246.7 mol:mol to remove As (initial As concentration = 10–26 µg/L) below 10 µg/L. Similarly, Roberts et al. (2004) showed a requirement of 146.7 mol:mol Fe/As ratio to remove 500 µg/L As below 50 µg/L via the aeration–filtration process. In such situations, chemical coagulants, such as FeCl₃, are dosed during aeration–filtration to achieve As concentrations meeting the drinking water guidelines (Ahmad et al., 2018).

Additionally, aeration leads to an elevation in groundwater pH due to CO₂ degassing. This pH increase may impede the adsorption of As(V) onto Fe(III)-precipitates, as As(V) adsorption is more favourable at lower pH levels (i.e., prior to aeration) (Annaduzzaman et al., 2021; Dixit & Hering, 2003).

1.3 Biological As(III) oxidation in sand filters

The biological oxidation of As(III) by arsenic oxidising bacteria (AsOB) has gained attention as a promising alternative to chemical oxidation methods. This approach does not generate toxic by-products and leads to reduced costs and logistical complexities, associated with chemical procurement and handling (Kamei-Ishikawa et al., 2017). AsOB oxidise As(III), either for detoxification (in heterotrophic microorganisms) or for energy generation and growth (in chemolithoautotrophic microbes), through their enzymatic activity involving arsenic oxidase (Muller et al., 2003; Santini et al., 2000). Native AsOB have originally been detected across various environments, including As-contaminated water and sediments (Ito et al., 2012). However, the occurrence of biological As(III) oxidation has also been reported in laboratory and large-scale rapid sand filters used in aeration–filtration for groundwater treatment (Crognale et al., 2019; Gude et al., 2018c; Lytle et al., 2007). Long-term exposure of rapid sand filter beds to As(III)-contaminated water transforms them into biofilters due to accumulation of a mixed biofilm (containing AsOB), that can effectively oxidise As(III) to As(V). For example, Lytle et al. (2007) documented biological oxidation of As(III) in granular media filters within a full-scale iron-removal plant treating raw groundwater.

Similarly, Gude et al. (2018c) demonstrated that continuous ripening of new sand filters with As(III)-spiked tap water led to the growth of a microbial community inside the bed, which was able to oxidise 98% of the influent 116 µg/L As(III) after 38 days of ripening.

In such biofilters, the oxidised As(V) could subsequently be co-removed by the Fe(III)-precipitates generated from the groundwater native-Fe(II) oxidation via aeration. However, complete biological As(III) oxidation predominantly occurs lower in the filter bed (around 40-60 cm from the top layer) (Gude et al., 2018a; Gude et al., 2018b; Yang et al., 2014), where the Fe(III)-precipitates, generated from groundwater native-Fe(II) oxidation, have already been removed and are unavailable for adsorption of As(V) (Gude et al., 2018a; Gude et al., 2018b). Consequently, an additional dosage of Fe is necessary to remove the oxidised As(V).

1.4 Iron Electrocoagulation

As an alternative to the direct dosage of Fe salts, iron electrocoagulation (FeEC) can serve as a Fe dosage technology to remove the biologically oxidised As(V) from biofilters, as well as in situations where the groundwater native-Fe(II) is insufficient to meet drinking water guidelines for As (Amrose et al., 2014; Bandaru et al., 2020a; Delaire et al., 2017; Holt et al., 2005; Mollah et al., 2004; Moussa et al., 2017). FeEC is an electrochemical water treatment process that utilises Fe(0) electrodes to introduce Fe into As-contaminated water. The technology resembles chemical coagulation; however, in FeEC, metal coagulants are generated in-situ through electrochemical reactions. FeEC involves applying a small electric current to Fe(0) electrodes (anode and cathode) in contact with As-contaminated water (Fig. 1.2). This results in the release of Fe(II) ions from the sacrificial Fe(0) anode due to oxidation. At the cathode, a reduction reaction occurs where H₂O converts into OH⁻ ions and H₂ gas. The Fe(II) ions are then oxidised by DO, present in the aerated water, producing reactive Fe(III)-precipitates that act as coagulants. As removal in FeEC takes place through co-precipitation and/or adsorption onto Fe(III)-precipitates. The As-laden Fe(III)-precipitates can subsequently be separated from the water using sedimentation, flotation, or filtration. During FeEC, generation of different types of Fe(III)-precipitates have been reported, ranging from poorly-ordered hydrous ferric oxides to crystalline magnetite (van Genuchten et al., 2012, 2014, 2019, 2020).

The modular design, affordability, adaptability, minimal infrastructure requirements, and potential for automation makes FeEC a highly suitable technology for low-income and resource-poor regions (Amrose et al., 2014; Bandaru et al., 2020a; Holt et al., 2005;

Kumar et al., 2004; Wan et al., 2011). Furthermore, FeEC has demonstrated effective As removal (up to 99%) (Wan et al., 2011). However, while FeEC can remove both As(III) and As(V) from water, the removal of As(V) requires lower levels of Fe dosage and treatment time compared to As(III). Therefore, pre-oxidising As(III) to As(V) during FeEC will substantially decrease the overall sludge production and energy consumption of the system (Kumar et al., 2004; Wan et al., 2011). Thus, applying FeEC after biological As(III) oxidation in the biofilters is advantageous in terms of waste management and energy requirements.

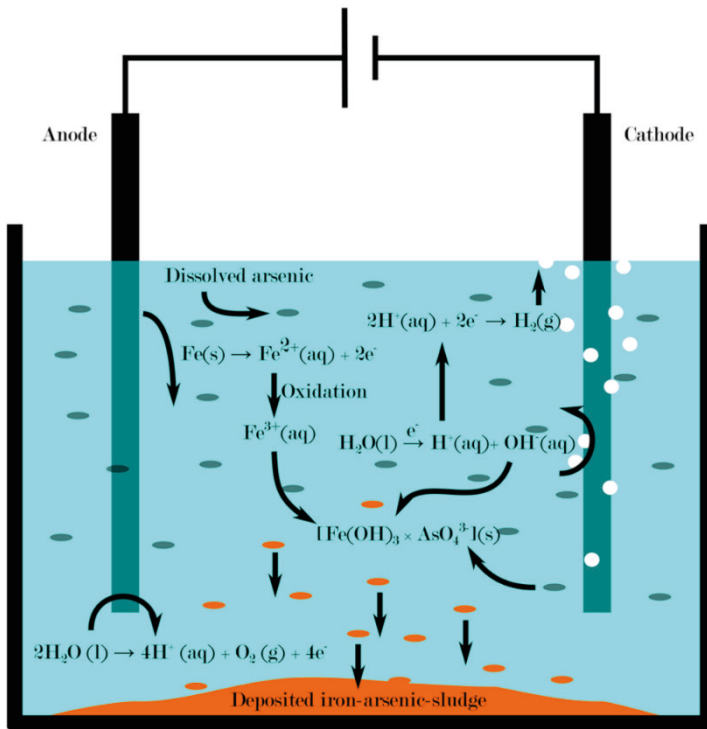


Fig. 1.2. Basic iron electrocoagulation setup (Müller et al., 2021).

1.5 Fe(II) oxidation with hydrogen peroxide

Fe(II)-based As removal is a common approach to treat groundwater, where either the groundwater native-Fe(II) or externally dosed Fe(II) (e.g. by FeEC) is oxidised by DO to generate Fe(III)-precipitates, adsorbing the As. However, as mentioned above, the oxidation state of As plays a major role in the removal efficacy of such approach. Although As(III) oxidation through DO is a slow process, partial oxidation of As(III)

occurs during Fe(II) oxidation. This partial As(III) co-oxidation is mainly performed by the reactive oxygen species (ROS) generated through Fenton reactions during the Fe(II) oxidation (Hug & Leupin, 2003). As an alternative, oxidation of Fe(II) by hydrogen peroxide (H_2O_2) has emerged to improve As(III) co-oxidation via such Fenton reactions. While H_2O_2 does not effectively oxidise As(III) (with a half-life of days), the oxidation of Fe(II) with H_2O_2 generates a higher stoichiometric yield of ROS compared to DO. Theoretically, using H_2O_2 , 1 mole of ROS can be generated from 1 mole of Fe(II), whereas it requires 3 moles of Fe(II) for the same yield with DO (Hug & Leupin, 2003).

Oxidising the groundwater native-Fe(II) and Fe(II) from FeEC with H_2O_2 can thus be promising due to higher ROS yields, in comparison with the oxidation of Fe(II) with DO. In addition, H_2O_2 can oxidise the groundwater native-Fe(II) or Fe(II) generated by FeEC anaerobically, before aeration, since Fe(II) oxidation rate with H_2O_2 is at four orders of magnitude higher than that of DO (Bandaru et al., 2020b). This process will then produce Fe(III)-precipitates at a relatively low pH, since during aeration groundwater pH rises due to CO_2 degassing. This is advantageous for As(V) adsorption since the positively charged Fe(III)-precipitates have a higher affinity to the negatively charged As(V) species at lower pH (Annaduzzaman et al., 2021; Dixit & Hering, 2003). Therefore, this novel Fe(II) oxidation approach with dosing H_2O_2 in anaerobic water, before aeration, can thus, potentially, optimise the use of Fe(II), including groundwater native-Fe(II) and Fe(II) generated during FeEC, while treating As(III)-contaminated water.

1.6 Knowledge gaps: Coupling iron electrocoagulation and hydrogen peroxide dosing to groundwater biofilters

Integrating biological As(III) oxidation in biofilters with FeEC represent a novel, (chemical-free) strategy to improve As(III) removal in aeration-filtration, however, such novel integrated systems have never been demonstrated before. An ideal approach would be to operate FeEC in a continuous flow mode, but so far FeEC reactors have mainly been studied in batch mode (Bandaru et al., 2020b; Chen et al., 2023; van Genuchten et al., 2012; Wan et al., 2011). To take advantage of biological oxidation in aeration-filtration, FeEC should further be applied after filtration, allowing oxidation to occur within the filter bed, followed by an additional filtration step to eliminate the As-laden Fe(III)-precipitates. To avoid this additional filtration step, one could also consider to integrate FeEC into the filter bed, entrapping the As-laden Fe(III)-precipitates within one single reactor system. However, this concept has never been studied for groundwater treatment and demands investigation to understand the

key performance indicators, such as overall As removal, energy consumption, and influence of operational parameters.

The application of H_2O_2 to oxidise Fe(II) for an improved As(III) co-removal has been reported previously. Krishna et al. (2001) demonstrated that when initially treating 2 mg/L of As(III) with a combination of 100 mg/L Fe(II) and 100 μ L/L of 30% H_2O_2 , followed by passing the mixture through zero valent iron columns and a sand bed, As removal below 10 μ g/L (WHO guideline) was achieved. Furthermore, Wang et al. (2013) reported 70% oxidation of 20 μ M As(III) when oxidising 20 μ M Fe(II) with 50 μ M H_2O_2 compared to 2.5% when oxidising the Fe(II) with DO. Although these studies provide valuable insights, their primary focus was on the enhanced co-oxidation of As(III) through ROS. The influence of the Fe(III)-precipitates structure was not a central aspect of their interpretations. Previous studies have reported that Fe(II) oxidation with H_2O_2 generates poorly-ordered Fe(III)-precipitates compared to moderately crystalline precipitates when DO is used as an oxidant (Bandaru et al., 2020b; van Genuchten & Peña, 2017). It is, however, not known if these poorly-ordered precipitates with higher reactive specific surface area can provide more (As) adsorption sites per mass of Fe. For oxidation with DO, Roberts et al. (2004) showed that to remove 500 μ g/L As(III) below 50 μ g/L through aeration-filtration, about five times more Fe(II) had to be dosed compared to the removal of 500 μ g/L As(V). Hence, understanding of Fe(III)-precipitates structure in relation to As speciation is critical to further understand to assess the added benefit of H_2O_2 dosing over DO.

Raw anaerobic groundwater often contains CO_2 , which is (partly) removed during the aeration process. This reduction in CO_2 concentration leads to an increase in groundwater pH during aeration, creating a less favourable environment for As(V) adsorption. This is because Fe(III)-precipitates have a higher affinity for adsorbing As(V) at lower pH (i.e., before aeration) (Annaduzzaman et al., 2021; Dixit & Hering, 2003). Therefore, generating Fe(III)-precipitates, either from native-Fe(II) in groundwater or through FeEC, anaerobically, before aeration, can be an advantageous step to enhance the adsorption capacity for As(V). This can be achieved e.g., by introducing H_2O_2 prior to aeration. This novel approach of anaerobic Fe(II) oxidation with H_2O_2 before aeration has not been thoroughly studied yet. The potential benefits of utilising the naturally occurring low pH to improve As removal in Fe(II)-based systems are often underestimated and demands careful consideration for optimising As removal during aeration-filtration.

Before implementing a new groundwater treatment technology on a larger scale, it is essential to test its effectiveness and feasibility in real-world conditions. While

laboratory experiments provide valuable insights into the treatment mechanisms, they often fail to account for site-specific factors such as natural variations in water quality. Therefore, field studies are necessary to assess the performance and effectiveness of the treatment technologies under diverse environmental conditions, validate laboratory findings, identify potential limitations, and develop targeted solutions that can be implemented at scale.

1.7 Research objective and questions

The primary objective of this thesis is to unravel the mechanisms underlying As removal in the coupling of FeEC and H_2O_2 dosing to groundwater biofilters, with the aim of enhancing the overall removal of As(III) from groundwater during aeration-(bio)filtration. To accomplish this main objective, the following research questions were addressed.

- *How does continuous flow FeEC after groundwater biofiltration improve the overall As(III) removal, sludge generation, and energy requirement compared to conventional FeEC?*
- *What is the impact of embedding and operating FeEC inside an As(III) oxidising biological filter bed on overall As(III) removal and energy consumption compared to FeEC in the filter supernatant, and how do operational parameters (Fe dosage, flow rate, pH) influence As removal in embedded-FeEC systems?*
- *What is the impact of oxidising Fe(II) anaerobically with H_2O_2 , compared to DO, on Fe(III)-precipitates structure, As(III) co-oxidation, and overall As(III) removal, and how does Fe: H_2O_2 dosing ratio influence the extent of Fe(II) oxidation and As removal?*
- *How does oxidation of native-Fe(II) (in groundwater) and Fe(II) generated by FeEC with H_2O_2 improve the overall As(III) removal, compared to DO, under varying groundwater composition in Assam (India), and what is the impact of pH on As/Fe uptake ratio when H_2O_2 oxidises the groundwater native-Fe(II)?*

1.8 Structure of the thesis

In **Chapter 2**, the influence of integrating FeEC with biofilters on As(III) removal, sludge generation, and energy consumption is discussed. In **Chapter 3** the use of a FeEC-embedded biological filter is demonstrated, and the impact of embedding and operating

FeEC within an As(III) oxidising filter bed on As(III) removal and energy consumption is determined. In addition, the effect of operational parameters such as Fe dosage (by FeEC), flow rate, and pH on As removal in embedded-FeEC systems is explored. The influence of oxidising Fe(II) anaerobically with H_2O_2 rather than with DO on Fe(III)-precipitates structure, As(III) co-oxidation, and overall As(III) co-removal is scrutinised in **Chapter 4**. Based on the findings reported in previous chapters, in **Chapter 5**, H_2O_2 dosing and FeEC were coupled in order to treat the As-contaminated groundwater's of Assam (India). Finally, the conclusions and outlook are presented in **Chapter 6**.

References

- Ahmad, A., Cornelissen, E., van de Wetering, S., van Dijk, T., van Genuchten, C., Bundschuh, J., van der Wal, A., & Bhattacharya, P. (2018). Arsenite removal in groundwater treatment plants by sequential Permanganate—Ferric treatment. *Journal of Water Process Engineering*, 26, 221–229. <https://doi.org/10.1016/J.JWPE.2018.10.014>
- Algieri, C., Pugliese, V., Coppola, G., Curcio, S., Calabro, V., & Chakraborty, S. (2022). Arsenic removal from groundwater by membrane technology: Advantages, disadvantages, and effect on human health. *Groundwater for Sustainable Development*, 19, 100815. <https://doi.org/10.1016/J.GSD.2022.100815>
- Alka, S., Shahir, S., Ibrahim, N., Ndejiko, M. J., Vo, D. V. N., & Manan, F. A. (2021). Arsenic removal technologies and future trends: A mini review. *Journal of Cleaner Production*, 278. <https://doi.org/10.1016/J.JCLEPRO.2020.123805>
- Amrose, S. E., Bandaru, S. R. S., Delaire, C., van Genuchten, C. M., Dutta, A., DebSarkar, A., Orr, C., Roy, J., Das, A., & Gadgil, A. J. (2014). Electro-chemical arsenic remediation: Field trials in West Bengal. *Science of the Total Environment*, 488–489(1), 539–546. <https://doi.org/10.1016/j.scitotenv.2013.11.074>
- Annaduzzaman, M., Rietveld, L. C., Hoque, B. A., Bari, M. N., & van Halem, D. (2021). Arsenic removal from iron-containing groundwater by delayed aeration in dual-media sand filters. *Journal of Hazardous Materials*, 411, 124823. <https://doi.org/10.1016/J.JHAZMAT.2020.124823>
- Annaduzzaman, M., Rietveld, L. C., Hoque, B. A., & van Halem, D. (2022). Sequential Fe²⁺ oxidation to mitigate the inhibiting effect of phosphate and silicate on arsenic removal. *Groundwater for Sustainable Development*, 17, 100749. <https://doi.org/10.1016/J.GSD.2022.100749>
- Bandaru, S. R. S., Roy, A., Gadgil, A. J., & van Genuchten, C. M. (2020a). Long-term electrode behavior during treatment of arsenic contaminated groundwater by a pilot-scale iron electrocoagulation system. *Water Research*, 175, 115668. <https://doi.org/10.1016/j.watres.2020.115668>
- Bandaru, S. R. S., van Genuchten, C. M., Kumar, A., Glade, S., Hernandez, D., Nahata, M., & Gadgil, A. (2020b). Rapid and Efficient Arsenic Removal by Iron Electrocoagulation Enabled with in Situ Generation of Hydrogen Peroxide. *Environmental Science and Technology*, 54(10), 6094–6103. <https://doi.org/10.1021/acs.est.0c00012>
- Berg, M., Stengel, C., Trang, P. T. K., Hung Viet, P., Sampson, M. L., Leng, M., Samreth, S., & Fredericks, D. (2007). Magnitude of arsenic pollution in the Mekong and Red River Deltas — Cambodia and Vietnam. *Science of The Total Environment*, 372(2–3), 413–425. <https://doi.org/10.1016/J.SCITOTENV.2006.09.010>
- Bhattacharya, P., Chatterjee, D., & Jacks, G. (1997). Occurrence of Arsenic-contaminated Groundwater in Alluvial Aquifers from Delta Plains, Eastern India: Options for Safe Drinking Water Supply. *International Journal of Water Resources Development*, 13(1), 79–92. <https://doi.org/10.1080/07900629749944>
- Bhattacharya, P., Welch, A. H., Ahmed, K. M., Jacks, G., & Naidu, R. (2004). Arsenic in groundwater of sedimentary aquifers. *Applied Geochemistry*, 19(2), 163–167. <https://doi.org/10.1016/J.APGEOCHEM.2003.09.004>
- Bissen, M., & Frimmel, F. H. (2003). Arsenic — a Review. Part II: Oxidation of Arsenic and its Removal in Water Treatment. *Acta Hydrochimica et Hydrobiologica*, 31(2), 97–107. <https://doi.org/10.1002/AHEH.200300485>
- Bora, A. J., Gogoi, S., Baruah, G., & Dutta, R. K. (2016). Utilization of co-existing iron in arsenic removal from groundwater by oxidation-coagulation at optimized pH. *Journal of Environmental Chemical Engineering*, 4(3), 2683–2691. <https://doi.org/10.1016/J.JECE.2016.05.012>

- Carrard, N., Foster, T., & Willetts, J. (2019). Groundwater as a Source of Drinking Water in Southeast Asia and the Pacific: A Multi-Country Review of Current Reliance and Resource Concerns. *Water* 2019, Vol. 11, Page 1605, 11(8), 1605. <https://doi.org/10.3390/W11081605>
- Chen, M., Hu, H., Chen, M., Wang, C., Wang, Q., Zeng, C., Shi, Q., Song, W., Li, X., & Zhang, Q. (2023). In-situ production of iron flocculation and reactive oxygen species by electrochemically decomposing siderite: An innovative Fe-EC route to remove trivalent arsenic. *Journal of Hazardous Materials*, 441, 129884. <https://doi.org/10.1016/j.jhazmat.2022.129884>
- Chiavola, A., D'Amato, E., Sirini, P., Caretti, C., & Gori, R. (2019). Arsenic Removal from a Highly Contaminated Groundwater by a Combined Coagulation-Filtration-Adsorption Process. *Water, Air, and Soil Pollution*, 230(4), 1–12. <https://doi.org/10.1007/S11270-019-4142-9/TABLES/3>
- Chiavola, Agostina, D'Amato, E., Gavasci, R., & Sirini, P. (2015). Arsenic removal from groundwater by ion exchange and adsorption processes: comparison of two different materials. *Water Supply*, 15(5), 981–989. <https://doi.org/10.2166/WS.2015.054>
- Chung, J. Y., Yu, S. Do, & Hong, Y. S. (2014). Environmental Source of Arsenic Exposure. *Journal of Preventive Medicine and Public Health*, 47(5), 253. <https://doi.org/10.3961/JPPMPH.14.036>
- Crognale, S., Casentini, B., Amalfitano, S., Fazi, S., Petruccioli, M., & Rossetti, S. (2019). Biological As(III) oxidation in biofilters by using native groundwater microorganisms. *Science of the Total Environment*, 651, 93–102. <https://doi.org/10.1016/j.scitotenv.2018.09.176>
- Delaire, C., Amrose, S., Zhang, M., Hake, J., & Gadgil, A. (2017). How do operating conditions affect As(III) removal by iron electrocoagulation? *Water Research*, 112, 185–194. <https://doi.org/10.1016/j.watres.2017.01.030>
- Dixit, S., & Hering, J. G. (2003). Comparison of Arsenic(V) and Arsenic(III) Sorption onto Iron Oxide Minerals: Implications for Arsenic Mobility. *Environmental Science and Technology*, 37(18), 4182–4189. <https://doi.org/10.1021/ES030309T>
- Fang, C., Yang, X., Ding, S., Luan, X., Xiao, R., Du, Z., Wang, P., An, W., & Chu, W. (2021). Characterization of Dissolved Organic Matter and Its Derived Disinfection Byproduct Formation along the Yangtze River. *Environmental Science and Technology*, 55(18), 12326–12336. https://doi.org/10.1021/ACS.EST.1C02378/ASSET/IMAGES/LARGE/ES1C02378_0007.JPEG
- George, C. M., Smith, A. H., Kalman, D. A., & Steinmaus, C. M. (2006). Reverse Osmosis Filter Use and High Arsenic Levels in Private Well Water. *Archives of Environmental & Occupational Health*, 61(4), 171–175. <https://doi.org/10.3200/AEOH.61.4.171-175>
- Gonzalez, B., Heijman, S. G. J., Rietveld, L. C., & van Halem, D. (2019). Arsenic removal from geothermal influenced groundwater with low pressure NF pilot plant for drinking water production in Nicaraguan rural communities. *Science of The Total Environment*, 667, 297–305. <https://doi.org/10.1016/J.SCIOTENV.2019.02.222>
- Gonzalez-Pech, N. I., Molloy, A. L., Zambrano, A., Lin, W., Bohloul, A., Zarate-Araiza, R., Avendano, C., & Colvin, V. L. (2022). Feasibility of iron-based sorbents for arsenic removal from groundwater. *Journal of Chemical Technology & Biotechnology*, 97(11), 3024–3034. <https://doi.org/10.1002/JCTB.7057>
- Goody, D. C., & Darling, W. G. (2005). The potential for methane emissions from groundwaters of the UK. *Science of the Total Environment*, 339(1–3), 117–126. <https://doi.org/10.1016/J.SCIOTENV.2004.07.019>
- Gude, J. C. J., Joris, K., Huysman, K., Rietveld, L. C., & van Halem, D. (2018a). Effect of supernatant water level on As removal in biological rapid sand filters. *Water Research X*, 1. <https://doi.org/10.1016/j.wroa.2018.100013>
- Gude, J. C. J., Rietveld, L. C., & van Halem, D. (2018b). As (III) removal in rapid filters: Effect of pH, Fe (II)/ Fe (III), filtration velocity and media size. *Water research*, 147, 342–349. <https://doi.org/10.1016/j.watres.2018.10.005>

- Gude, J. C. J., Rietveld, L. C., & van Halem, D. (2016). Fate of low arsenic concentrations during full-scale aeration and rapid filtration. *Water Research*, 88, 566–574. <https://doi.org/10.1016/j.watres.2015.10.034>
- Gude, J. C. J., Rietveld, L. C., & van Halem, D. (2017). As(III) oxidation by MnO₂ during groundwater treatment. *Water Research*, 111, 41–51. <https://doi.org/10.1016/j.watres.2016.12.041>
- Gude, J. C. J., Rietveld, L. C., & van Halem, D. (2018c). Biological As(III) oxidation in rapid sand filters. *Journal of Water Process Engineering*, 21, 107–115. <https://doi.org/10.1016/j.jwpe.2017.12.003>
- Guppy, L., Uyttendaele, P., Villholth, K. G., & Smakhtin, V. U. (2018). Groundwater and Sustainable Development Goals: Analysis of Interlinkages. 26. <https://cgspace.cgiar.org/handle/10568/98576>
- Han, M., Zhao, Z. wei, Gao, W., & Cui, F. yi. (2013). Study on the factors affecting simultaneous removal of ammonia and manganese by pilot-scale biological aerated filter (BAF) for drinking water pre-treatment. *Bioresource Technology*, 145, 17–24. <https://doi.org/10.1016/J.BIORTECH.2013.02.101>
- Hesami, F., Bina, B., Ebrahimi, A., & Amin, M. M. (2012). Arsenic removal by coagulation using ferric chloride and chitosan from water. *International Journal of Environmental Health Engineering*, 1(9). <https://doi.org/10.4103/2277-9183.110170>
- Holm, T. R., & Wilson, S. D. (2006). Chemical oxidation for arsenic removal. ISWS Contract Report CR-2006-10.
- Holt, P. K., Barton, G. W., & Mitchell, C. A. (2005). The future for electrocoagulation as a localised water treatment technology. *Chemosphere*, 59(3), 355–367. <https://doi.org/10.1016/j.chemosphere.2004.10.023>
- Hug, S. J., & Leupin, O. (2003). Iron-catalyzed oxidation of Arsenic(III) by oxygen and by hydrogen peroxide: pH-dependent formation of oxidants in the Fenton reaction. *Environmental Science and Technology*, 37(12), 2734–2742. <https://doi.org/10.1021/es026208x>
- International Association of Hydrogeologists (2020) Groundwater— more about the hidden resource. <https://iah.org/education/general-public/groundwater-hidden-resource>.
- Ito, A., Miura, J. I., Ishikawa, N., & Umita, T. (2012). Biological oxidation of arsenite in synthetic groundwater using immobilised bacteria. *Water Research*, 46(15), 4825–4831. <https://doi.org/10.1016/j.watres.2012.06.013>
- Jackman, T. A., & Hughes, C. L. (2010). Formation of Trihalomethanes in Soil and Groundwater by the Release of Sodium Hypochlorite. *Ground Water Monitoring & Remediation*, 30(1), 74–78. <https://doi.org/10.1111/j.1745-6592.2009.01266.x>
- Johnston, R., Heijnen, H., & Wurzel, P. (2001). Safe Water Technology, in United Nations Synthesis Report on Arsenic in Drinking water, World Health Organisation.
- Kamei-Ishikawa, N., Segawa, N., Yamazaki, D., Ito, A., & Umita, T. (2017). Arsenic removal from arsenic-contaminated water by biological arsenite oxidation and chemical ferrous iron oxidation using a down-flow hanging sponge reactor. *Water Science and Technology: Water Supply*, 17(5), 1249–1259. <https://doi.org/10.2166/ws.2017.025>
- Kanel, S. R., Manning, B., Charlet, L., & Choi, H. (2005). Removal of arsenic(III) from groundwater by nanoscale zero-valent iron. *Environmental Science and Technology*, 39(5), 1291–1298. <https://doi.org/10.1021/ES048991U/ASSET/IMAGES/LARGE/ES048991UF00010.JPEG>
- Kapaj, S., Peterson, H., Liber, K., & Bhattacharya, P. (2006). Human health effects from chronic arsenic poisoning - A review. *Journal of Environmental Science and Health - Part A Toxic/Hazardous Substances and Environmental Engineering*, 41(10), 2399–2428. <https://doi.org/10.1080/10934520600873571>

- Katsoyiannis, I. A., Zikoudi, A., & Hug, S. J. (2008). Arsenic removal from groundwaters containing iron, ammonium, manganese and phosphate: A case study from a treatment unit in northern Greece. *Desalination*, 224(1–3), 330–339. <https://doi.org/10.1016/j.desal.2007.06.014>
- Katsoyiannis, I. A., & Zouboulis, A. I. (2004). Application of biological processes for the removal of arsenic from groundwaters. *Water Research*, 38(1), 17–26. <https://doi.org/10.1016/j.watres.2003.09.011>
- Khan, M. M. T., Yamamoto, K., & Ahmed, M. F. (2002). A low cost technique of arsenic removal from drinking water by coagulation using ferric chloride salt and alum. *Water Supply*, 2(2), 281–288. <https://doi.org/10.2166/WS.2002.0074>
- Kim, L., Thanh, N. T., Toan, P. Van, Minh, H. V. T., & Kumar, P. (2022). Removal of Arsenic in Groundwater Using Fe(III) Oxyhydroxide Coated Sand: A Case Study in Mekong Delta, Vietnam. *Hydrology* 2022, Vol. 9, Page 15, 9(1), 15. <https://doi.org/10.3390/HYDROLOGY9010015>
- Kim, M. J., & Nriagu, J. (2000). Oxidation of arsenite in groundwater using ozone and oxygen. *Science of the Total Environment*, 247(1), 71–79. [https://doi.org/10.1016/S0048-9697\(99\)00470-2](https://doi.org/10.1016/S0048-9697(99)00470-2)
- Krishna, M. V. B., Chandrasekaran, K., Karunasagar, D., & Arunachalam, J. (2001). A combined treatment approach using Fenton's reagent and zero valent iron for the removal of arsenic from drinking water. *Journal of Hazardous Materials*, 84(2–3), 229–240. [https://doi.org/10.1016/S0304-3894\(01\)00205-9](https://doi.org/10.1016/S0304-3894(01)00205-9)
- Kumar, P. R., Chaudhari, S., Khilar, K. C., & Mahajan, S. P. (2004). Removal of arsenic from water by electrocoagulation. *Chemosphere*, 55(9), 1245–1252. <https://doi.org/10.1016/j.chemosphere.2003.12.025>
- Lakshmanan, D., Clifford, D., & Samanta, G. (2008). Arsenic Removal by Coagulation With Aluminum, Iron, Titanium, and Zirconium. *Journal - American Water Works Association*, 100(2), 76–88. <https://doi.org/10.1002/J.1551-8833.2008.TB08144.X>
- Li, Y., Bland, G. D., & Yan, W. (2016). Enhanced arsenite removal through surface-catalyzed oxidative coagulation treatment. *Chemosphere*, 150, 650–658. <https://doi.org/10.1016/j.chemosphere.2016.02.006>
- Liang, Y., Ma, R., Nghiem, A., Xu, J., Tang, L., Wei, W., Prommer, H., & Gan, Y. (2022). Sources of ammonium enriched in groundwater in the central Yangtze River Basin: Anthropogenic or geogenic? *Environmental Pollution*, 306, 119463. <https://doi.org/10.1016/j.envpol.2022.119463>
- Lytle, D. A., Chen, A. S., Sorg, T. J., Phillips, S., & French, K. (2007). Microbial As(III) oxidation in water treatment plant filters. *Journal - American Water Works Association*, 99(12), 72–86. <https://doi.org/10.1002/j.1551-8833.2007.tb08108.x>
- Mohan, D., & Pittman, C. U. (2007). Arsenic removal from water/wastewater using adsorbents—A critical review. *Journal of Hazardous Materials*, 142(1–2), 1–53. <https://doi.org/10.1016/J.JHAZMAT.2007.01.006>
- Mohanty, D. (2017). Conventional as well as Emerging Arsenic Removal Technologies—a Critical Review. *Water, Air, & Soil Pollution* 2017 228:10, 228(10), 1–21. <https://doi.org/10.1007/S11270-017-3549-4>
- Mollah, M. Y. A., Morkovsky, P., Gomes, J. A. G., Kesmez, M., Parga, J., & Cocke, D. L. (2004). Fundamentals, present and future perspectives of electrocoagulation. *Journal of Hazardous Materials*, 114(1–3), 199–210. <https://doi.org/10.1016/j.jhazmat.2004.08.009>
- Morrison, C. M., Hogard, S., Pearce, R., Mohan, A., Pisarenko, A. N., Dickenson, E. R. V., von Gunten, U., & Wert, E. C. (2023). Critical Review on Bromate Formation during Ozonation and Control Options for Its Minimization. *Environmental Science and Technology*. https://doi.org/10.1021/ACS.EST.3C00538/ASSET/IMAGES/LARGE/ES3C00538_0006.JPEG
- Moussa, D. T., El-Naas, M. H., Nasser, M., & Al-Marri, M. J. (2017). A comprehensive review of electrocoagulation for water treatment: Potentials and challenges. In *Journal of Environmental Management* (Vol. 186, pp. 24–41). Academic Press. <https://doi.org/10.1016/j.jenvman.2016.10.032>

- Muller, D., Lièvremon, D., Simeonova, D. D., Hubert, J. C., & Lett, M. C. (2003). Arsenite oxidase aox genes from a metal-resistant β -proteobacterium. *Journal of Bacteriology*, 185(1), 135–141. <https://doi.org/10.1128/JB.185.1.135-141.2003>
- Müller, D., Nina Stirn, C., & Veit Maier, M. (2021). Arsenic Removal from Highly Contaminated Groundwater by Iron Electrocoagulation—Investigation of Process Parameters and Iron Dosage Calculation. *Water* 2021, Vol. 13, Page 687, 13(5), 687. <https://doi.org/10.3390/W13050687>
- Neisan, R. S., Saady, N. M. C., Bazan, C., Zendeheboudi, S., Al-nayili, A., Abbassi, B., & Chatterjee, P. (2023). Arsenic Removal by Adsorbents from Water for Small Communities' Decentralized Systems: Performance, Characterization, and Effective Parameters. *Clean Technologies* 2023, Vol. 5, Pages 352–402, 5(1), 352–402. <https://doi.org/10.3390/CLEANTECHNOL5010019>
- Nickson, R. T., Mearthur, J. M., Ravenscroft, P., Burgess, W. G., & Ahmed, K. M. (2000). Mechanism of arsenic release to groundwater, Bangladesh and West Bengal. *Applied Geochemistry*, 15(4), 403–413. [https://doi.org/10.1016/S0883-2927\(99\)00086-4](https://doi.org/10.1016/S0883-2927(99)00086-4)
- Podgorski, J., & Berg, M. (2020). Global threat of arsenic in groundwater. *Science*, 368(6493), 845–850. <https://doi.org/10.1126/science.aba1510>
- Podgorski, J., & Berg, M. (2022). Global analysis and prediction of fluoride in groundwater. *Nature Communications* 2022 13:1, 13(1), 1–9. <https://doi.org/10.1038/s41467-022-31940-x>
- Podgorski, J., Araya, D., & Berg, M. (2022). Geogenic manganese and iron in groundwater of Southeast Asia and Bangladesh – Machine learning spatial prediction modeling and comparison with arsenic. *Science of The Total Environment*, 833, 155131. <https://doi.org/10.1016/J.SCITOTENV.2022.155131>
- Rajendran, R. M., Garg, S., & Bajpai, S. (2021). Economic feasibility of arsenic removal using nanofiltration membrane: A mini review. *Chemical Papers*, 75(9), 4431–4444. <https://doi.org/10.1007/S11696-021-01694-9/TABLES/2>
- Ravenscroft, P., Brammer, H., & Richards, K. (2009). Arsenic Pollution: A Global Synthesis. *Arsenic Pollution: A Global Synthesis*, 1–588. <https://doi.org/10.1002/9781444308785>
- Richardson, S. D., & Plewa, M. J. (2020). To regulate or not to regulate? What to do with more toxic disinfection by-products? *Journal of Environmental Chemical Engineering*, 8(4), 103939. <https://doi.org/10.1016/J.JECE.2020.103939>
- Roberts, L. C., Hug, S. J., Ruettimann, T., Billah, M., Khan, A. W., & Rahman, M. T. (2004). Arsenic Removal with Iron(II) and Iron(III) in Waters with High Silicate and Phosphate Concentrations. *Environmental Science and Technology*, 38(1), 307–315. <https://doi.org/10.1021/es0343205>
- Sancha, A. M. (2006). Review of Coagulation Technology for Removal of Arsenic: Case of Chile. *Journal of Health, Population, and Nutrition*, 24(3), 267. [/pmc/articles/PMC3013246/](https://pubmed.ncbi.nlm.nih.gov/1613246/)
- Santini, J. M., Sly, L. I., Schnagl, R. D., & Macy, J. M. (2000). A new chemolithoautotrophic arsenite-oxidizing bacterium isolated from a gold mine: Phylogenetic, physiological, and preliminary biochemical studies. *Applied and Environmental Microbiology*, 66(1), 92–97. <https://doi.org/10.1128/AEM.66.1.92-97.2000>
- Schmoll, O., Howard, G., Chilton, J., Chorus, I. (2006). *Protecting Groundwater for Health. Managing the Quality of Drinking Water Sources.* World Health Organization, IWA Publishing, London, UK.
- Shaji, E., Santosh, M., Sarath, K. V., Prakash, P., Deepchand, V., & Divya, B. V. (2021). Arsenic contamination of groundwater: A global synopsis with focus on the Indian Peninsula. *Geoscience Frontiers*, 12(3), 101079. <https://doi.org/10.1016/J.GSF.2020.08.015>
- Shankar, S., Shanker, U., & Shikha. (2014). Arsenic contamination of groundwater: A review of sources, prevalence, health risks, and strategies for mitigation. *Scientific World Journal*, 2014. <https://doi.org/10.1155/2014/304524>

- Smedley, P. L., & Kinniburgh, D. G. (2002). A review of the source, behaviour and distribution of arsenic in natural waters. *Applied Geochemistry*, 17(5), 517–568. [https://doi.org/10.1016/S0883-2927\(02\)00018-5](https://doi.org/10.1016/S0883-2927(02)00018-5)
- Smedley, P. L., Zhang, M., Zhang, G., & Luo, Z. (2003). Mobilisation of arsenic and other trace elements in fluviolacustrine aquifers of the Huhhot Basin, Inner Mongolia. *Applied Geochemistry*, 18(9), 1453–1477. [https://doi.org/10.1016/S0883-2927\(03\)00062-3](https://doi.org/10.1016/S0883-2927(03)00062-3)
- Sorlini, S., & Gialdini, F. (2010). Conventional oxidation treatments for the removal of arsenic with chlorine dioxide, hypochlorite, potassium permanganate and monochloramine. *Water Research*, 44(19), 5653–5659. <https://doi.org/10.1016/j.watres.2010.06.032>
- Tseng, W. P. (1977). Effects and dose response relationships of skin cancer and blackfoot disease with arsenic. *Environmental Health Perspectives*, Vol.19, 109–119. <https://doi.org/10.1289/ehp.7719109>
- van Genuchten, C. M., Behrends, T., & Dideriksen, K. (2019). Emerging investigator series: Interdependency of green rust transformation and the partitioning and binding mode of arsenic. *Environmental Science: Processes and Impacts*, 21(9), 1459–1476. <https://doi.org/10.1039/C9EM00267G>
- van Genuchten, Case M., Addy, S. E. A., Peña, J., & Gadgil, A. J. (2012). Removing arsenic from synthetic groundwater with iron electrocoagulation: An Fe and As K-edge EXAFS study. *Environmental Science and Technology*, 46(2), 986–994. <https://doi.org/10.1021/es201913a>
- van Genuchten, Case M., Peña, J., Amrose, S. E., & Gadgil, A. J. (2014). Structure of Fe(III) precipitates generated by the electrolytic dissolution of Fe(0) in the presence of groundwater ions. *Geochimica et Cosmochimica Acta*, 127, 285–304. <https://doi.org/10.1016/J.GCA.2013.11.044>
- van Genuchten, C. M., & Ahmad, A. (2020). Groundwater As Removal by As(III), Fe(II), and Mn(II) Co-Oxidation: Contrasting As Removal Pathways with O₂, NaOCl, and KMnO₄. *Environmental Science & Technology*, 54(23), 15454–15464. <https://doi.org/10.1021/acs.est.0c05424>
- van Genuchten, C. M., Behrends, T., Stipp, S. L. S., & Dideriksen, K. (2020). Achieving arsenic concentrations of <1 µg/L by Fe(0) electrolysis: The exceptional performance of magnetite. *Water Research*, 168, 115170. <https://doi.org/10.1016/j.watres.2019.115170>
- van Genuchten, C. M., & Peña, J. (2017). Mn(II) Oxidation in Fenton and Fenton Type Systems: Identification of Reaction Efficiency and Reaction Products. *Environmental Science and Technology*, 51(5), 2982–2991. <https://doi.org/10.1021/acs.est.6b05584>
- Vries, D., Bertelkamp, C., Schoonenberg Kegel, F., Hofs, B., Dusseldorp, J., Bruins, J. H., de Vet, W., & van den Akker, B. (2017). Iron and manganese removal: Recent advances in modelling treatment efficiency by rapid sand filtration. *Water Research*, 109, 35–45. <https://doi.org/10.1016/J.WATRES.2016.11.032>
- Wan, W., Pepping, T. J., Banerji, T., Chaudhari, S., & Giammar, D. E. (2011). Effects of water chemistry on arsenic removal from drinking water by electrocoagulation. *Water Research*, 45(1), 384–392. <https://doi.org/10.1016/j.watres.2010.08.016>
- Wang, Z., Bush, R. T., & Liu, J. (2013). Arsenic(III) and iron(II) co-oxidation by oxygen and hydrogen peroxide: Divergent reactions in the presence of organic ligands. *Chemosphere*, 93(9), 1936–1941. <https://doi.org/10.1016/j.chemosphere.2013.06.076>
- Welch, A. H., Lico, M. S., & Hughes, J. L. (1988). Arsenic in Ground Water of the Western United States. *Groundwater*, 26(3), 333–347. <https://doi.org/10.1111/J.1745-6584.1988.TB00397.X>
- World Health Organisation. (1993). Guidelines for drinking-water quality. Second Edition. Recommendations: WHO Press.
- Wickramasinghe, S. R., Han, B., Zimbron, J., Shen, Z., & Karim, M. N. (2004). Arsenic removal by coagulation and filtration: comparison of groundwaters from the United States and Bangladesh. *Desalination*, 169(3), 231–244. <https://doi.org/10.1016/J.DESAL.2004.03.013>

- Wilkie, J. A., & Hering, J. G. (1998). Rapid oxidation of geothermal arsenic(III) in streamwaters of the eastern Sierra Nevada. *Environmental Science and Technology*, 32(5), 657–662. <https://doi.org/10.1021/ES970637R/ASSET/IMAGES/LARGE/ES970637RF00005.JPEG>
- Wolthoorn, A. (2003). Subsurface aeration of anaerobic groundwater: iron colloid formation and the nitrification process. Wageningen University and Research.
- Yadav, M. K., Saidulu, D., Gupta, A. K., Ghosal, P. S., & Mukherjee, A. (2021). Status and management of arsenic pollution in groundwater: A comprehensive appraisal of recent global scenario, human health impacts, sustainable field-scale treatment technologies. *Journal of Environmental Chemical Engineering*, 9(3), 105203. <https://doi.org/10.1016/J.JECE.2021.105203>
- Yang, L., Li, X., Chu, Z., Ren, Y., & Zhang, J. (2014). Distribution and genetic diversity of the microorganisms in the biofilter for the simultaneous removal of arsenic, iron and manganese from simulated groundwater. *Bioresource Technology*, 156, 384–388. <https://doi.org/10.1016/J.BIORTECH.2014.01.067>.



Chapter 2

Integrating biological As(III) oxidation with Fe(o) electrocoagulation for As removal from groundwater

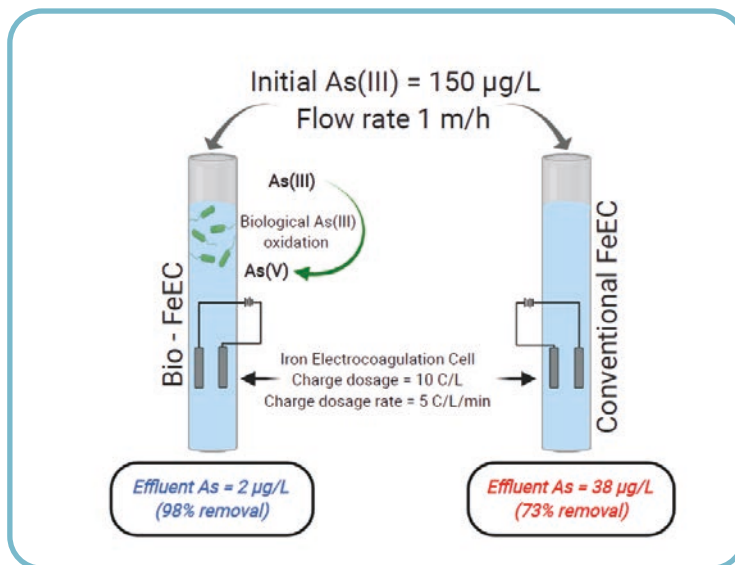


Image created in Biorender

This chapter is based on:

Roy, M., van Genuchten, C. M., Rietveld, L., & van Halem, D. (2021). Integrating biological As (III) oxidation with Fe (o) electrocoagulation for arsenic removal from groundwater.

Water Research, 188, 116531.

Abstract

Arsenic (As) is a toxic element present in many (ground)water sources in the world. Most conventional As removal techniques require pre-oxidation of the neutral arsenite (As(III)) species to the negatively charged arsenate (As(V)) oxyanion to optimise As removal and minimise chemical use. In this work, a novel, continuous-flow As removal system was developed that combines biological As(III) oxidation by bacteria with iron electrocoagulation (FeEC), an Fe(o)-based electrochemical technology that generates reactive Fe(III)-precipitates to bind As. The bio-integrated FeEC system (bio-FeEC) showed effective oxidation and removal of 150 µg/L As(III), without the need of chemicals. To remove As to below the WHO guideline of 10 µg/L, 10 times lower charge dosage was required for the bio-FeEC system compared to conventional FeEC. This lower Fe dosage requirement reduced sludge production and energy consumption. The As(III) oxidising biomass was found to consist of bacteria belonging to *Comamonadaceae*, *Rhodobacteraceae* and *Acidovorax*, which are capable of oxidising As(III) and are common in drinking water biofilms. Characterisation of the As-laden Fe(III)-precipitates by X-ray absorption spectroscopy indicated that both bio-FeEC and conventional FeEC produced precipitates consistent with a mixture of lepidocrocite and 2-line ferrihydrite. Arsenic bound to the precipitates was dominantly As(V), but a slightly higher fraction of As(V) was detected in the bio-FeEC precipitates compared to the conventional FeEC.

Keywords: Arsenic, Electrocoagulation, Drinking Water, Iron, Groundwater

2.1 Introduction

Arsenic (As) contamination of drinking water sources, especially groundwater, has been a major global concern affecting many countries in the world, including Argentina, Bangladesh, Cambodia, China, India, Mexico, the United States and Vietnam. It has been estimated that around 94 to 220 million people worldwide have been exposed to groundwater with toxic As concentrations (Podgorski & Berg, 2020). In water sources, As is mainly present in two inorganic forms: arsenite (As(III)) and arsenate (As(V)) (Wan et al., 2011), with the As(III) species being more toxic and more prevalent in reduced groundwater aquifers than As(V) (Katsoyiannis & Zouboulis, 2004; Nicomel et al., 2015). Chronic exposure to As in drinking water causes various diseases, such as skin, bladder and lung cancers, reproductive disorders and neurodevelopmental disease in children (Kapaj et al., 2006; Tseng, 1977). Hence, it is essential to remove As from contaminated water meant for drinking purposes, with the provisional drinking water guideline of 10 µg/L set by the World Health Organization (WHO) (WHO, 2004).

Many techniques have been proposed to remove As from drinking water, such as coagulation and flocculation, ion exchange, adsorption to activated alumina or iron based sorbents, and reverse osmosis (Feenstra et al., 2007; Mondal et al., 2013). The efficacy of these techniques is improved by pre-oxidation of the neutral As(III) species to the negatively charged As(V) oxyanion ($\text{H}_2\text{AsO}_4^-/\text{HAsO}_4^{2-}$) (Goren et al., 2020; Kim & Nriagu, 2000), which is removed more readily by ion exchange, precipitation, and adsorption (Kumar et al., 2004; Wan et al., 2011). Effective As(III) oxidation can be performed with chemical oxidants, including O_3 , NaClO and KMnO_4 (Kim & Nriagu, 2000; Sorlini & Gialdini, 2010). However, chemical oxidants can be expensive and can generate unwanted by-products (Jackman & Hughes, 2010) that require additional treatment, which increases the cost and complexity of treatment (Katsoyiannis & Zouboulis, 2004). Hence, new methods are needed that can overcome the drawbacks of conventional chemical methods to oxidise and remove As(III).

The biological oxidation of As(III) by arsenic oxidising bacteria (AsOB) is a promising alternative to chemical oxidation because AsOBs do not need auxiliary chemicals to oxidise As(III), which reduces the supply chain and costs of As removal (Kamei-Ishikawa et al., 2017). Native AsOBs have been detected in a wide range of conditions, including in As-contaminated water and sediments (Ito et al., 2012), and are hypothesised to oxidise As(III) as a detoxification or energy generation (for growth) mechanism (Muller et al., 2003; Santini et al., 2000). Recently, biological oxidation of As(III) has also been reported in laboratory and industrial scale rapid sand filter systems, due to growth and accumulation of an AsOB community in filter beds, ripened with As(III) contaminated groundwater (Crognale et al., 2019; Gude et al., 2018; Lytle et al., 2007).

After biological As(III) oxidation, an additional treatment step is subsequently required to remove the dissolved As(V). One low-cost and chemical-free method is Fe(0) electrolysis, also known as iron electrocoagulation (FeEC), which involves in-situ generation of Fe(III)-precipitates to potentially bind As (Holt et al., 2005; Mollah et al., 2004; Moussa et al., 2017). In FeEC, a small electric current is applied to Fe(0) electrodes in contact with contaminated water to generate Fe(II) ions, which are then oxidised by dissolved oxygen (DO) to produce reactive Fe(III)-precipitates with a high As sorption affinity (van Genuchten et al., 2012). After As sorption, the As-laden Fe(III)-precipitates generated by FeEC can be removed by rapid sand filtration or gravitational settling. While FeEC can remove both As(III) and As(V) from water, the removal of As(III) requires substantially more Fe (proportional to charge passed) and treatment time than As(V) (Amrose et al., 2013; Wan et al., 2011). Therefore, pre-oxidising As(III) should be considered to decrease the required energy and amount of produced sludge for equivalent As removal.

In this study, biological As(III) oxidation and FeEC were combined in a continuous flow setup. This type of bio-FeEC system, as per knowledge, has not been demonstrated previously, but has the potential to substantially reduce Fe sludge production and energy consumption. We evaluated the As removal efficacy of bio-integrated FeEC and conventional FeEC in view of the biological conversion of dissolved As(III) and the molecular-scale structure and As uptake mechanism of the generated Fe(III)-precipitates.

2.2 Materials and methods

2.2.1 Chemicals

Dutch non-chlorinated, tap water (characteristics in Table S2.1) was used as the model water for all experiments. Both As(III) and As(V) were added to the tap water from As(III) and As(V) stock solutions that were prepared by dissolving defined amounts of sodium (meta)arsenite (NaAsO_2) or sodium arsenate dibasic heptahydrate ($\text{Na}_2\text{HAsO}_4 \cdot 7\text{H}_2\text{O}$) (Sigma-Aldrich) to 18.2 m Ω .cm ultrapure water. The pH of the experimental solutions was adjusted with NaOH or H_2SO_4 (Merck Millipore) and the water conductivity was increased to 1200 ± 300 $\mu\text{S}/\text{cm}$ by adding NaCl (Sigma-Aldrich).

2.2.2 Experimental setup

2.2.2.1 FeEC batch reactor

Batch FeEC experiments were conducted to understand the impact of charge dosage (CD), charge dosage rate (CDR), and initial As oxidation state on As removal, which

informed the selection of operating parameters during the pilot-scale continuous flow experiments. The FeEC batch reactor consisted of a 1 L glass beaker containing 0.8 L As solution (tap water spiked with As(III) or As(V)) and two Fe electrodes (one cathode and one anode, Steel S235) in contact with the solution (Fig. 2.1(A)). The electrodes had dimensions of 50 mm x 20 mm x 0.5 mm, with a total submerged surface area of 12 cm² each and an inter-electrode gap of 1 cm. Before experiments, the electrodes were immersed in 0.01 M H₂SO₄ for 2 min and abraded with sand paper to remove any scale and rinsed with demineralised water. The electrodes were connected to a direct current (DC) power supply (TENMA® 72-10500) to generate the Fe(III)-precipitates. The initial pH of the solution in all experiments was measured using a multimeter (WTW™ MultiLine™ Multi 3630 IDS) and was maintained between 7.0-8.0 by manual additions of 0.01 M H₂SO₄ and 0.1 M NaOH. In all FeEC batch experiments, the solutions were stirred using a magnetic stirrer (LABINCO L23) at 150 rpm. The initial DO was measured between 8.0-9.0 mg/L using the multimeter.

In FeEC, the As removal efficacy depends on the amount of Fe generated in the solution and the rate at which it is generated (Amrose et al., 2013). The amount and rate of Fe generated is proportional to the CD, (*q* in C/L) and CDR, (*dq/dt* in C/L/min) by Faraday's law (eq. 2.1 and 2.2).

$$W = \frac{qM}{nF} = \frac{itM}{nFV} \quad (2.1)$$

$$\frac{dq}{dt} = \frac{i}{V} \quad (2.2)$$

where, *W* = amount of dissolved electrode material (mg/L); *i* = current (mA); *t* = electrolysis time (min); *M* = molecular weight of Fe (mg/mol) = 55845; *F* = Faraday's constant (96485 C/mol); *n* = number of transferred electrons (2 for Fe); *V* = solution volume (L).

The batch experiments were performed by applying a range of CD and CDRs to tap water containing 150 µg/L As(III) or As(V). Table 2.1 shows the applied CD and CDRs for the batch experiments along with the corresponding electrolysis time, applied current, and the theoretical amount of Fe generated by Faraday's law. To determine As removal for a given CD, water samples were collected before and after EC (without additional mixing time or precipitate settling) and analysed for total As and Fe, as well as aqueous As(III) and As(V).

Table 2.1. List of operational parameters varied during FeEC batch experiments

| CD | CDR | EC Time | Solution Volume | Applied Current | Theoretical Fe conc. |
|-------|-----------|---------------|-----------------|-----------------|----------------------|
| (C/L) | (C/L/min) | (min) | (L) | (Ampere) | (mg/L) |
| 10 | 5/15/60 | 2/0.67/0.17 | 0.8 | 0.07/0.2/0.8 | 2.90 |
| 25 | 5/15/60 | 5/1.67/0.42 | 0.8 | 0.07/0.2/0.8 | 7.26 |
| 50 | 5/15/60 | 10/3.33/0.83 | 0.8 | 0.07/0.2/0.8 | 14.51 |
| 100 | 5/15/60 | 20/6.67/1.67 | 0.8 | 0.07/0.2/0.8 | 29.02 |
| 150 | 5/15/60 | 30/10/2.50 | 0.8 | 0.07/0.2/0.8 | 43.53 |
| 200 | 5/15/60 | 40/13.33/3.33 | 0.8 | 0.07/0.2/0.8 | 58.04 |

2.2.2.2 Biological filter columns

Biological filter columns were used to establish an As(III) oxidising microbial community in the filter beds, through ripening with As(III) water. The setup consisted of two duplicate down flow cylindrical columns (2 m high, 9 cm diameter, made from PVC) containing an anthracite layer (size fraction = 2.0 - 4.0 mm), coarse sand layer (size fraction = 1.4 - 2.0 mm), and garnet layer (size fraction = 0.3 - 0.6 mm), each 30 cm high (Fig. 2.1(B)). Before the experiments, the columns were backwashed with tap water until the supernatant was visually clear. The columns were then loaded continuously with tap water spiked with 150 µg/L As(III) for 49 days at a flow rate of 1 m/h to establish the oxidising biomass. A supernatant level of 40 cm was maintained above the anthracite bed. The development of As(III) oxidation in the columns was monitored by measuring As speciation in the influent and effluent at 7 day intervals.

After ripening, column effluents from both columns were taken from the bottom location of the anthracite bed (As speciation showed >95% oxidation of 150 µg/L influent As(III) in the anthracite bed at 49 days) and FeEC was applied in batch mode. These separate experiments were performed to verify the performance of FeEC in solutions where As(III) was oxidised biologically and to determine the minimum CD (i.e., Fe dosage) required to remove 150 µg/L oxidised As(V) below 10 µg/L.

2.2.2.3 Bio-FeEC system

After performing the FeEC batch experiments and establishing the As(III) oxidising biomass, the integrated bio-FeEC set-up was assembled. The setup for the bio-FeEC system consisted of a similar down flow column as described in section 2.2.2.2, augmented with an FeEC electrochemical cell. The column contained the ripened anthracite layer (containing oxidising biomass) at the top followed by an FeEC cell,

consisting of two Fe-electrodes (60 mm x 30 mm x 0.5 mm) connected to the DC power supply. The bottom of the column contained sand layers to collect the generated Fe(III)-precipitates during FeEC (Fig. 2.1(C)). An identical control FeEC flow-through system was created that consisted of only a conventional FeEC cell without a biological oxidation pre-layer (Fig. 2.1(C)). Tap water spiked with 150 µg/L As(III) was introduced to both systems at 1 m/h.

The bio-FeEC and conventional FeEC systems were run for 3 days, with an experimental run time of 6 hours each day during which the FeEC cell was operated. After 6 hours, the current applied to the FeEC cell was stopped and the As(III)-spiked tap water was allowed to flow through the columns continuously. After 3 days, the two systems were backwashed to collect the As-laden Fe(III)-precipitates that were trapped in the bottom sand layers for molecular-scale characterisation by Fe and As K-edge X-ray absorption spectroscopy (XAS). For both column systems, the As removal efficacy was determined over the 6 hour operating cycles by measuring the difference in dissolved As concentrations at the influent and just above the lower sand layers.

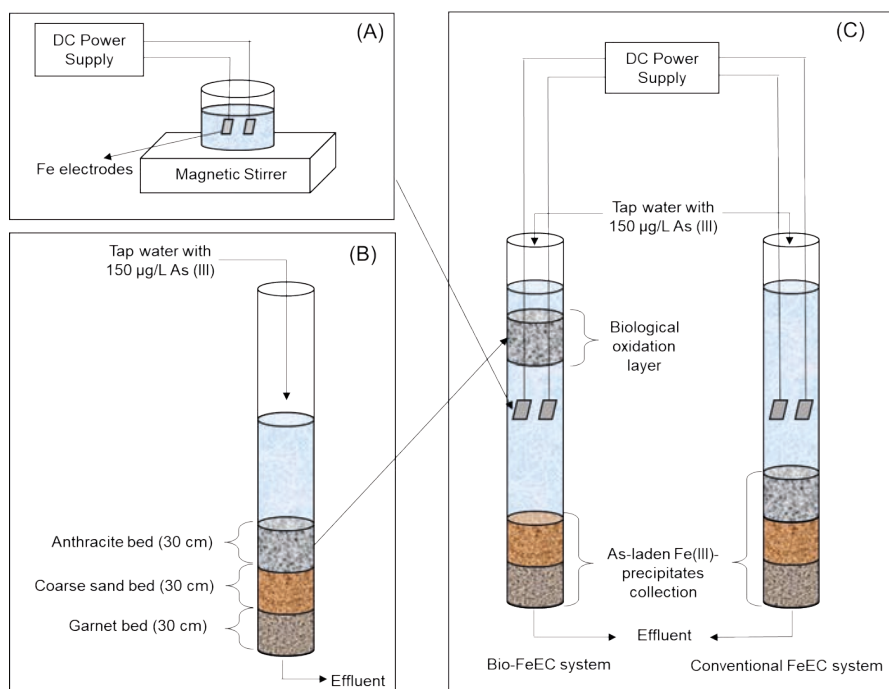


Fig. 2.1. Schematic diagram of the various experimental setups: batch FeEC experiments (A), biological column experiment (B), and integrated bio-FeEC and conventional FeEC systems (C) used during this study.

2.2.3 Chemical analysis

Water samples (in triplicates) were collected (1) unfiltered, (2) filtered over 0.45 μm polystyrenesulfone filters (Macherey-Nagel GmbH & Co. KG), and (3) filtered over 0.45 μm filters and an anionic resin (for As speciation). After collection, the samples were acidified using ultrapure nitric acid (ROTIPURAN® Ultra 69%) to dissolve any Fe(III)-precipitates. The samples were then stored at 4°C before analysis for total As and Fe, as well as aqueous As(III) and As(V) by inductively coupled plasma mass spectrometry (ICP-MS, Analytikal Jena model PlasmaQuant MS). For As speciation, an anionic exchange resin (Amberlite* IRA-400 chlorite form resin) was used following the Clifford method as explained in Gude et al. (2018).

2.2.4 X-ray absorption spectroscopy

Precipitates for Fe and As K-edge XAS analysis were obtained by backwashing the bio-FeEC and conventional FeEC columns and filtering the backwashed water with filter papers. The filter papers containing the precipitates were then stored at -80°C before preparation for XAS analysis. Fe and As K-edge XAS data were collected at beam line 2-2 of the Stanford Synchrotron Radiation Lightsource (SSRL, Menlo Park, USA). Fe K-edge XAS data were recorded at room temperature out to k of 13 \AA^{-1} and As K-edge XAS data were recorded at liquid nitrogen temperatures ($\approx 80^\circ\text{K}$) in fluorescence mode out to k of 14 \AA^{-1} . Beam calibration was performed by setting the maximum of the first derivative of Fe(O) to 7112 eV or Au(O) to 11919 eV for Fe and As K-edge XAS data, respectively. The SixPack software was used for spectral alignment, averaging and background subtraction (Webb, 2005), following standard procedures (van Genuchten et al., 2012). The EXAFS spectra were extracted using k^3 -weighting and were Fourier-transformed using a Kaiser-Bessel window with dk of 3 \AA^{-1} over the k -range 2 to 11 \AA^{-1} for Fe data or 2 to 13 \AA^{-1} for As data.

The As K-edge XAS data were analysed by linear combination fits (LCFs) of the XANES spectra and shell-by-shell fits of the EXAFS spectra using the SixPack software. The LCFs were performed over the energy range of 11860 to 11880 eV using reference spectra of As(III) and As(V) adsorbed to two line ferrihydrite (2LFh), which were collected previously at beam line 4-1 of SSRL under similar conditions as the current data set. The shell-by-shell fits were performed in $R+\Delta R$ -space based on algorithms derived from IFEFFIT (Newville, 2001). Theoretical phase and amplitude functions for single and multiple scattering paths used in the fits were calculated using FEFF6 (Rehr et al., 1992) and were derived from the structure of scorodite (Kitahama et al., 1975). Additional details on XAS sample preparation and data collection and the shell-by-shell fitting procedure are provided in the appendix (section S2.1).

2.2.5 Microbial characterisation

To characterise the As(III) oxidising biomass that grew and accumulated in the biological sand filters due to ripening with As(III)-rich water, a set of duplicate up-flow biological sand columns (1 m x 4 cm diameter, PVC) containing quartz filter sand (size fraction = 0.7 to 1.25 mm; bed height = 75 cm) was ripened with tap water containing 100 µg/L As(III) for a period of 60 days (Fig. S2.1). After establishing the oxidising biomass on the sand bed, sand samples (100 ml) were taken for DNA extraction at the bottom (15 cm) of the columns (location of influent) to characterise the biomass by high-throughput sequencing (HTS) of 16S rRNA genes.

Total genome DNA of the biomass on the sand samples was extracted using CTAB/SDS method. The concentration and purity of the DNA was monitored on 1% agarose gels and the DNA was diluted to 1 ng/µL using sterile water depending on the concentration. The bacterial 16s rRNA genes were amplified using specific primer and the PCR reactions were carried out with a Phusion® High-Fidelity PCR Master Mix (New England Biolabs). The PCR products were mixed with same volume of 1X loading buffer to operate electrophoresis on 2% agarose gel for detection. Samples with a bright main strip between 400-450 bp were considered for further analysis. The PCR products were then mixed in equidensity ratios and purified using Qiagen Gel Extraction Kit (Qiagen, Germany). NEBNext® Ultra™ DNA Library Pre Kit (Illumina) was then used to generate sequencing libraries. The library quality was assessed on the Qubit® 2.0 Fluorometer (Thermo Scientific) and Agilent Bioanalyzer 2100 system and sequenced on an Illumina platform to generate 250 bp paired-end reads. Paired-end reads were merged using FLASH (V1.2.7) (Magoč et al., 2011) to generate raw tags on which quality filtering was performed according to the QIIME(V1.7.0) (Caporaso et al., 2010) to generate high-quality clean tags. The tags were then compared with the reference Gold database using the UCHIME algorithm (Edgar et al., 2011) to obtain effective tags by detecting and removing chimera sequences.

Uparse software (Uparse v7.0.100) (Edgar, 2013) was used for sequence analysis and sequences with ≥97% similarity were assigned to the same Operational Taxonomic Units (OTUs). To obtain taxonomic information the representative sequence for each OTU was annotated by the RDP classifier (Version 2.2) (Wang et al., 2007) algorithm using GreenGene Database (Desantis et al., 2006).

2.3 Results and discussion

2.3.1 As removal in FeEC batch experiments

In order to understand the dependency of As(V) and As(III) removal on different FeEC operational parameters in the specific test water matrix, batch FeEC experiments were conducted. Fig. 2.2 shows the changes in dissolved As(III) and As(V) concentrations over the various applied CD values (0 to 200 C/L) at a CDR of 15 C/L/min. It was observed that as the CD increased, the dissolved As concentration decreased, which is consistent with previously reported FeEC batch studies (Amrose et al., 2013; Delaire et al., 2017; Goren et al., 2020; van Genuchten et al., 2012; Wan et al., 2011). The concentration of total Fe increased linearly with CD and matched the theoretical Fe concentration based on Faraday's law (eq. 2.1), (i.e., Faradaic efficiency = 1) (Müller et al., 2019). At CD values of 100 C/L and above (i.e., Fe dosages > 29 mg/L or Fe:As > 260 (mol:mol)), the dissolved As level decreased below the WHO guideline of 10 µg/L regardless the initial As oxidation state, and reached as low as ≤ 2 µg/L for CDs of 150 and 200 C/L. Since As removal in FeEC occurs via sorption to co-precipitated Fe(III)-precipitates (Kobya et al., 2016), the enhanced As removal at increasing CD can be explained by a higher concentration of Fe(III)-precipitates and the corresponding availability of more As sorption sites.

Although both As(III) and As(V) removal was observed in FeEC batch experiments, solutions initially containing As(V) required a lower CD (10 C/L or Fe:As = 26 (mol:mol)) than As(III) (100 C/L or Fe:As = 260 (mol:mol)) to meet the WHO guideline of 10 µg/L. This result can be explained by the higher affinity of the generated Fe(III)-precipitates for As(V) than As(III) (Roberts et al., 2004).

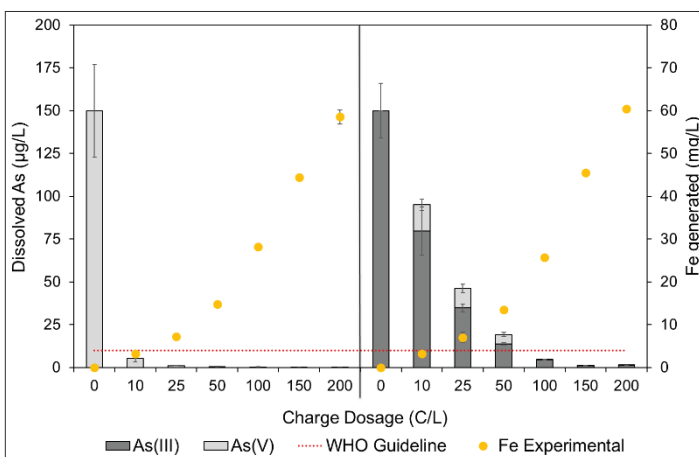


Fig. 2.2. Dissolved As concentration after FeEC in batch mode by applying various CD (0 to 200) C/L at 15 C/L/min CDR in tap water containing 150 µg/L As(V) (left) and As (III) (right) as initial As species.

With As(III) as the initial species, the oxidation to As(V) in solution was observed for CD values of 10, 25 and 50 C/L, which is consistent with the formation of reactive intermediates during FeEC operation that oxidise As(III) to As(V) (van Genuchten et al., 2012). At higher CD, dissolved As(V) was not observed, which can be explained by the presence of excess Fe leading to complete adsorption of dissolved As(V) (Dixit & Hering, 2003; Raven et al., 1998). When CDR was varied, slightly more effective As(III) removal was observed at the lowest CDR of 5 C/L/min (Fig. S2.2 and S2.3), consistent with previous work (Delaire et al., 2017; Li et al., 2012).

2.3.2 Biological As(III) oxidation in filter columns

The As speciation in the effluent of the duplicate down-flow biological filter columns over the experimental period of 49 days is shown in Fig. 2.3. At the start of this ripening stage (day 1 to 28), 30±10% of the influent As(III) was recovered in the filtrate. However, by 35 days, complete oxidation of 150 µg/L As(III) developed in the columns, which remained stable until the end of the experiment. The pH, DO, electrical conductivity, and temperature were steady during the experimental period at 7.5±0.5, 8±1 mg/L, 300±100 µS/cm and 20±2°C, respectively. Also, it must be noted that the total As concentration in the effluent was consistently lower (3 to 26%) than in influent, indicating adsorption to the fresh filter materials (anthracite, sand and garnet). On day 49, additional samples were collected for As speciation after the anthracite layer, revealing that >95% of As(III) was oxidised in the top layer. Therefore, this 30 cm layer was considered suitable for biological pre-treatment and was shifted upward prior to FeEC for follow-up experiments.

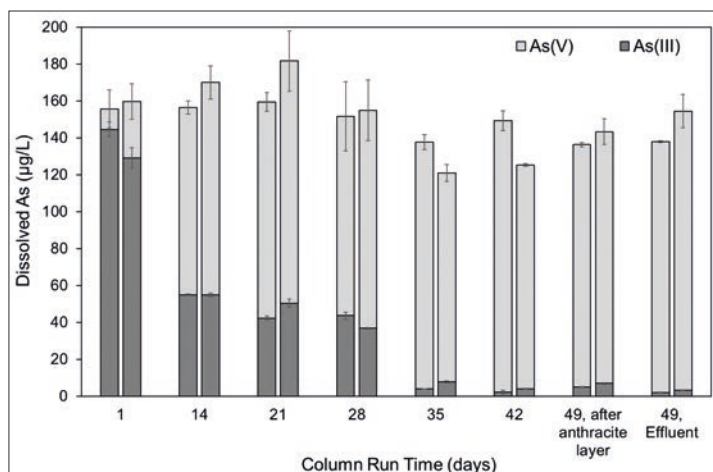


Fig. 2.3. As(III) and As(V) concentrations in the effluent of the duplicate biological filter columns during 49 days ripening with 150±30 µg/L As(III) spiked tap water.

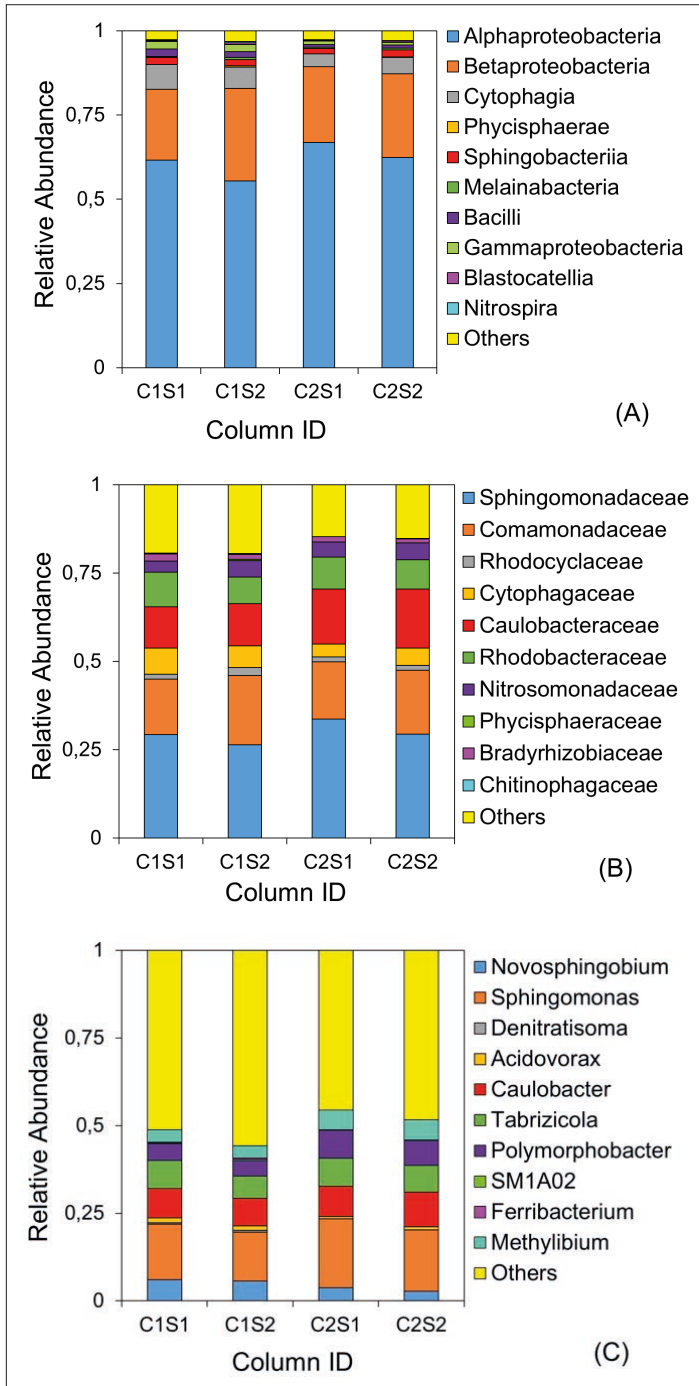


Fig. 2.4. Relative abundance (% of total OTUs) of the predominant bacterial communities in the accumulated As(III) oxidising biomass of the duplicate up-flow biological columns at class **(A)**, family **(B)** and genus **(C)** level. (C1, C2 = 2 columns; S1, S2 = duplicate sand samples from each column)

A similar As(III) oxidation pattern was observed in the two up-flow columns, which were used for characterisation of the accumulated As(III) oxidising biomass (Fig. S2.4). High-throughput sequencing (HTS) of the biomass DNA generated OTUs of 730 and 811, and 609 and 562 from duplicate samples of each column, respectively. Fig. 2.4(A) depicts the relative abundance (RA) (percentage of total OTUs) of the top 10 classes, which accounted for more than 97% of the entire biomass in each sample. *Alphaproteobacteria* and *Betaproteobacteria* were the two most abundant classes in the two columns having a RA of 55 to 67% and 21 to 28%, respectively, which is in agreement with findings of Cavalca et al. (2013). Both of these classes belong to the most abundant phylum *Proteobacteria* (Fig. S2.5). Furthermore, classification at the family level showed the presence of microorganisms affiliated with *Comamonadaceae* (RA: 15 to 20%; Class: *Betaproteobacteria*) and *Rhodobacteraceae* (RA: 7.5 to 10%; Class: *Alphaproteobacteria*) (Fig. 2.4(B)), which are known to oxidise As(III) (Crognale et al., 2019). Additionally, the As(III) oxidising genus *Acidovorax* (RA: 0.6 to 1.4%) in the *Comamonadaceae* family was also observed (Fig. 2.4(C)), which is a genus that is common in the rapid sand filters of drinking water treatment plants treating As-free water (Vandermaesen et al., 2017), but that also oxidise As(III) (Cavalca et al., 2013). While As(III) oxidising biomass is commonly reported in sand filters for groundwater treatment (Crognale et al., 2019; Gude et al., 2018; Katsoyiannis & Zouboulis, 2004), the results indicate that a similar As(III) oxidising biomass can also develop in sand filters running on chlorine-free tap water, sourced from a surface water body.

2.3.3 As(III) removal by bio-FeEC

2.3.3.1 Batch experiments

After ripening of the biological columns, batch FeEC experiments were performed on the column effluent, which contained 150 µg/L As(V), to determine the optimal operational parameters for the continuous flow experiments. Fig. 2.5 shows the change in dissolved As(III) and As(V) concentrations after applying various CDs (0 to 200 C/L) at a CDR of 5 C/L/min to the column effluent and to an unoxidised As(III)-spiked tap water solution for reference. The As removal in the column effluent was similar to that of the FeEC experiment using tap water containing As(V) as the initial As species (Fig. S2.2 (left)). For FeEC experiments in both the biological column effluent and the As(V) solution, a CD of 10 C/L (at CDR of 5 C/L/min) was able to remove 150 µg/L As to below the 10 µg/L WHO guideline, whereas a CD of 100 C/L was needed to achieve the same level with the reference As(III) solution.

The Faradaic efficiency for the FeEC experiments in the column effluents containing oxidised As(V) was near 1, which was similar to the values obtained for FeEC

experiments in standard As(V) solution (Fig. S2.2 (left)). This result suggests that biological As(III) oxidation did not impact the electrochemical oxidation of Fe(O) and the release of Fe(II) to the bulk solution.

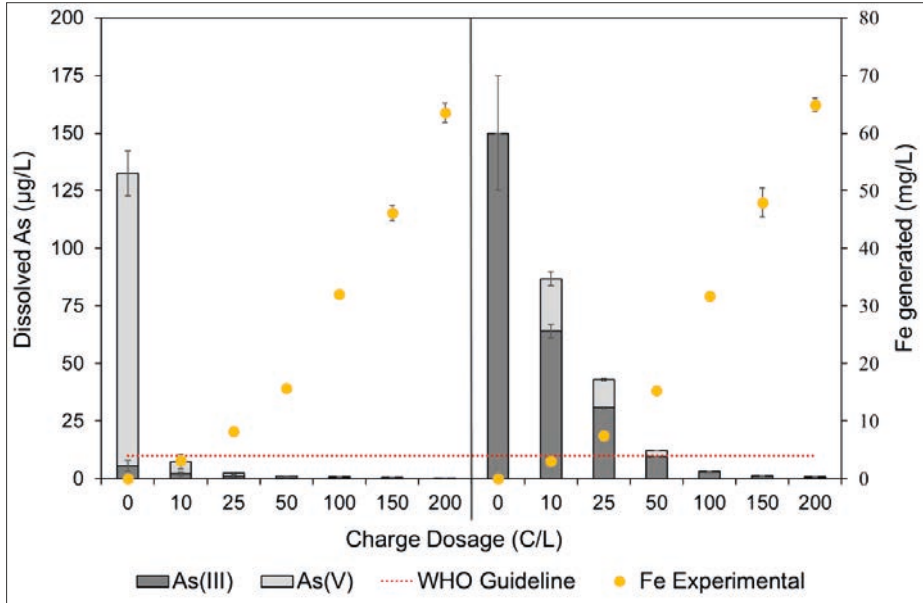


Fig. 2.5. Batch mode bio-FeEC (left) and conventional FeEC (right) treatment of 150 µg/L As(III) as a function of CD applied at 5 C/L/min CDR. The bio-FeEC experiments were conducted with the effluent of the biological anthracite layer; the conventional FeEC experiments are shown again in Fig. S2.2 (right).

2.3.3.2 Continuous flow experiments

The operating parameters of CD = 10 C/L applied at CDR = 5 C/L/min were selected for the continuous flow bio-FeEC experiments based on the results from the batch EC experiments using the biological column effluent. The voltage observed in the DC current supplier to achieve the required CD and CDR in both column systems was 2.1 V. Fig. 2.6 depicts the results during the 3 day experimental duration for both the bio-FeEC (left) and the conventional FeEC (right) continuous flow systems. The results indicate that both systems removed As, but only the bio-FeEC system was able to decrease As levels to below the WHO guideline of 10 µg/L, despite identical operating parameters (i.e. flow rate, CD, CDR). In the bio-FeEC system, the dissolved As concentration decreased from 150 ± 30 µg/L to approximately 2 ± 1 µg/L (98% removal). The dissolved As concentration was consistently higher than the WHO guideline in the conventional FeEC system, with approximately 38 ± 4 µg/L remaining in solution (73% removal), which consisted of 75±5% As(III).

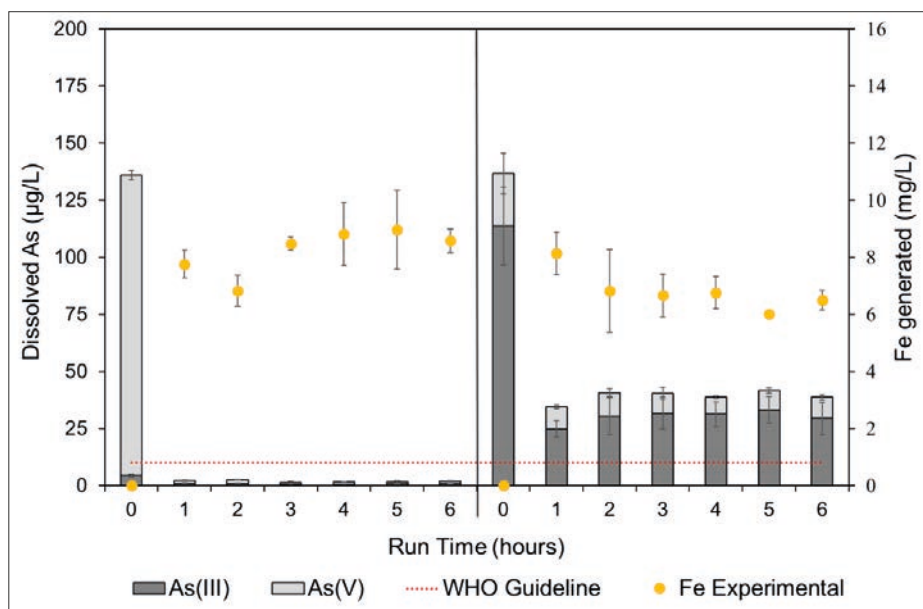


Fig. 2.6. Average As(III) removal during continuous flow mode bio-FeEC (left) and conventional FeEC (right) during 6 hours experimental run time (executed in triplicate). FeEC was operated under 10 C/L CD at 5 C/L/min CDR.

It was also observed that the As(III) removal efficacy of the conventional FeEC column was higher (73% As removal) than the FeEC batch experiments using the As(III)-spiked tap water (42% As removal), despite the similar operating parameters (CD = 10 C/L and CDR = 5 C/L/min). This result can be explained by the accumulation of Fe(III)-precipitates on top of the supporting filter layers in the continuous flow system. This explanation is based on the measured total Fe concentration of approximately 7 mg/L in unfiltered samples of the conventional FeEC column system, which is greater than the theoretical Fe value of 3 mg/L (eq. 2.1) expected based on Faraday's law. The accumulated Fe(III)-precipitates allow for extended contact time with dissolved As, resulting in greater As adsorption per Fe mass. Although the Fe concentration was also significantly higher than the theoretical Faradaic value in the bio-FeEC column, no difference in As removal per charge passed was observed in the bio-FeEC because of the nearly complete removal of the oxidised As(V). However, the accumulation of Fe in both continuous flow systems suggests that the bio-FeEC column could be operated at even lower CD and still achieve As(III) removal to below 10 µg/L.

2.3.4 Characterisation of As-laden Fe(III)-precipitates

After the 6 h operating cycles over the 3-day experimental duration, the filter columns were backwashed and the precipitates were characterised by Fe and As K-edge XAS

(Fig. 2.7). The Fe K-edge EXAFS spectra showed no notable difference in line shape or phase of the oscillations for samples collected from the bio-FeEC and conventional FeEC columns, indicating a similar average structure of the generated Fe(III)-precipitates. Based on characteristic fingerprints in the EXAFS spectra, including the asymmetric first oscillation from 3 to 5.5 Å⁻¹, the precipitates are consistent with a mixture of lepidocrocite (Lp) and poorly-ordered Fe(III)-precipitates (e.g. 2-line ferrihydrite (2LFh)) (Fig. 2.7(A)). The formation of a mixture of Lp and 2LFh can be attributed to the composition of the As(III)-rich tap water (Table S2.1) and is consistent with precipitates formed in previous FeEC studies at similar pH and total As/Fe ratios (van Genuchten et al., 2014; Wan et al., 2011). Previous studies on Fe oxidising bacteria have shown that Fe(III)-precipitates produced by various types of bacteria often have unique structures because biogenic dissolved organic compounds can interfere with Fe(III) (oxyhydr)oxide crystallisation pathway (Toner et al., 2009). However, the Fe K-edge EXAFS spectra of Fe(III)-precipitates from both systems were similar, indicating that the bacteria upstream of the FeEC cell did not interfere with Fe(III) polymerisation. Instead, the inorganic composition of the solution played a more important role in determining the Fe(III)-precipitates structure. The formation of poorly-ordered precipitates, such as 2LFh, in the bio-FeEC and conventional FeEC system can be advantageous for As adsorption because of their higher proportion of reactive surface area per mass (i.e. specific surface area) compared to more crystalline Fe phases (Dixit & Hering, 2003).

The As K-edge XANES data for samples collected from the bio-FeEC and conventional FeEC systems indicate that the oxidation state of As bound to the precipitates was predominantly As(V) for both systems based on the position of the absorption maximum near 11875 eV (Fig. 2.7(B) and (C)). The predominance of solid-phase As(V) in the conventional FeEC system is in line with the oxidation of As(III) during FeEC due to the formation of reactive intermediates (Li et al., 2012; van Genuchten et al., 2012). Although As(V) was the major species inbound to both bio-FeEC and conventional FeEC precipitates, the LCFs of the XANES spectra indicated a slightly higher As(III) percentage for precipitates in the conventional FeEC system (8%) compared to those of the bio-FeEC system (2%). These results confirm that the As removal pathway for both columns involved As(III) oxidation. However, unlike the bio-FeEC system, the abiotic As(III) oxidation pathway of the conventional FeEC column was not sufficient to oxidise all As(III). Consequently, As(III) was observed bound to the Fe(III)-precipitates of the conventional FeEC column and was the dominant form of As in effluent, which was substantially higher (38±4 µg/L) than the bio-FeEC system (2±1 µg/L).

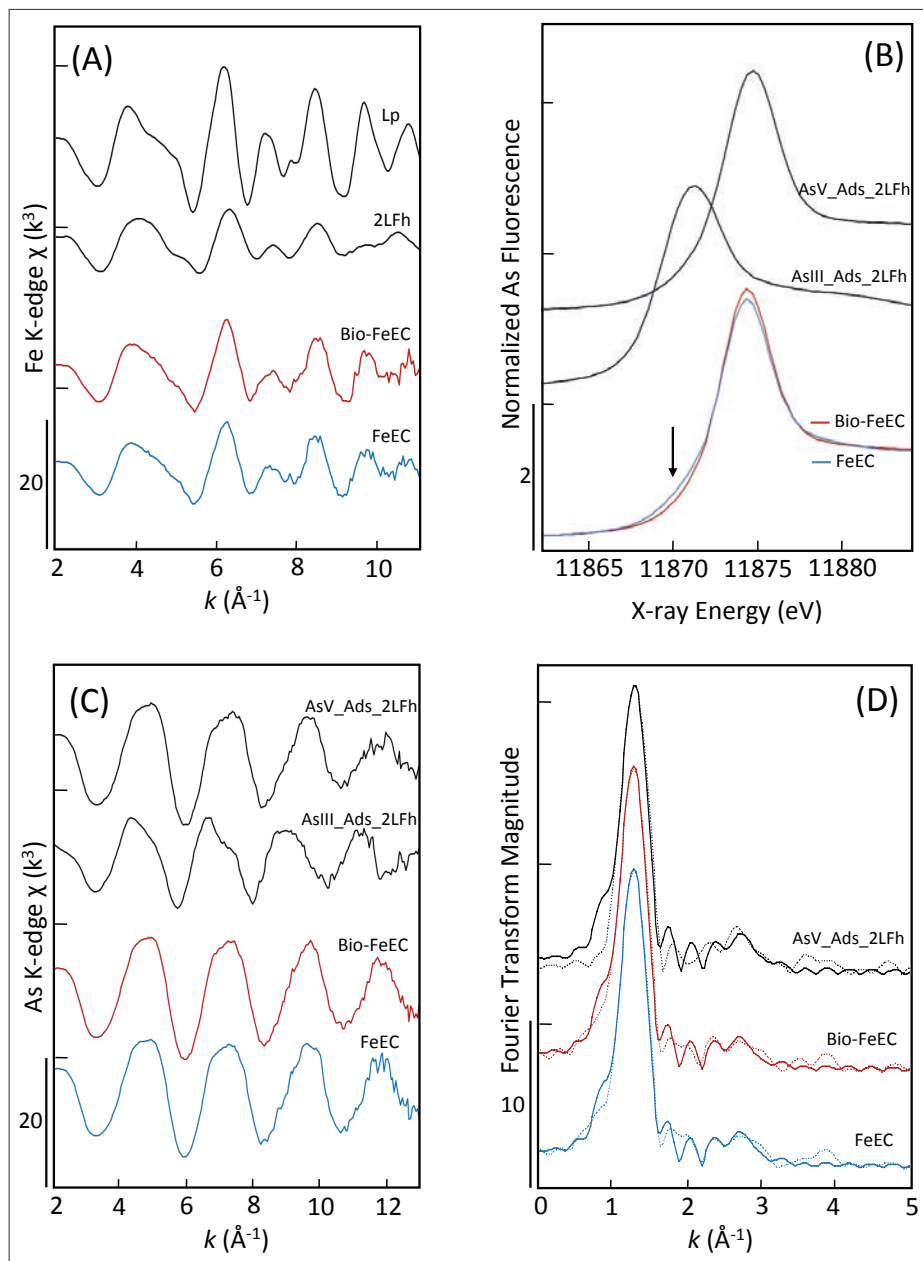


Fig 2.7. (A) Fe K-edge EXAFS spectra of the precipitates produced in the bio-FeEC and conventional FeEC columns plotted below reference spectra of lepidocrocite (Lp) and 2-line ferrihydrite (2LFh). (B) As K-edge XANES spectra of the precipitates produced in the bio-FeEC and conventional FeEC columns plotted below reference spectra of As(III) and As(V) adsorbed to 2LFh. The arrow in B highlights a small shoulder indicative of As(III). (C) As K-edge EXAFS spectra of samples compared to the reference spectra of As(III) and As(V) adsorbed to 2LFh. (D) Fourier-transformed As K-edge EXAFS spectra (data in dotted lines) and output of the shell-by-shell fits (model output in solid lines).

The As K-edge EXAFS spectra of the precipitates collected from both continuous flow systems were similar, consistent with the As K-edge XANES data, and both matched the reference spectrum of As(V) adsorbed to 2LFh. To confirm the exact As bonding mode to the Fe(III)-precipitates in both systems, shell-by-shell fits of the Fourier-transformed EXAFS spectra were performed. The output of the fits is overlain to the data in Fig. 2.7(D) and the fitting parameters are summarised in Table S2.2. The fitting results were identical for both conventional FeEC and bio-FeEC samples within fit-derived standard errors, indicating a similar As uptake mode. The fitting output for both samples also matched that of the reference spectrum of As(V) adsorbed 2LFh. The first shell fits of the samples returned values for the As-O coordination number (CN_{As-O}) of 4.3 to 4.6 and As-O interatomic distance (R_{As-O}) of 1.69 Å, which is consistent with tetrahedrally-coordinated As(V) (Waychunas et al., 1993). The second shell fits of both samples yielded CN_{As-Fe} values of 1.4 to 1.6 and an R_{As-Fe} of 3.28 Å, which was identical to the fits of As(V) adsorbed to 2LFh, within fit-derived standard errors (Table S2.2). Based on these fit-derived parameters, we conclude that As was taken up by the precipitates produced in both bio-FeEC and conventional FeEC systems via the binuclear corner-sharing (2C) surface complex, where As(V) tetrahedra bind to the apical oxygen atoms of two adjacent edge-sharing FeO_6 octahedra (van Genuchten et al., 2012; Waychunas et al., 1993). We noted that the XANES LCFs revealed a slightly larger fraction of As(III) in the conventional FeEC sample that was not reflected in the shell-by-shell fitting results, which can be explained by the higher sensitivity of XANES analysis to small changes in As oxidation state. Therefore, the conclusions obtained with shell-by-shell fits of the EXAFS data did not account for the additional complexity of the FeEC precipitates, which contained 8% sorbed As(III).

2.3.5 Benefits and challenges of bio-FeEC

Our results indicate that integrating biological As(III) oxidation with FeEC can be advantageous to treat As(III) contaminated water because of the lower Fe dosage or CD requirement to achieve sufficiently low As levels in the effluent. At a CD value of 10 C/L, the bio-FeEC column removed As(III) to well below 10 µg/L, whereas As in the effluent of the conventional FeEC column was considerably greater than the WHO recommended limit. Based on the results of the batch experiments, the conventional FeEC column could have eventually achieved As removal to below 10 µg/L, but a much higher CD would be needed. This higher CD for equivalent As removal requires a substantially higher applied current or electrolysis time, which would lead to greater electricity consumption and a larger amount of Fe sludge generated. For instance in the bio-FeEC column, the average energy consumption and sludge production to remove 150 µg/L As(III) below 10 µg/L for a CD of 10 C/L under a constant voltage (U)

of 2.1 V was 0.006 kWh/m³ (by eq. 2.3) and 0.007 kg/m³, respectively. Similarly for the conventional FeEC column to remove 150 µg/L As(III) below 10 µg/L a CD of 100 C/L might be necessary (as observed in the batch FeEC system, (Fig. 2.2)), which is 10 times higher than bio-FeEC, resulting in a tenfold increase in energy consumption and sludge generation of 0.06 kWh/m³ (by eq. 2.3) and 0.07 kg/m³, respectively. Compared to other removal techniques, the power required for treating the As-contaminated water by bio-FeEC (0.06 kWh/m³) is nearly two orders of magnitude lower than the power requirement (3 to 4 kWh/m³) reported for As treatment by membrane techniques (Schmidt et al., 2016). Furthermore, because Fe(III)-precipitates form in the presence of As during FeEC, the amount of reactive surface area available for As sorption per mass of solid (50 µg As/mg Fe) is significantly higher than for other Fe-based strategies, including adsorption to pre-synthesised Fe(III)-oxide adsorbents or Fe-oxide coated sand filters (Thirunavukkarasu et al., 2003). Therefore, the amount of sludge generated by bio-FeEC for a given electrolyte composition is lower than other methods. However, it is important to note that direct comparisons of the power requirement and sludge production of different techniques is difficult because these parameters are highly dependent on solution composition. Hence, the values of power consumption and sludge generation obtained for the bio-FeEC system are relevant to the solution conditions used in this study and might not reflect exactly the values obtained in other types of As-contaminated water.

$$C_{\text{energy}} = Uq \quad (2.3)$$

where C_{energy} = Consumption of electricity per m³ of water treated (Wh/m³); U = Total cell potential (V); q = Charge dosage (C/L)

The advantage of pre-oxidising As(III) in FeEC in terms of lower CD and Fe required for complete removal has been reported previously in systems where As(III) was oxidised by chemical or electrochemical methods (Flores et al., 2013; Zhang et al., 2014). However, in the bio-FeEC system, the oxidation is performed biologically without the need of chemicals or electricity, which is a benefit because chemicals can create secondary by-products in water (disinfection by-products for NaClO; (Jackman & Hughes, 2010)) and more electricity would lead to higher energy consumption. Furthermore, a separate chemical oxidation step can lead to more complex supply chains for As treatment, which is a major barrier to sustained operation of technologies, particularly in decentralised areas. Finally, the lower Fe sludge production in the bio-FeEC system compared to conventional FeEC also requires less waste management (i.e., landfill disposal) and reduces the backwashing frequency of the post filtration step due to less clogging of the filter beds. Although the bio-FeEC system produces less As-rich

Fe sludge than conventional FeEC, proper handling and disposal of the sludge is still important from the perspective of safety and circularity. Identifying the most appropriate sludge disposal method is beyond the scope of our study, but one method could be to dewater the sludge by passive settling and subsequent drying for re-use in industry (e.g. brick production) (Hassan et al., 2014; Sullivan et al., 2010). Another approach can be stabilising the sludge in concrete for re-use in local construction (Roy et al., 2019). However, in both cases, the toxicity characteristic leaching procedure (TCLP) test must be performed first to identify the leaching behaviour of the waste, which ensures minimal environmental contamination (Sullivan et al., 2010).

Although this work suggests that the bio-FeEC system can be an effective alternative to conventional FeEC or other standard As removal techniques, some potential challenges of the system must be investigated before implementing it in practice. For example, whereas the biological layer can oxidise ammonium (NH_4^+) in groundwater (Gude et al., 2018), which is an added benefit, the biological layer can also enhance Fe(II) and manganese (Mn(II)) oxidation (Gülay et al., 2018; Vandenabeele et al., 1992). The oxidation of Fe(II) and Mn(II) in the biological layer can result in their removal due to deposition of the solid oxidation products in the layer, but this can also be disadvantageous as the deposited precipitates can clog the layer, requiring more frequent backwashing or a conventional aeration-filtration step prior to bio-FeEC. Furthermore, the presence of high concentrations of natural organic matter (NOM) and total organic carbon (TOC) in groundwater can impact the speciation of aqueous Fe(II) by complexation (Sundman, 2014), which alters Fe(II) oxidation kinetics, can decrease As adsorption on Fe(III)-precipitates by competing for sorption sites (Redman et al., 2002), and can enhance growth of the biological layer (Kott et al., 1997), which can potentially lead to increased amounts of organic matter in subsequent treatment stages due to washout of biological material. However, we note that FeEC is effective at removing organic matter, which suggests that washout from the biological layer might not substantially decrease the quality of treated water (McBeath et al., 2020). The bio-FeEC system also requires a startup period to establish the AsOB-containing biofilm on the sand bed, which can lead to additional energy needed for continuous water pumping during ripening. This disadvantage can be avoided through accelerating the ripening phase by inoculating with already ripened sand from an existing As(III) treatment plant or by adding more Fe via FeEC to achieve sufficient As removal at the onset of treatment. Overall, the attractiveness of the bio-FeEC system lies particularly in that it can be implemented using locally available materials in conventional or decentralised systems (with electricity consumption offset by solar panels) which is appropriate for rural areas of South Asia, where As contamination of drinking water sources has led to catastrophic health impacts (Chakraborti et al., 2010).

2.4 Conclusions

In this study, the novel integrated system of biological As(III) oxidation and FeEC to treat As(III)-contaminated water was investigated. Compared to the abiotic, conventional FeEC system, the integrated biological FeEC system showed more effective oxidation and removal of 150 µg/L As(III) to below 10 µg/L without the need of chemicals. The bio-FeEC system reduced the Fe dosage required (by 10 times) compared to conventional FeEC. Hence, we propose that this integrated biological and electrochemical system can be a sustainable approach to remove As(III) from water, particularly in areas where costly and complex supply chains inhibit sustained operation of treatment methods.

References

- Amrose, S., Gadgil, A., Srinivasan, V., Kowolik, K., Muller, M., Huang, J., & Kostecki, R. (2013). Arsenic removal from groundwater using iron electrocoagulation: Effect of charge dosage rate. *Journal of Environmental Science and Health - Part A Toxic/Hazardous Substances and Environmental Engineering*, 48(9), 1019–1030. <https://doi.org/10.1080/10934529.2013.773215>
- Caporaso, J. G., Kuczynski, J., Stombaugh, J., Bittinger, K., Bushman, F. D., Costello, E. K., Fierer, N., Gonzalez Peña, A., Goodrich, J. K., Gordon, J. I., Huttley, G. A., Kelley, S. T., Knights, D., Koenig, J. E., Ley, R. E., Lozupone, C. A., McDonald, D., Muegge, B. D., Pirrung, M., ... Knight, R. (2010). QIIME allows analysis of high-throughput community sequencing data. *Nat Methods*, 7(5), 335–336. <https://doi.org/10.1038/nmeth.f.303>
- Cavalca, L., Corsini, A., Zaccheo, P., Andreoni, V., & Muyzer, G. (2013). Microbial transformations of arsenic: Perspectives for biological removal of arsenic from water. In *Future Microbiology* (Vol. 8, Issue 6, pp. 753–768). <https://doi.org/10.2217/fmb.13.38>
- Chakraborti, D., Rahman, M. M., Das, B., Murrill, M., Dey, S., Chandra Mukherjee, S., Dhar, R. K., Biswas, B. K., Chowdhury, U. K., Roy, S., Sorif, S., Selim, M., Rahman, M., & Quamruzzaman, Q. (2010). Status of groundwater arsenic contamination in Bangladesh: A 14-year study report. *Water Research*, 44(19), 5789–5802. <https://doi.org/10.1016/j.watres.2010.06.051>
- Crognale, S., Casentini, B., Amalfitano, S., Fazi, S., Petruccioli, M., & Rossetti, S. (2019). Biological As(III) oxidation in biofilters by using native groundwater microorganisms. *Science of the Total Environment*, 651, 93–102. <https://doi.org/10.1016/j.scitotenv.2018.09.176>
- Delaire, C., Amrose, S., Zhang, M., Hake, J., & Gadgil, A. (2017). How do operating conditions affect As(III) removal by iron electrocoagulation? *Water Research*, 112, 185–194. <https://doi.org/10.1016/j.watres.2017.01.030>
- Desantis, T. Z., Hugenholtz, P., Larsen, N., Rojas, M., Brodie, E. L., Keller, K., Huber, T., Dalevi, D., Hu, P., & Andersen, G. L. (2006). Greengenes, a Chimera-Checked 16S rRNA Gene Database and Workbench Compatible with ARB. *APPLIED AND ENVIRONMENTAL MICROBIOLOGY*, 72(7), 5069–5072. <https://doi.org/10.1128/AEM.03006-05>
- Dixit, S., & Hering, J. G. (2003). Comparison of arsenic(V) and arsenic(III) sorption onto iron oxide minerals: Implications for arsenic mobility. *Environmental Science and Technology*, 37(18), 4182–4189. <https://doi.org/10.1021/es030309t>
- Edgar, R. C. (2013). UPARSE: Highly accurate OTU sequences from microbial amplicon reads. *Nature Methods*, 10(10), 996–998. <https://doi.org/10.1038/nmeth.2604>
- Edgar, R. C., Haas, B. J., Clemente, J. C., Quince, C., & Knight, R. (2011). UCHIME improves sensitivity and speed of chimera detection. 27(16), 2194–2200. <https://doi.org/10.1093/bioinformatics/btr381>
- Feenstra, L., Van Erkel, J., & Utrecht, L. V. (2007). *Arsenic in groundwater: Overview and evaluation of removal methods*.
- Flores, O. J., Nava, J. L., Carreño, G., Elorza, E., & Martínez, F. (2013). Arsenic removal from groundwater by electrocoagulation in a pre-pilot-scale continuous filter press reactor. *Chemical Engineering Science*, 97, 1–6. <https://doi.org/10.1016/j.ces.2013.04.029>
- Goren, A. Y., Kobya, M., & Oncel, M. S. (2020). Arsenite removal from groundwater by aerated electrocoagulation reactor with Al ball electrodes: Human health risk assessment. *Chemosphere*, 251, 126363. <https://doi.org/10.1016/j.chemosphere.2020.126363>
- Gude, J. C. J., Rietveld, L. C., & van Halem, D. (2018). Biological As(III) oxidation in rapid sand filters. *Journal of Water Process Engineering*, 21, 107–115. <https://doi.org/10.1016/j.jwpe.2017.12.003>

- Gülay, A., Çekiç, Y., Musovic, S., Albrechtsen, H.-J., & Smets, B. F. (2018). Diversity of Iron Oxidizers in Groundwater-Fed Rapid Sand Filters: Evidence of Fe(II)-Dependent Growth by *Curvibacter* and *Undibacterium* spp. *Frontiers in Microbiology*, 9. <https://doi.org/10.3389/fmicb.2018.02808>
- Hassan, K. M., Fukushi, K., Turikuzzaman, K., & Moniruzzaman, S. M. (2014). Effects of using arsenic-iron sludge wastes in brick making. *Waste Management*, 34(6), 1072–1078. <https://doi.org/10.1016/j.wasman.2013.09.022>
- Holt, P. K., Barton, G. W., & Mitchell, C. A. (2005). The future for electrocoagulation as a localised water treatment technology. *Chemosphere*, 59(3), 355–367. <https://doi.org/10.1016/j.chemosphere.2004.10.023>
- Ito, A., Miura, J. I., Ishikawa, N., & Umita, T. (2012). Biological oxidation of arsenite in synthetic groundwater using immobilised bacteria. *Water Research*, 46(15), 4825–4831. <https://doi.org/10.1016/j.watres.2012.06.013>
- Jackman, T. A., & Hughes, C. L. (2010). Formation of Trihalomethanes in Soil and Groundwater by the Release of Sodium Hypochlorite. *Ground Water Monitoring & Remediation*, 30(1), 74–78. <https://doi.org/10.1111/j.1745-6592.2009.01266.x>
- Kamei-Ishikawa, N., Segawa, N., Yamazaki, D., Ito, A., & Umita, T. (2017). Arsenic removal from arsenic-contaminated water by biological arsenite oxidation and chemical ferrous iron oxidation using a down-flow hanging sponge reactor. *Water Science and Technology: Water Supply*, 17(5), 1249–1259. <https://doi.org/10.2166/ws.2017.025>
- Kapaj, S., Peterson, H., Liber, K., & Bhattacharya, P. (2006). Human health effects from chronic arsenic poisoning - A review. *Journal of Environmental Science and Health - Part A Toxic/Hazardous Substances and Environmental Engineering*, 41(10), 2399–2428. <https://doi.org/10.1080/10934520600873571>
- Katsoyiannis, I. A., & Zouboulis, A. I. (2004). Application of biological processes for the removal of arsenic from groundwaters. *Water Research*, 38(1), 17–26. <https://doi.org/10.1016/j.watres.2003.09.011>
- Kim, M. J., & Nriagu, J. (2000). Oxidation of arsenite in groundwater using ozone and oxygen. *Science of the Total Environment*, 247(1), 71–79. [https://doi.org/10.1016/S0048-9697\(99\)00470-2](https://doi.org/10.1016/S0048-9697(99)00470-2)
- Kitahama, K., Kiriya, R., & Baba, Y. (1975). Refinement of the crystal structure of scorodite. *Acta Crystallographica Section B Structural Crystallography and Crystal Chemistry*, 31(1), 322–324. <https://doi.org/10.1107/s056774087500266x>
- Koby, M., Demirbas, E., & Ulu, F. (2016). Evaluation of operating parameters with respect to charge loading on the removal efficiency of arsenic from potable water by electrocoagulation. *Journal of Environmental Chemical Engineering*, 4(2), 1484–1494. <https://doi.org/10.1016/j.jece.2016.02.016>
- Kott, Y., Ribas, F., Frías, J., & Lucena, F. (1997). Comparison between the evaluation of bacterial regrowth capability in a turbidimeter and biodegradable dissolved organic carbon bioreactor measurements in water. In *Journal of Applied Microbiology* (Vol. 83).
- Kumar, P. R., Chaudhari, S., Khilar, K. C., & Mahajan, S. P. (2004). Removal of arsenic from water by electrocoagulation. *Chemosphere*, 55(9), 1245–1252. <https://doi.org/10.1016/j.chemosphere.2003.12.025>
- Li, L., Van Genuchten, C. M., Addy, S. E. A., Yao, J., Gao, N., & Gadgil, A. J. (2012). *Modeling As(III) Oxidation and Removal with Iron Electrocoagulation in Groundwater*. <https://doi.org/10.1021/es302456b>
- Lytle, D. A., Chen, A. S., Sorg, T. J., Phillips, S., & French, K. (2007). Microbial As(III) oxidation in water treatment plant filters. *Journal - American Water Works Association*, 99(12), 72–86. <https://doi.org/10.1002/j.1551-8833.2007.tb08108.x>

- Magoč, T., Magoč, M., & Salzberg, S. L. (2011). FLASH: fast length adjustment of short reads to improve genome assemblies. *27*(21), 2957–2963. <https://doi.org/10.1093/bioinformatics/btr507>
- McBeath, S. T., Mohseni, M., & Wilkinson, D. P. (2020). Pilot-scale iron electrocoagulation treatment for natural organic matter removal. *Environmental Technology (United Kingdom)*, *41*(5), 577–585. <https://doi.org/10.1080/09593330.2018.1505965>
- Mikutta, C., Frommer, J., Voegelin, A., Kaegi, R., & Kretzschmar, R. (2010). Effect of citrate on the local Fe coordination in ferrihydrite, arsenate binding, and ternary arsenate complex formation. *Geochimica et Cosmochimica Acta*, *74*(19), 5574–5592. <https://doi.org/10.1016/j.gca.2010.06.024>
- Mollah, M. Y. A., Morkovsky, P., Gomes, J. A. G., Kesmez, M., Parga, J., & Cocke, D. L. (2004). Fundamentals, present and future perspectives of electrocoagulation. *Journal of Hazardous Materials*, *114*(1–3), 199–210. <https://doi.org/10.1016/j.jhazmat.2004.08.009>
- Mondal, P., Bhowmick, S., Chatterjee, D., Figoli, A., & Van der Bruggen, B. (2013). Remediation of inorganic arsenic in groundwater for safe water supply: A critical assessment of technological solutions. In *Chemosphere* (Vol. 92, Issue 2, pp. 157–170). Pergamon. <https://doi.org/10.1016/j.chemosphere.2013.01.097>
- Moussa, D. T., El-Naas, M. H., Nasser, M., & Al-Marri, M. J. (2017). A comprehensive review of electrocoagulation for water treatment: Potentials and challenges. In *Journal of Environmental Management* (Vol. 186, pp. 24–41). Academic Press. <https://doi.org/10.1016/j.jenvman.2016.10.032>
- Muller, D., Lièvreumont, D., Simeonova, D. D., Hubert, J. C., & Lett, M. C. (2003). Arsenite oxidase *aox* genes from a metal-resistant β -proteobacterium. *Journal of Bacteriology*, *185*(1), 135–141. <https://doi.org/10.1128/JB.185.1.135-141.2003>
- Müller, S., Behrends, T., & van Genuchten, C. M. (2019). Sustaining efficient production of aqueous iron during repeated operation of Fe(0)-electrocoagulation. *Water Research*, *155*, 455–464. <https://doi.org/10.1016/j.watres.2018.11.060>
- Newville, M. (2001). IFEFFIT: Interactive XAFS analysis and FEFF fitting. *Journal of Synchrotron Radiation*, *8*(2), 322–324. <https://doi.org/10.1107/S0909049500016964>
- Nicomel, N. R., Leus, K., Folens, K., Van Der Voort, P., & Du Laing, G. (2015). Technologies for arsenic removal from water: Current status and future perspectives. In *International Journal of Environmental Research and Public Health* (Vol. 13, Issue 1, p. ijerph13010062). MDPI AG. <https://doi.org/10.3390/ijerph13010062>
- Podgorski, J., & Berg, M. (2020). Global threat of arsenic in groundwater. *Science*, *368*(6493), 845–850. <https://doi.org/10.1126/science.aba1510>
- Raven, K. P., Jain, A., & Loeppert, R. H. (1998). Arsenite and arsenate adsorption on ferrihydrite: Kinetics, equilibrium, and adsorption envelopes. *Environmental Science and Technology*, *32*(3), 344–349. <https://doi.org/10.1021/es970421p>
- Redman, A. D., Macalady, D. L., & Ahmann, D. (2002). Natural organic matter affects Arsenic speciation and sorption onto hematite. *Environmental Science and Technology*, *36*(13), 2889–2896. <https://doi.org/10.1021/es0112801>
- Rehr, J. J., Albers, R. C., & Zabinsky, S. I. (1992). High-order multiple-scattering calculations of x-ray-absorption fine structure. *Physical Review Letters*, *69*(23), 3397–3400. <https://doi.org/10.1103/PhysRevLett.69.3397>
- Roberts, L. C., Hug, S. J., Ruettimann, T., Billah, M., Khan, A. W., & Rahman, M. T. (2004). Arsenic Removal with Iron(II) and Iron(III) in Waters with High Silicate and Phosphate Concentrations. *Environmental Science and Technology*, *38*(1), 307–315. <https://doi.org/10.1021/es0343205>

- Roy, A., van Genuchten, C. M., Mookherjee, I., Debsarkar, A., & Dutta, A. (2019). Concrete stabilization of arsenic-bearing iron sludge generated from an electrochemical arsenic remediation plant. *Journal of Environmental Management*, 233, 141–150. <https://doi.org/10.1016/j.jenvman.2018.11.062>
- Santini, J. M., Sly, L. I., Schnagl, R. D., & Macy, J. M. (2000). A new chemolithoautotrophic arsenite-oxidizing bacterium isolated from a gold mine: Phylogenetic, physiological, and preliminary biochemical studies. *Applied and Environmental Microbiology*, 66(1), 92–97. <https://doi.org/10.1128/AEM.66.1.92-97.2000>
- Schmidt, S. A., Gukelberger, E., Hermann, M., Fiedler, F., Großmann, B., Hoinkis, J., Ghosh, A., Chatterjee, D., & Bundschuh, J. (2016). Pilot study on arsenic removal from groundwater using a small-scale reverse osmosis system—Towards sustainable drinking water production. *Journal of Hazardous Materials*, 318, 671–678. <https://doi.org/10.1016/j.jhazmat.2016.06.005>
- Sorlini, S., & Gialdini, F. (2010). Conventional oxidation treatments for the removal of arsenic with chlorine dioxide, hypochlorite, potassium permanganate and monochloramine. *Water Research*, 44(19), 5653–5659. <https://doi.org/10.1016/j.watres.2010.06.032>
- Sullivan, C., Tyrer, M., Cheeseman, C. R., & Graham, N. J. D. (2010). Disposal of water treatment wastes containing arsenic - A review. In *Science of the Total Environment* (Vol. 408, Issue 8, pp. 1770–1778). Elsevier. <https://doi.org/10.1016/j.scitotenv.2010.01.010>
- Sundman, A. (2014). *Interactions between Fe and organic matter and their impact on As(V) and P(V)*. Doctoral dissertation, Umeå Universitet. <http://umu.diva-portal.org/>
- Thirunavukkarasu, O. S., Viraraghavan, T., & Subramanian, K. S. (2003). Arsenic removal from drinking water using iron oxide-coated sand. In *Water, Air, and Soil Pollution* (Vol. 142, Issues 1–4, pp. 95–111). Springer. <https://doi.org/10.1023/A:1022073721853>
- Toner, B. M., Santelli, C. M., Marcus, M. A., Wirth, R., Chan, C. S., McCollom, T., Bach, W., & Edwards, K. J. (2009). Biogenic iron oxyhydroxide formation at mid-ocean ridge hydrothermal vents: Juan de Fuca Ridge. *Geochimica et Cosmochimica Acta*, 73(2), 388–403. <https://doi.org/10.1016/j.gca.2008.09.035>
- Tseng, W. P. (1977). Effects and dose response relationships of skin cancer and blackfoot disease with arsenic. *Environmental Health Perspectives*, Vol.19, 109–119. <https://doi.org/10.1289/ehp.7719109>
- van Genuchten, C. M., Addy, S. E. A., Peña, J., & Gadgil, A. J. (2012). Removing arsenic from synthetic groundwater with iron electrocoagulation: An Fe and As K-edge EXAFS study. *Environmental Science and Technology*, 46(2), 986–994. <https://doi.org/10.1021/es201913a>
- van Genuchten, C. M., Peña, J., Amrose, S. E., & Gadgil, A. J. (2014). Structure of Fe(III) precipitates generated by the electrolytic dissolution of Fe(0) in the presence of groundwater ions. *Geochimica et Cosmochimica Acta*, 127, 285–304. <https://doi.org/10.1016/j.gca.2013.11.044>
- Vandenabeele, J., de Beer, D., Germonpré, R., & Verstraete, W. (1992). Manganese oxidation by microbial consortia from sand filters. *Microbial Ecology*, 24(1), 91–108. <https://doi.org/10.1007/BF00171973>
- Vandermaesen, J., Lievens, B., & Springael, D. (2017). Isolation and identification of culturable bacteria, capable of heterotrophic growth, from rapid sand filters of drinking water treatment plants. *Research in Microbiology*, 168(6), 594–607. <https://doi.org/10.1016/j.resmic.2017.03.008>
- Wan, W., Pepping, T. J., Banerji, T., Chaudhari, S., & Giammar, D. E. (2011). Effects of water chemistry on arsenic removal from drinking water by electrocoagulation. *Water Research*, 45(1), 384–392. <https://doi.org/10.1016/j.watres.2010.08.016>
- Wang, Q., Garrity, G. M., Tiedje, J. M., & Cole, J. R. (2007). Naïve Bayesian classifier for rapid assignment of rRNA sequences into the new bacterial taxonomy. *Applied and Environmental Microbiology*, 73(16), 5261–5267. <https://doi.org/10.1128/AEM.00062-07>

- Waychunas, G. A., Rea, B. A., Fuller, C. C., & Davis, J. A. (1993). Surface chemistry of ferrihydrite: Part 1. EXAFS studies of the geometry of coprecipitated and adsorbed arsenate. *Geochimica et Cosmochimica Acta*, 57(10), 2251–2269. [https://doi.org/10.1016/0016-7037\(93\)90567-G](https://doi.org/10.1016/0016-7037(93)90567-G)
- Webb, S. M. (2005). SIXpack: A graphical user interface for XAS analysis using IFEFFIT. *Physica Scripta T*, T115(T115), 1011–1014. <https://doi.org/10.1238/Physica.Topical.115a01011>
- World Health Organization. (2004). Guidelines for Drinking-water Quality, vol. 1. Recommendations, 3rd ed. World Health Organization, Geneva, Switzerland.
- Zhang, P., Tong, M., Yuan, S., & Liao, P. (2014). Transformation and removal of arsenic in groundwater by sequential anodic oxidation and electrocoagulation. *Journal of Contaminant Hydrology*, 164, 299–307. <https://doi.org/10.1016/j.jconhyd.2014.06.009>

Appendix

S2.1 X-ray absorption spectroscopy

The Fe(III)-precipitates generated in the bio-FeEC and control FeEC column systems were collected by backwashing the columns and filtering the backwashed water using filter paper. The filter paper containing the precipitates were then immediately stored at -80°C before being used for Fe and As K-edge (XAS) analysis. Following previous approaches, the filter paper bearing the precipitates was cut into small sections and the small sections were stacked to maximise the homogeneity of the precipitates within the path of the X-ray beam. The stacks were then affixed to custom sample holders with Kapton tape. All samples and sample holders were kept cool in an air-tight container until analysis at the beam line.

S2.1.1 Data collection

Fe and As K-edge XAS data were collected at beam line 2-2 of the Stanford Synchrotron Radiation Lightsource (SSRL, Menlo Park, USA). Fe K-edge XAS data were recorded at room temperature out to k of 13 \AA^{-1} . As K-edge XAS data were recorded at liquid nitrogen temperatures ($\approx 80^{\circ}\text{K}$) in fluorescence mode out to k of 14 \AA^{-1} . Samples were measured simultaneously in transmission and fluorescence mode using ion chambers for transmission measurements (I_0 and I_f) and a solid state PIPS detector for fluorescence measurements. The vertical dimension of the X-ray beam during data collection was 1 mm and the horizontal dimension was 6 mm. To prevent second-order harmonics, the X-ray beam was detuned 40%. Beam calibration was performed by setting the maximum of the first derivative of Fe(0) to 7112 eV for Fe K-edge XAS data or by setting the maximum of the first derivative of Au(0) to 11919 eV for As K-edge XAS data. The XANES region for both Fe and As spectra was measured with 0.35 eV steps, whereas step sizes of 0.05 \AA^{-1} were used for the EXAFS region. Two to six scans were collected for each sample, depending on data quality. During data collection, changes in line shape and peak position indicative of beam-induced redox reactions were examined and no beam damage was observed. Spectra were aligned, averaged, and background-subtracted using SixPack software following standard methods described previously (van Genuchten et al., 2012). The EXAFS spectra were extracted using k^3 -weighting and were Fourier-transformed using a Kaiser-Bessel window with dk of 3 \AA^{-1} over the k -range 2 to 11 \AA^{-1} for Fe data or 2 to 13 \AA^{-1} for As data.

S2.1.2 As K-edge XANES and EXAFS analysis

The fraction of sorbed As(III) and As(V) in the samples was quantified by linear combination fits (LCFs) using the SixPack software. The XANES LCFs were performed over the range of 11860 to 11880 eV using reference spectra of As(III) and As(V) adsorbed

to 2LFh. The As(III) and As(V) reference spectra were collected previously at beam line 4-1 of SSRL under similar conditions as the current data set.

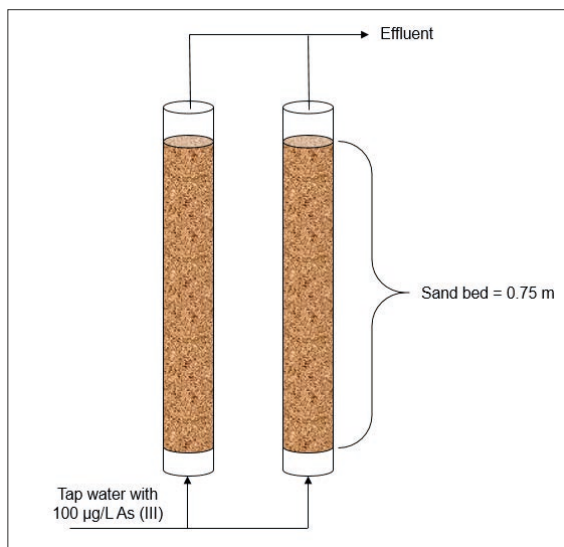


Fig. S2.1. Schematic diagram of the up-flow sand columns used for microbial characterisation of the arsenite oxidising biomass.

Shell-by-shell fitting of the EXAFS spectra was used to derive arsenic sorption configurations for an adsorption standard (As(V) adsorbed to 2LFh) and the continuous flow column samples. The fits were performed from 1 to 3.5 Å in $R+\Delta R$ -space using the SixPack software. Parameters that were varied in the fits typically included the interatomic distance (R), the coordination number (CN) and the change in threshold energy (ΔE_0). Following previous approaches, we constrained σ^2 to the value of previous EXAFS studies of As(V) adsorbed Fe(III) (oxyhydr)oxide precipitates to 0.010 to avoid large fit-derived uncertainties due to the high correlation between CN and σ^2 (Mikutta et al., 2010; Waychunas et al., 1993). For all fits, the passive electron reduction parameter, S_0^2 , was set to 1.0. The goodness-of-fit was assessed using the R-factor, which is the mean square difference between the fit and the data on a point-by-point basis: $R = \sum_i (\text{data}_i - \text{fit}_i)^2 / \sum_i (\text{data}_i)^2$. A reasonable fit is considered to yield an R-factor less than 0.05.

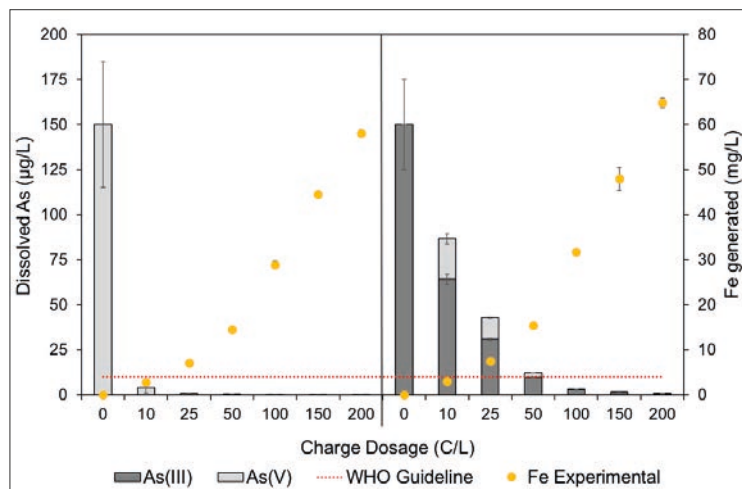


Fig. S2.2. Dissolved As concentration after FeEC in batch mode by applying various CD (0 to 200) C/L at 5 C/L/min CDR in tap water containing 150 µg/L As(V) (left) and As (III) (right) as the initial As species.

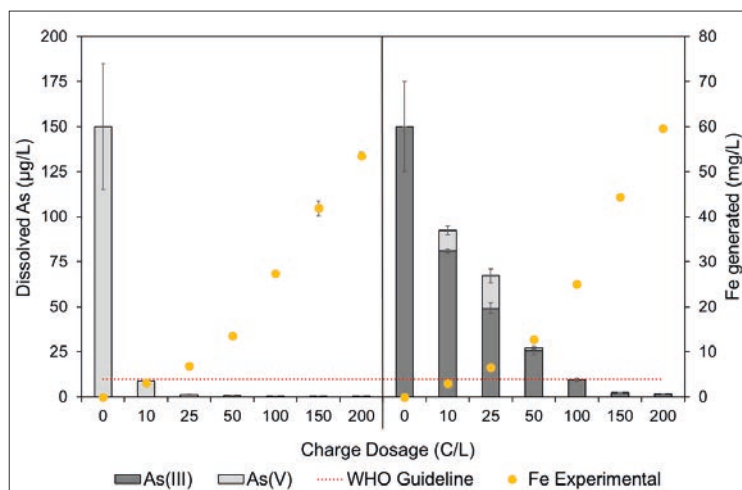


Fig. S2.3. Dissolved As concentration after FeEC in batch mode by applying various CD (0 to 200) C/L at 60 C/L/min CDR in tap water containing 150 µg/L As(V) (left) and As (III) (right) as the initial As species.

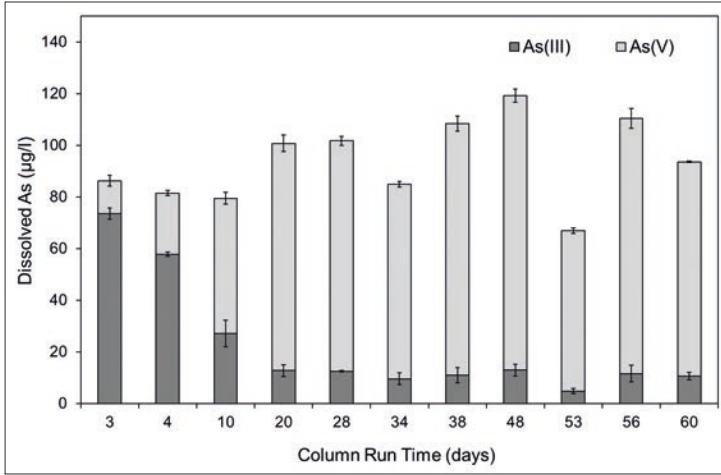


Fig. S2.4. As(III) and As(V) concentration in the effluent of the duplicate up-flow sand columns during 60 days ripening with 100 ± 20 µg/L As(III) spiked tap water.

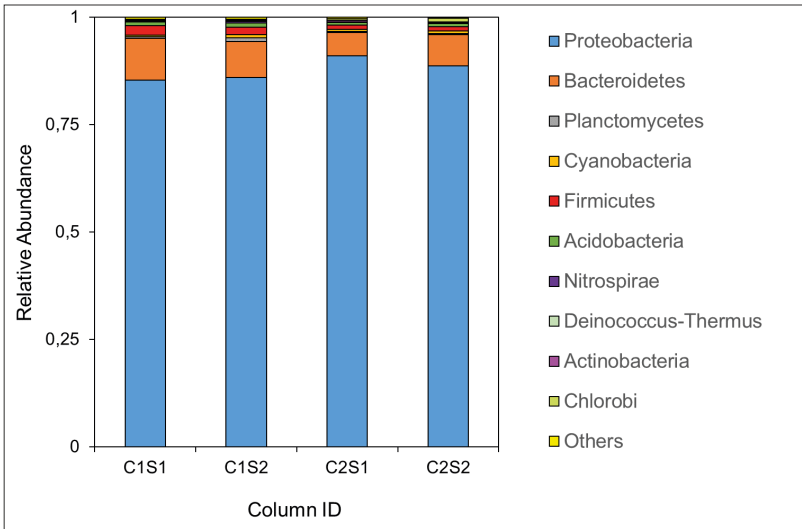


Fig. S2.5. Relative abundance (% of total OTUs) of the predominant bacterial communities in the accumulated As(III) oxidising biomass of the duplicate up-flow biological columns at phylum level. (C1, C2 = 2 columns; S1, S2 = duplicate sand samples from each column)

Table S2.1. Tap water composition

| Ion | Initial value |
|-------------------------------|---------------|
| pH | 7.0-8.0 |
| PO ₄ ³⁻ | 0 |
| SO ₄ ²⁻ | 52.1±1 mg/L |
| NO ₂ ⁻ | 0 |
| NO ₃ ⁻ | 2.4±0.3 mg/L |
| NH ₄ ⁺ | 0 |
| Fe | 0 |
| As | 0 |
| Ca ²⁺ | 49.8±0.3 mg/L |
| Na ⁺ | 41.5±0.4 mg/L |
| Si | 2.2±0.1 mg/L |
| Mg ²⁺ | 7±0.1 mg/L |

Table S2.2. Summary of As Shell-by-shell Fitting results

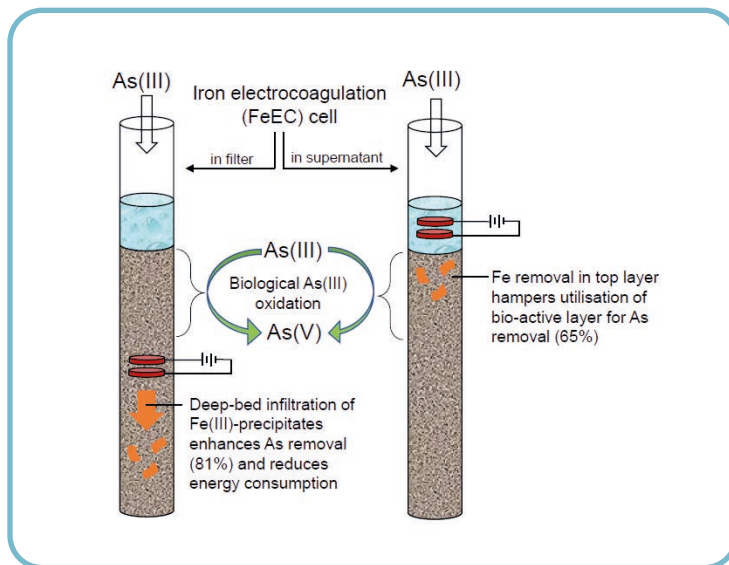
| Sample | Atomic Pairs | CN | R (Å) | σ ² (Å ²) | ΔE _o (eV) | R-Factor |
|------------------------------|--------------|-----------|---------------------------------|----------------------------------|----------------------|----------|
| As(V) adsorbed to 2LFh | As-O | 4.1 (0.4) | 1.70 (0.01) | 0.003 (0.001) | 7.8 (1.9) | 0.0356 |
| | As-O-O | 12 | 1.82(R _{As-O}) = 3.09 | σ ² (As-O) | | |
| | As-Fe | 1.8 (1.1) | 3.29 (0.04) | 0.010 | | |
| Bio-FeEC | As-O | 4.6 (0.4) | 1.69 (0.01) | 0.003 (0.001) | 5.4 (1.2) | 0.012 |
| | As-O-O | 12 | 1.82(R _{As-O}) = 3.08 | σ ² (As-O) | | |
| | As-Fe | 1.4 (0.6) | 3.28 (0.03) | 0.010 | | |
| FeEC | As-O | 4.3 (0.4) | 1.69 (0.01) | 0.003 (0.001) | 5.2 (1.2) | 0.013 |
| | As-O-O | 12 | 1.82(R _{As-O}) = 3.08 | σ ² (As-O) | | |
| | As-Fe | 1.6 (0.7) | 3.28 (0.03) | 0.010 | | |

CN represents the coordination number, R the interatomic distance, σ² the mean squared atomic displacement and ΔE_o represents the change in threshold energy. The passive electron reduction factor, S_o², was fixed at 1.0. Fitting parameters allowed to float are accompanied by fit-determined standard errors in parenthesis, while constrained parameters appear without a parenthesis. The multiple scattering As-O-O path (CN = 12) was constrained geometrically to the single scattering As-O path (R_{As-O-O} = 1.82 R_{As-O}). All fits were carried out from 1 to 3.5 Å in R+ΔR-space. The number of independent point (N_{IDP}) in the fits was 15.0 and the number of variables (N_{Var}) was 6.



Chapter 3

Embedding Fe(0) electrocoagulation in a biologically active As(III) oxidising filter bed



This chapter is based on:

Roy, M., Kraaijeveld, E., Gude, J. C. J., van Genuchten, C. M., Rietveld, L., & van Halem, D. (2024). Embedding Fe(0) electrocoagulation in a biologically active As(III) oxidising filter bed. *Water Research*, 121233.

Abstract

Long-term consumption of groundwater containing elevated levels of arsenic (As) can have severe health consequences, including cancer. To effectively remove As, conventional treatment technologies require expensive chemical oxidants to oxidise neutral arsenite (As(III)) in groundwater to negatively charged arsenate (As(V)), which is more easily removed. Rapid sand filter beds used in conventional aeration-filtration to treat anaerobic groundwater can naturally oxidise As(III) through biological processes but require an additional step to remove the generated As(V), adding complexity and cost. This study introduces a novel approach where As(V), produced through biological As(III) oxidation in a sand filter, is effectively removed within the same filter by embedding and operating an iron electrocoagulation (FeEC) system inside the filter. Operating FeEC within the biological filter achieved higher As(III) removal (81%) compared to operating FeEC in the filter supernatant (67%). This performance was similar to an analogous embedded-FeEC system treating As(V)-contaminated water (85%), confirming the benefits of incorporating FeEC in a biological bed for comparable As(III) and As(V) removal. However, operating FeEC in the sand matrix consumed more energy (14 Wh/m³) compared to FeEC operated in a water matrix (7 Wh/m³). The efficacy of As removal increased and energy requirements decreased in such embedded-FeEC systems by deep-bed infiltration of Fe(III)-precipitates, which can be controlled by adjusting flow rate and pH. This study is one of the first to demonstrate the feasibility of embedding FeEC systems in sand filters for groundwater arsenic removal. Such systems capitalise on biological As(III) oxidation in aeration-filtration, effectively eliminating As(V) within the same setup without the need for chemicals or major modifications.

Keywords: Arsenic, Groundwater, Iron electrocoagulation, Drinking water

3.1 Introduction

To minimise the potential health risks associated with elevated levels of arsenic (As) in groundwater, it is crucial to treat the water before consumption. Exposure to such contaminated water has been linked to various cancers, including skin, lung, prostate, and kidney cancer, as well as neurodevelopmental issues in children (Kapaj et al., 2006; Sodhi et al., 2019; Steinmaus et al., 2014). Consequently, the World Health Organization (WHO) has established a provisional guideline value of less than 10 µg/L As in drinking water (WHO, 2004).

Extensive research has been conducted on various standard technologies, such as adsorption, coagulation, precipitation, and filtration, to address the removal of arsenic (As) from groundwater (Alka et al., 2021; Kowalski, 2014). However, these methods often face limitations in terms of their efficacy, primarily due to the oxidation state of As. In raw anaerobic groundwater, As exists as neutrally charged arsenite (As(III)) (H_3AsO_3), which is more difficult to remove compared to the oxidised form, arsenate (As(V)), a negatively charged oxyanion at neutral pH ($\text{H}_2\text{AsO}_4^-/\text{HAsO}_4^{2-}$) (Roberts et al., 2004).

While aeration is commonly employed after extracting raw anaerobic groundwater, the oxidation of As(III) to As(V) through aeration (i.e., oxidation by molecular oxygen) at near-neutral pH is a slow process, taking several days for completion (Hug & Leupin, 2003). Consequently, to enhance the removal of As(III) using the aforementioned technologies, pre-oxidation to As(V) using strong chemical oxidants like NaOCl and KMnO_4 has been reported (Ahmad et al., 2018; Sorlini & Gialdini, 2010). However, the use of chemical oxidants increases costs, can lead to operational difficulties, and generates unwanted by-products that necessitate additional treatment (Jackman & Hughes, 2010; Katsoyiannis & Zouboulis, 2004).

Other studies have proposed a chemical-free approach to achieve effective oxidation of As(III) during conventional aeration-filtration by employing arsenic oxidising bacteria (AsOB) to biologically oxidise As(III) (Gude et al., 2018c; Katsoyiannis & Zouboulis, 2004; Lytle et al., 2007). Long-term exposure of rapid sand filter (RSF) beds to As(III)-contaminated water leads to the development and accumulation of a diverse microbial community, including AsOB, which effectively oxidise As(III) throughout the filter bed depth (Gude et al., 2018c; Roy et al., 2020). Additionally, aeration-filtration is commonly employed to remove native-Fe(II) from groundwater by oxidising it to form Fe(III)-precipitates, which can potentially adsorb the oxidised As(V) and remove it during this treatment step. However, complete biological As(III) oxidation predominantly occurs at a specific depth within the filter bed (around 40-60 cm

from the top layer) (Gude et al., 2018a; Gude et al., 2018b; Yang et al., 2014), where the Fe(III)-precipitates have already been removed and are unavailable for adsorption of As(V) (Gude et al., 2018a; Gude et al., 2018b). Therefore, additional dosing of Fe is necessary to remove the biologically oxidised As(V) after aeration-filtration.

Iron electrocoagulation (FeEC) is a chemical-free method that can be employed to introduce Fe into water and remove the oxidised As(V), as demonstrated in numerous studies focusing on treating As-contaminated water (Amrose et al., 2014; Bandaru et al., 2020; Delaire et al., 2017; Mollah et al., 2004). In FeEC, an electric current is passed through Fe(0) electrodes, releasing Fe(II) ions from the sacrificial Fe(0) anode into the solution. These Fe(II) ions can be oxidised by dissolved oxygen (DO) to produce Fe(III)-precipitates with a high affinity for adsorbing As (van Genuchten et al., 2012). Various forms of Fe(III)-precipitates, ranging from poorly-ordered hydrous ferric oxides to crystalline magnetite, have been observed during FeEC, with As being either adsorbed or incorporated into the solid structure (van Genuchten et al., 2012, 2014, 2019, 2020). However, conventional FeEC has primarily been applied in a water matrix. Therefore, to harness the benefits of biological As(III) oxidation in conventional aeration-filtration, FeEC should be positioned post-filtration, allowing oxidation to occur within the filter bed. The conventional approach would involve applying FeEC to the filtrate of the biological bed, followed by an additional filtration step to remove the As-laden Fe(III)-precipitates, which would require constructing additional infrastructure. By contrast, an ideal system would utilise a single integrated reactor to couple both biological As(III) oxidation and Fe(III) production via FeEC. Such a system could be achieved by embedding and operating FeEC within the biological sand filter to generate and filter Fe within a single system. However, to the best of our knowledge, embedding FeEC has only recently been investigated for As removal in soils and has not been studied in the context of a sand filter (Kumpiene et al., 2023). Examining embedded-FeEC within a sand filter is crucial for understanding key parameters, including overall As removal efficacy, energy consumption, and the role of FeEC operating conditions, before implementing such a system at scale.

In this study, we evaluated three specific systems: FeEC embedded and operated inside a biotic filter bed, FeEC in the supernatant of a biotic filter bed, and FeEC embedded inside an abiotic filter bed. The performance of these different systems was compared in terms of As removal efficacy, energy consumption, and deep-bed Fe infiltration, with additional consideration of the impact of FeEC location, biological As(III) oxidation, initial As oxidation state, and operational conditions (Fe dosage, flow rate, and pH). The novelty of this work lies in effectively utilising the biological As(III) oxidation step in conventional aeration-filtration and removing the oxidised As(V) within the

same filtration step, without any chemicals and major structural changes. The results from this study improve the understanding of the operation of such embedded-FeEC systems for As removal under a range of realistic conditions.

3.2 Materials and methods

3.2.1 Experimental setup

3.2.1.1 Batch FeEC

The quantity of iron (Fe) released from the anode during FeEC is directly related to the charge dosage (CD) (q in C/L) and can be determined using Faraday's law (eq. 3.1) (Roy et al., 2020).

$$W = \frac{qM}{nF} = \frac{ItM}{nFV} = \frac{IM}{nFQ} \quad (3.1)$$

where, W = Amount of generated Fe (mg/L); I = Applied current (A); t = Electrolysis time (s); M = Molecular weight of Fe (mg/mol) = 55845; F = Faraday's constant (96485 C/mol); n = Number of transferred electrons (2 for Fe); V = Solution volume (L); Q = Flow rate (L/s).

To determine the appropriate CD or Fe dosage for the subsequent flow-through embedded-FeEC experiments, batch FeEC experiments were conducted. A comprehensive description of the batch FeEC reactor, operational parameters, and the obtained results can be found in the appendix (section S3.1 and S3.2).

3.2.1.2 Column setup

The experimental setup consisted of four PVC down-flow columns, each with a height of 1.7 m and a diameter of 7.4 cm (Fig. 3.1(A)). These columns contained fresh anthracite, serving as the filter material, with a bed height of 80 cm. The anthracite material had a porosity of 0.43 ± 0.01 and a median particle size (d_{50}) of 1.9 mm. During the experiments, a supernatant water level of 20 to 25 cm above the anthracite bed was maintained. Prior to the experiments, the anthracite beds were thoroughly backwashed with tap water until the supernatant appeared visually clean, ensuring the removal of solids.

Two of the four columns were initially used to establish a microbial community capable of oxidising As(III) within the anthracite beds (referred to as biotic columns) (Fig. 3.1(B)) (further details in section 3.2.2.1). Subsequently, modifications were made

to the two biotic columns: one had a FeEC cell placed inside the bed (referred to as biotic embedded-FeEC), and the other had the FeEC cell placed in the supernatant water (referred to as supernatant-FeEC) (Fig. 3.1(C)) (further details in section 3.2.2.2). A clean layer of sand (height = 40 cm; porosity = 0.40 ± 0.01 ; $d_{50} = 1.2$ mm) was also added at the bottom of the biotic embedded-FeEC and supernatant-FeEC columns to enhance filtration. The remaining two columns were duplicates, with anthracite beds that were abiotic but embedded with a FeEC cell (referred to as abiotic embedded-FeEC) (Fig. 3.1(D)) (further details in section 3.2.2.3).

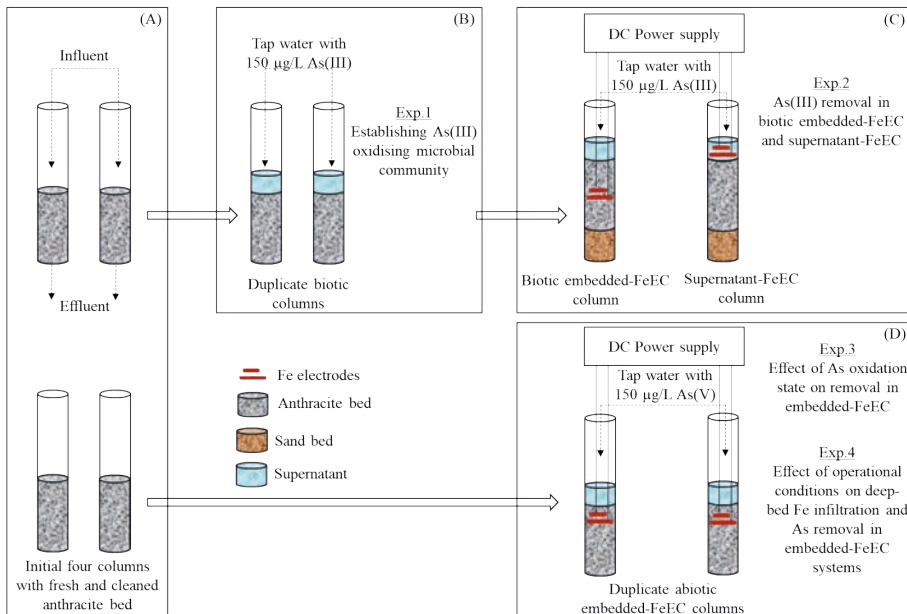


Fig. 3.1. Schematic diagram of the different columns used and overview of the experiments performed during this study.

The FeEC cell in all four columns consisted of two perforated Fe electrodes (anode diameter = 75 mm; cathode diameter = 55 mm; perforation diameter = 12 mm; open surface area = 51%) (Fig. S3.4 and S3.5), connected to a DC power supply (TENMA 72-10500 Power Supply, 30V, 3A). The electrodes were horizontally positioned within the anthracite bed or in the supernatant water. The perforations allowed for easy placement and removal of the electrodes during backwashing of the filter bed. The anode was positioned downstream of the cathode, and an inter-electrode gap of 1.5 cm was maintained using a plastic spacer (Fig. S3.5). Nylon wire was used to secure the electrodes and maintain a consistent configuration throughout the experiment. Before and after the FeEC operation, backwashing was performed with tap water to achieve

a visually clean supernatant (approximately 15 minutes before and 30 minutes after FeEC operation), resulting in a bed expansion of 25 to 30%. During these backwashing periods, the electrodes were lowered into and removed from the fluidised bed. Prior to placement, the electrodes were cleaned following the procedure described in the batch study (section S3.1). When the FeEC cell was not operational, the electrodes were kept dry outside the columns. Sample points were located on the sides of the columns, corresponding to different heights within the bed.

3.2.2 Overview of column experiments

3.2.2.1 Establishing As(III) oxidising microbial community

The procedure for establishing an As(III)-oxidising biomass on a sand bed resembled the methodologies outlined in the previous studies by Gude et al. (2018c), and Roy et al. (2020). These studies focused on the establishment and characterisation of AsOB in sand filters for biological As(III) oxidation. To establish an As(III)-oxidising biomass, the two biotic filter columns were subjected to a nine-week ripening period with 150 µg/L As(III)-spiked tap water flowing at a rate of 3 m/h (Fig. 3.1(B)). During this period, aluminium foil was wrapped around the columns to shield the filter material from light exposure. The pH of the water was consistently maintained at 7.9 ± 0.1 using HNO₃ acid, which was the pH of the tap water used in this study (Table S3.2). The extent of biological As(III) oxidation within the columns was assessed on a weekly basis by analysing the speciation of dissolved As in the influent and effluent (speciation procedure in section 3.2.4). Once the microbial biomass in the filter beds had been established, capable of oxidising over 95% of the influent 150 µg/L As(III) in the effluent (after nine weeks), an As(III) oxidation profile across the bed height was obtained to determine the optimal placement of Fe electrodes within the biological bed.

3.2.2.2 As(III) removal in biotic embedded- and supernatant-FeEC columns

The biotic embedded-FeEC and supernatant-FeEC columns were utilised for these experiments (Fig. 3.1(C)). In the biotic embedded-FeEC column, the Fe electrodes were positioned at a filter depth of 50 cm from the top of the filter bed, where 85% of the As(III) oxidation was observed in the ripened anthracite bed during week 9. In the supernatant-FeEC column, the Fe electrodes were placed in the supernatant water, 15 cm above the top of the bed.

To assess and compare the removal of As(III) in the two columns, tap water spiked with 150 µg/L As(III) was fed into both columns at a flow rate of 3 m/h, pH of 8.0, and FeEC operated at a CD of 6.4 C/L (or $I = 0.022$ A as per eq. 3.1). The CD value was determined based on the batch FeEC experiments (section S3.2). The two columns were operated

continuously for three consecutive days, with FeEC operated for 11 hours each day. Water samples were collected from the influent and effluent at the 7th, 9th, and 11th hour of operation. At the 11th hour, additional samples were collected at depths of 40 cm and 80 cm from the top of the bed to obtain As and Fe oxidation/removal profiles, followed by a backwashing step. After 11 hours of FeEC operation and backwashing, the columns were flushed with tap water (without As) until the subsequent trial, which occurred approximately 12 hours later, to minimise the impact of As desorption from the filter bed.

3.2.2.3 Effect of As oxidation state on removal in embedded-FeEC systems

To investigate the influence of the As oxidation state on the performance of embedded-FeEC and the potential advantages of embedding FeEC in a biological bed for As(III) removal, a separate set of experiments were conducted using As(V)-spiked tap water. In these experiments, the duplicate abiotic embedded-FeEC columns were utilised, with the Fe electrodes embedded 10 cm from the top of the abiotic anthracite bed (Fig. 3.1(D)). Both columns were operated with tap water spiked with 150 µg/L As(V), while maintaining similar pH, flow rate, and CD as the biotic embedded-FeEC column (section 3.2.2.2). Consequently, the abiotic embedded-FeEC columns served as control, and the results were then compared to As(III) removal in the biotic embedded-FeEC column (section 3.2.2.2). The experiments were carried out continuously for three consecutive days, with FeEC operated for 7 hours each day. Water samples were collected from the influent and effluent at the 4th, 5th, 6th, and 7th hour of operation. At the 7th hour, additional samples were collected at depths of 20 cm, 40 cm, and 60 cm from the top of the bed to obtain As and Fe oxidation/removal profiles, followed by the backwashing procedure.

3.2.2.4 Effect of operational conditions on deep-bed Fe infiltration and As removal in embedded-FeEC systems

Since the distribution of Fe(III)-precipitates deep within the sand filter can increase As removal, experiments were conducted to investigate the effects of charge dosage (CD), flow rate, and pH on the infiltration of Fe(III)-precipitates within the embedded-FeEC systems and its impact on As removal. The duplicate abiotic embedded-FeEC columns (Fig. 3.1(D)) were utilised for these experiments, operating under different conditions compared to the reference condition in section 3.2.2.3 (CD = 6.4 C/L, flow rate = 3 m/h, pH = 8.0). The columns were run under modified conditions by either increasing the CD to 9.4 C/L (higher CD), increasing the flow rate to 5 m/h (higher flow rate), or lowering the pH to 7.0 (using HNO₃). The Fe and As depth profiles obtained during these experiments with varying operational conditions were then compared to the reference condition described in section 3.2.2.3. The experimental duration,

sampling procedures, and other protocols were consistent with those of the reference condition in section 3.2.2.3.

3.2.3 Energy consumption

The energy consumption in the embedded- and supernatant-FeEC columns was estimated by monitoring the cell potential (E) and the applied current (I) during the experimental period and represented per unit of water treated, see eq. 3.2.

$$\text{Energy consumption (Wh/m}^3\text{)} = mV + \frac{EI}{Q} \quad (3.2)$$

where m = Rate of increase in energy consumption per unit of treated water (Wh/m³/L); V = Volume of treated water (L); EI/Q = Initial energy consumption (Wh/m³) at the start of the experiment; E = Total cell potential (V); I = Applied current (A); Q = Flow rate (m³/h).

3.2.4 Used water, chemicals, sampling and analytical methods

Chlorine-free Dutch tap water was used in all experiments, and its composition can be found in Table S3.2. To introduce As(III)/As(V) into the tap water, stock solutions were freshly prepared by dissolving sodium (meta)arsenite (NaAsO₂) or sodium arsenate dibasic heptahydrate (Na₂HAsO₄·7H₂O) from Sigma-Aldrich in ultrapure water. Ultrapure nitric acid (ROTIPURAN Ultra 69%) was employed for pH adjustment, and the pH levels were monitored using a WTW SenTix 940 pH meter.

Water samples were collected for analysis in triplicate using three different methods: (a) unfiltered, (b) filtered through a 0.20 μm polystyrene sulfone filter from Macherey-Nagel GmbH & Co. KG, and (c) filtered through a 0.20 μm polystyrene sulfone filter followed by an anion exchange resin. All three types of samples were acidified with ultrapure nitric acid (ROTIPURAN® Ultra 69%) and stored at 4°C before analysis. The speciation of dissolved As (i.e., As(III) and As(V)) was determined using an anion exchange resin (Amberlite® IRA-402 chlorite form resin) following the method described by Gude et al. (2018c). In the case of column samples, the Fe concentration after filtration with a 0.20 μm polystyrene sulfone filter was considered as dissolved Fe (or Fe(II)), while the difference in Fe concentration between the unfiltered and 0.20 μm polystyrene sulfone filtered samples represented particulate Fe (Fe(III)-precipitates that were not retained by the filter bed). As and Fe concentrations were analysed using inductively coupled plasma mass spectrometry (ICP-MS) with an Analytik Jena PlasmaQuant MS instrument. The values presented in the graphs in the "Results and discussion" section represent the average of the collected water samples for each data point, and the error bars indicate the corresponding standard deviation.

3.3 Results and discussion

3.3.1 Ripening of biotic columns

Fig. S3.3 illustrates the As speciation in the effluent of the duplicate biotic columns (Fig. 3.1(B)) after being ripened with 150 ± 20 $\mu\text{g/L}$ As(III)-spiked tap water for nine weeks before their modification into the biotic embedded- and supernatant-FeEC columns. Throughout the nine-week ripening period, the oxidation of influent As(III) began within the anthracite beds, and by the 9th week, approximately 95% of the initial 150 ± 20 $\mu\text{g/L}$ As(III) had been converted to As(V) in the effluent (Fig. S3.3). This trend of As(III) oxidation within the filter bed over time aligns with previous studies that focused on the establishment and characterisation of AsOB in sand filters for biological As(III) oxidation (Gude et al., 2018b; Gude et al., 2018c; Roy et al., 2020). Furthermore, the As(III) speciation across the ripened anthracite bed depths in week 9 revealed that approximately 88% of the influent As(III) had been oxidised at a depth of 40 cm (Fig. 3.2). This finding is consistent with earlier research indicating that biological activity is highest in the upper section of the filter bed (Gude et al., 2016; Gude et al., 2018c). Consequently, when assembling the biotic embedded-FeEC column (Fig. 3.1(C)) using one of the ripened anthracite columns, the Fe electrodes were positioned at a depth of 50 cm from the top of the filter bed.

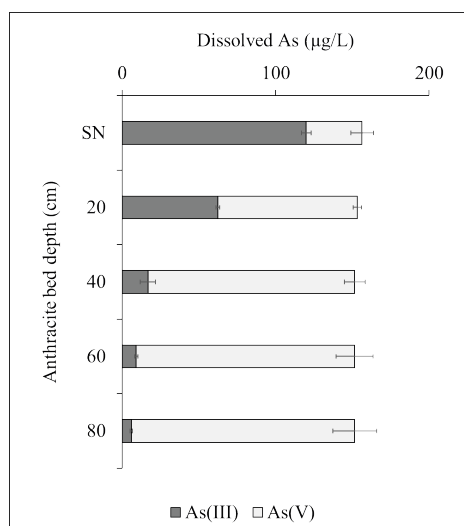


Fig. 3.2. As(III) oxidation profile over the depth in the duplicate biotic columns after nine weeks of ripening with 150 ± 20 $\mu\text{g/L}$ As(III)-spiked tap water. SN = supernatant.

3.3.2 Fe and As depth profile in biotic embedded-FeEC and supernatant-FeEC columns

The As and Fe depth profiles during the runs in the biotic embedded- and supernatant-FeEC columns, which were assembled by modifying the duplicate abiotic columns after ripening, are presented in Fig. 3.3(A) and (B). Both columns were operated with tap water spiked with $150 \pm 20 \mu\text{g/L}$ As ($130 \pm 10 \mu\text{g/L}$ As(III)) as the influent, at a flow rate of 3 m/h, and pH of 8.0. The FeEC cell was operated at a CD of 6.4 C/L, which was determined from the batch FeEC experiments (section S3.2).

The Fe profiles in both columns demonstrate that Fe generation by FeEC within the sand matrix was similar to conventional FeEC in a water matrix. In this process, Fe(II) was released from the anode, oxidised to Fe(III)-precipitates, and distributed across the height of the bed. In the supernatant-FeEC column, a total Fe concentration of $1.7 \pm 0.2 \text{ mg/L}$ was measured in the supernatant water just below the FeEC cell. This released Fe corresponds to a Faradaic efficiency of approximately 1 (see eq. 3.1; theoretical Fe release of 1.85 mg/L), under the conditions of CD = 6.4 C/L and flow rate = 3 m/h, which aligns with literature findings (van Genuchten et al., 2018; van Genuchten et al., 2017). It was assumed that a similar Fe release occurred in the biotic embedded-FeEC column (indicated by the yellow circle in Fig. 3.3(A)) since both systems were operated at a constant CD and flow rate. However, the actual Fe released by the embedded-FeEC could not be measured accurately due to filtration effects.

The Fe depth profiles in both columns exhibited rapid oxidation, precipitation, and filtration of the anodically-generated Fe(II). This could be attributed to the relatively high pH (8.0) and the saturated DO concentration of the solution. In the biotic embedded-FeEC column, at a bed depth of 30 cm below the FeEC cell, a dissolved Fe concentration of 0.1 mg/L and a particulate Fe concentration of 0.5 mg/L were measured, corresponding to 94% oxidation and precipitation, as well as 67% filtration of the released Fe(II) (considering a theoretical release of 1.85 mg/L Fe) (Fig. 3.3(A)). Similar trends were observed in the supernatant-FeEC column. Below the anode in the supernatant, a dissolved Fe concentration of 0.1 mg/L was measured, indicating 94% oxidation and precipitation of the released $1.7 \pm 0.2 \text{ mg/L}$ Fe(II). At a depth of 40 cm within the filter bed, 70% (0.5 mg/L measured as dissolved + particulate) of the released $1.7 \pm 0.2 \text{ mg/L}$ Fe(II) was filtered (Fig. 3.3(B)). These findings align with previous studies that demonstrated effective Fe removal in rapid sand filter beds (Gude et al., 2018b; Yang et al., 2014). Deeper within the bed, further oxidation and filtration of the remaining Fe were observed, which resulted in presence of only 0.2 mg/L Fe (0.1 mg/L particulate Fe) and 0.1 mg/L Fe (0.09 mg/L particulate Fe) in the effluent of the biotic embedded- and supernatant-

FeEC columns, respectively. With optimisation of the filter media size, bed depth, and contact time, the removal of the remaining Fe in the effluent can be further improved.

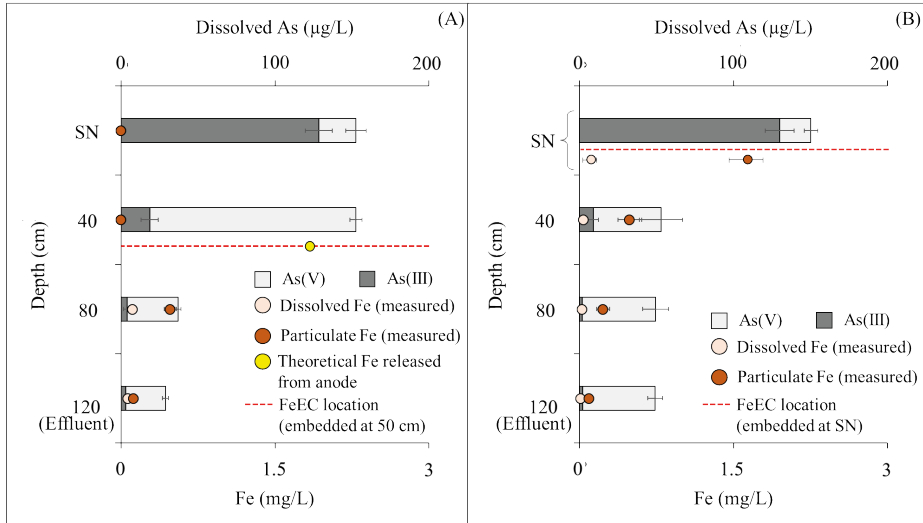


Fig. 3.3. Fe and As depth profile over the bed height in the biotic embedded-FeEC (A) and supernatant-FeEC (B) filter columns. Tap water spiked with As(III) was dosed as the influent and the columns were operated at CD = 6.4 C/L, flow rate = 3 m/h, and pH = 8.0. The Fe graph shows the concentration of dissolved Fe and particulate Fe that was not filtered by the bed. The yellow circle in (A) indicates the theoretical 1.85 mg/L Fe released by FeEC at CD = 6.4 C/L and flow rate = 3 m/h, as per eq. 3.1. SN = supernatant.

The Fe released from the FeEC cell played a significant role in the removal of a large portion of the influent As(III) in both columns. Fig. 3.3(A) and (B) illustrate the removal of the influent 150 ± 20 $\mu\text{g/L}$ As (130 ± 10 $\mu\text{g/L}$ As(III)) over the depth of the two columns during the experimental runs. The effluent As concentrations in the biotic embedded- and supernatant-FeEC columns were 28.9 ± 2.5 $\mu\text{g/L}$ (3.2 ± 0.6 $\mu\text{g/L}$ As(III)) and 49.1 ± 5.3 $\mu\text{g/L}$ (2.0 ± 0.5 $\mu\text{g/L}$ As(III)), respectively. This indicates that the Fe(III)-precipitates generated by FeEC effectively adsorbed and removed the As, leading to a decrease in concentration across the filter depths. However, the biotic embedded-FeEC system (81% removal) outperformed the supernatant-FeEC system (67% removal), with nearly double the residual As in the effluent of the supernatant-FeEC system. The higher As removal in the biotic embedded-FeEC column can be attributed to the biological oxidation of influent As(III) to As(V) in the ripened anthracite bed prior to the FeEC cell (Fig. 3.3(A)) (Roy et al., 2020). Fig. 3.3(A) demonstrates that at a depth of 40 cm, over 85% of the influent As(III) was oxidised to As(V). Therefore, the FeEC in the biotic embedded-FeEC column (positioned at a depth of 50 cm) mainly operated

in water containing As(V), which was not the case for the supernatant-FeEC column (Fig. 3.3(B)). The pre-oxidation of As(III) by biological processes in the biotic embedded-FeEC column resulted in a higher removal of the influent As(III), as Fe(III)-precipitates generated by FeEC have a greater affinity to adsorb As(V) than As(III) (Roberts et al., 2004). In the supernatant-FeEC column, biological oxidation of the unadsorbed As(III) was also observed in the filter bed at depths of 40 cm and 80 cm, respectively (Fig. 3.3(B)). However, due to insufficient remaining concentrations of Fe, the oxidised As(V) was not further removed.

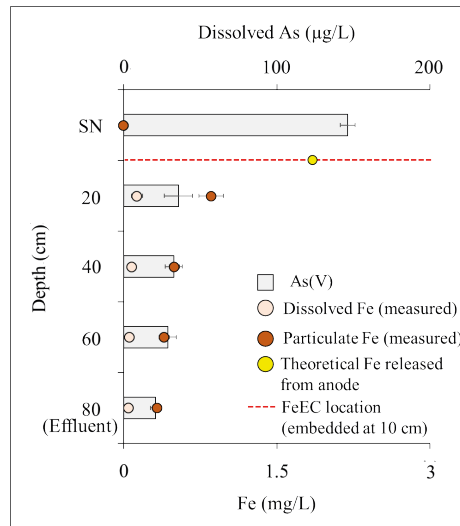


Fig. 3.4. Fe and As depth profile over the bed height in the duplicate abiotic embedded-FeEC filter columns. Tap water spiked with As(V) was dosed as the influent and the columns were operated at CD = 6.4 C/L, flow rate = 3 m/h, and pH = 8.0. The Fe graph shows the concentration of dissolved and particulate Fe that was not filtered by the bed. The yellow circle indicates the theoretical 1.85 mg/L Fe released by FeEC at CD = 6.4 C/L and flow rate = 3 m/h, as per eq. 3.1. SN = supernatant.

3.3.3 Effect of As oxidation state on removal in embedded-FeEC

To further validate the improved As(III) removal in the biotic embedded-FeEC column (section 3.3.2) and study the influence of As oxidation state on the removal performance of the embedded-FeEC system, experiments were conducted by embedding FeEC (depth = 10 cm) in an abiotic bed (duplicate abiotic embedded-FeEC columns) operated with As(V) (Fig. 3.1(D)). The Fe and As depth profiles during these runs are shown in Fig. 3.4. The charge dosage (CD), flow rate, and pH were similar to the biotic embedded-FeEC system, except that the influent tap water contained $146 \pm 5 \mu\text{g/L}$ As(V). The results demonstrate that, similar to the biotic embedded-FeEC system in section 3.3.2, Fe(II) was released in the abiotic bed, rapidly oxidised to Fe(III)-precipitates,

and filtered below the FeEC cell. Within 10 cm and 30 cm of the filter bed (below the FeEC cell), approximately 46% and 69% of the released Fe(II) was oxidised and filtered, respectively (considering a theoretical Fe release of 1.85 mg/L). This release of Fe inside the bed led to the removal of the influent As(V) (Fig. 3.4), with the effluent dissolved As(V) concentration being $21 \pm 3.4 \mu\text{g/L}$, corresponding to 85% removal. These findings align with the results of the biotic embedded-FeEC column presented in section 3.3.2, where, due to biological As(III) oxidation to As(V), a removal efficacy of 81% for influent As(III) was observed. This validates the advantage of embedding FeEC in a biological bed, where As(III) removal achieved by embedded-FeEC (under similar Fe dosage) is comparable to that of As(V).

3.3.4 Enhancing deep-bed infiltration of Fe in embedded-FeEC filter beds

Previous studies have indicated that deep-bed infiltration of Fe(III)-precipitates in sand filters can have a positive effect on As removal (Gude et al., 2018b). However, the rapid filtration observed in the biotic and abiotic embedded-FeEC columns suggested that deep-bed infiltration was not occurring, potentially limiting As removal due to a shorter contact time with the precipitates. To investigate this further, a set of experiments were conducted to assess the impact of varying operational parameters (CD, flow rate, pH) on achieving deep-bed infiltration of the Fe(III)-precipitates in the embedded-FeEC system and the corresponding impact on As removal. The duplicate abiotic embedded-FeEC columns discussed in section 3.3.3 were used for these experiments, with the CD, flow rate, or pH being altered. Fig. 3.5(A), (B), and (C) depict the Fe and As depth profiles in the abiotic embedded-FeEC columns under higher CD (9.4 C/L), higher flow rate (5 m/h), and lower pH (7.0) conditions compared to the reference condition in section 3.3.3 (CD = 6.4 C/L, flow rate = 3 m/h, pH = 8.0).

The Fe depth profile observed with a CD of 9.4 C/L was similar to that with 6.4 C/L (Fig. 3.5(A)). Approximately 79% of the released Fe (theoretical value of 2.7 mg/L based on eq. 3.1) from the embedded-FeEC was oxidised and filtered within a 30 cm filtration depth below the FeEC cell. However, the effluent As concentration with a CD of 9.4 C/L was $10.7 \pm 1.4 \mu\text{g/L}$, corresponding to 93% removal (influent concentration = $156 \pm 0.3 \mu\text{g/L}$ As(V)) (Fig. 3.5(A)), compared to 85% removal with a CD of 6.4 C/L (Fig. 3.4). The higher removal of As(V) with higher CD can be attributed to the increased amount of Fe generated from electrolysis, which is consistent with previous studies conducted in a water matrix in batch mode (van Genuchten et al., 2012; Wan et al., 2011).

Deeper penetration of Fe was observed with a higher flow rate (5 m/h compared to 3 m/h), where the Fe concentration at 10 and 30 cm below the FeEC cell was 1.4 and 0.7 mg/L, respectively, with a flow rate of 5 m/h (Fig. 3.5(B)). In comparison, with a flow

rate of 3 m/h, the corresponding Fe concentrations were 1 and 0.6 mg/L, respectively (Fig. 3.4). However, a lower removal of As(V) was observed with the flow rate of 5 m/h, where the dissolved As concentration in the effluent was $29 \pm 3.4 \mu\text{g/L}$, corresponding to 81% removal ($149.7 \pm 5 \mu\text{g/L}$ As(V) influent) (Fig. 3.5(B)), compared to 85% with a flow rate of 3 m/h (Fig. 3.4). This could be attributed to the reduced residence time, resulting in less contact time between As(V) and the released Fe. Furthermore, the higher flow rate also affected the oxidation of Fe(II), as indicated by the higher dissolved Fe concentration (or Fe(II)) of 0.10 mg/L at 5 m/h compared to 0.05 mg/L at 3 m/h, which could have adversely impacted As removal by reducing the availability of Fe(III)-precipitates for As adsorption. Therefore, while an increased flow rate facilitated deep-bed Fe infiltration, the residence time played a crucial role in overall As removal.

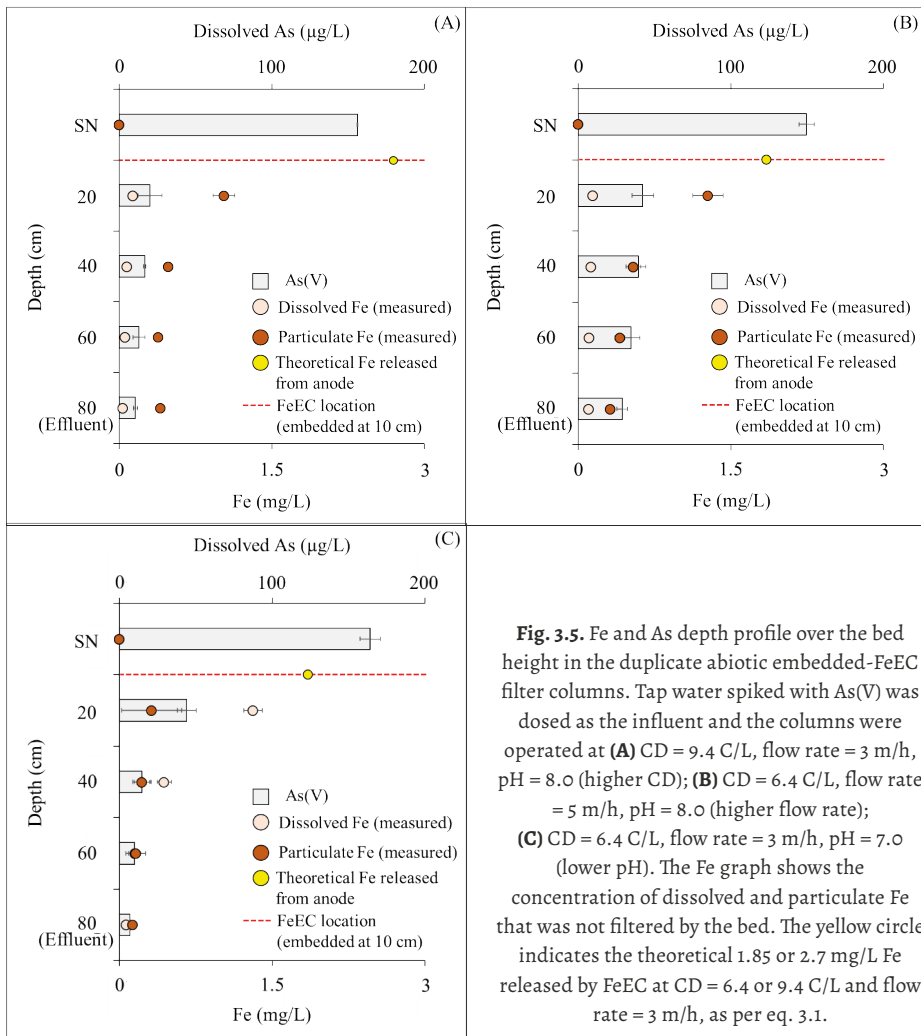


Fig. 3.5. Fe and As depth profile over the bed height in the duplicate abiotic embedded-FeEC filter columns. Tap water spiked with As(V) was dosed as the influent and the columns were operated at (A) CD = 9.4 C/L, flow rate = 3 m/h, pH = 8.0 (higher CD); (B) CD = 6.4 C/L, flow rate = 5 m/h, pH = 8.0 (higher flow rate); (C) CD = 6.4 C/L, flow rate = 3 m/h, pH = 7.0 (lower pH). The Fe graph shows the concentration of dissolved and particulate Fe that was not filtered by the bed. The yellow circle indicates the theoretical 1.85 or 2.7 mg/L Fe released by FeEC at CD = 6.4 or 9.4 C/L and flow rate = 3 m/h, as per eq. 3.1. SN = supernatant.

Operating the embedded-FeEC system at a lower pH (7.0 compared to 8.0) aimed to decrease the oxidation rate of the released Fe(II) and allow for its deeper distribution within the bed. The Fe depth profile at pH = 7.0 supported this hypothesis, as the dissolved Fe (Fe(II)) concentration at 10 and 30 cm below the FeEC cell was the highest among the different operational conditions (Fig. 3.5(C)). However, the total Fe concentration in the effluent was the lowest among the different conditions. At 10, 30, and 70 cm below the FeEC cell (effluent), the Fe concentrations were 1.6 (80% dissolved), 0.7 (67% dissolved), and 0.2 mg/L at pH = 7.0 (Fig. 3.5(C)), compared to 1 (13% dissolved), 0.6 (14% dissolved), and 0.4 mg/L at pH = 8.0 (Fig. 3.4), respectively. This indicates that Fe(II) oxidation, precipitation, and filtration occurred at deeper locations within the bed at pH = 7.0, resulting in a higher concentration of Fe at lower depths compared to the experiments at pH = 8.0. The presence of Fe at deeper locations could be likely contributed to the improved As removal at pH = 7.0, where the As concentration in the effluent was $7 \pm 1.4 \mu\text{g/L}$, corresponding to a 94% removal ($164 \pm 6.6 \mu\text{g/L As(V)}$ influent) (Fig. 3.5(C)), compared to 85% at pH = 8.0 (Fig. 3.4). However, the higher As removal at a lower pH (7.0 over 8.0) can also be attributed to enhanced As(V) adsorption to the Fe(III)-precipitates, as mentioned in previous studies (Dixit & Hering, 2003; Gude et al., 2016). We note here that while As(V) removal improved at lower pH in these experiments, similar trends with pH might not be observed for abiotic experiments performed with initial As(III) since the kinetics of Fe(II) and As(III) co-oxidation decrease significantly with decreasing pH (Garg et al., 2018; King et al., 1995).

3.3.5 Energy consumption in embedded-FeEC systems

Energy consumption in the abiotic embedded-FeEC columns under different conditions and the supernatant-FeEC column was monitored throughout the experiments and is presented as energy consumption per volume of treated water (Wh/m^3), as calculated using eq. 3.2. The results obtained under various conditions are shown in Fig. 3.6.

In the abiotic embedded-FeEC columns operated at $\text{CD} = 6.4 \text{ C/L}$, flow rate = 3 m/h, and pH = 8.0 or 7.0 (reference or lower pH condition), the initial energy consumption was in the same range, ranging between 12 and 14 Wh/m^3 , respectively. However, a higher initial energy consumption was observed for the experiments with a flow rate of 5 m/h (higher flow rate) and $\text{CD} = 9.4 \text{ C/L}$ (higher CD), which were approximately 22 and 30 Wh/m^3 , respectively. This difference in the initial consumption value can be explained by the Butler-Volmer relationship (Müller et al., 2019), where an increase in current (I) leads to an increase in the cell potential (E) and, consequently, in the energy consumption. In the case of $\text{CD} = 9.4 \text{ C/L}$ (higher CD), a higher current (I) had to be applied compared to $\text{CD} = 6.4 \text{ C/L}$. Similarly, for experiments with a flow rate of 5 m/h

(higher flow rate), maintaining a constant I/Q (or $CD = 6.4 \text{ C/L}$) value as the 3 m/h experiments required a comparatively higher applied current (I) (0.040 A compared to 0.023 A), resulting in an increased cell potential from 8 V (3 m/h) to 12.5 V (5 m/h).

The impact of operating FeEC in a filter bed on cell potential and energy consumption was highlighted in the supernatant-FeEC column. Under constant CD , flow rate, and pH , the supernatant-FeEC column exhibited the lowest initial energy consumption, around 7 Wh/m^3 , which was half the value of 14 Wh/m^3 observed in the embedded-FeEC (reference condition) (Fig. 3.6). This suggests that operating FeEC in a biological filter bed may require more energy compared to supernatant operation. However, achieving efficient As(III) removal similar to the biotic embedded-FeEC column would necessitate a relatively higher CD in the supernatant-FeEC column, resulting in higher energy consumption.

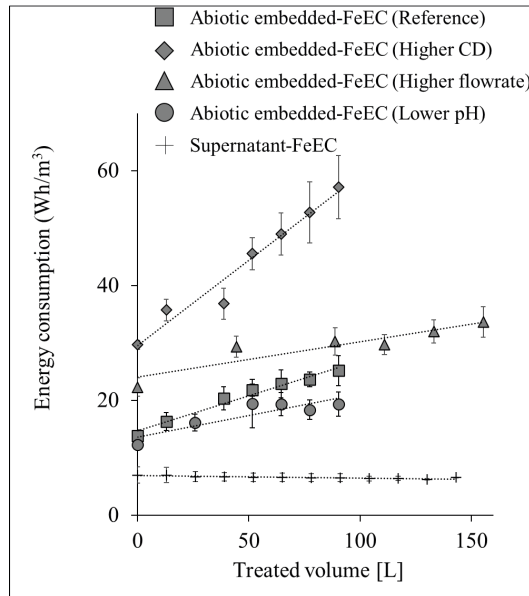


Fig. 3.6. Energy consumption during the experiments in abiotic embedded-FeEC columns operated under different conditions and the supernatant-FeEC column.

In the embedded-FeEC columns, the cell potential (E) at a constant applied current (I) showed an increasing trend over the course of the experiments. This led to an increase in energy consumption during treatment, as depicted in Fig. 3.6. For example, in the abiotic embedded-FeEC columns operated under the reference condition, higher CD , higher flow rate, and lower pH , the energy consumption at the end of the experiment increased by 82%, 92%, 51%, and 57%, respectively, compared to the initial value. This

rise in energy consumption over time could be attributed to the accumulation of Fe(III)-precipitates between the electrodes, which increased the cell resistance. Additionally, the accumulation of Fe(III)-precipitates on the electrode surface may have reduced the effective electrode area, resulting in an increase in current density and elevated cell potential (E) and, consequently, increased the energy consumption (Müller et al., 2019). In contrast, the energy consumption over time in the supernatant-FeEC system did not show an increasing trend. This suggests that the cell remained unaffected throughout the experiments, with no changes in cell resistance or effective electrode area.

3.3.6 Benefits and challenges of embedded-FeEC systems

The findings of this study demonstrate the feasibility of embedding FeEC within a biological filter bed for effective As removal. This embedded-FeEC concept can be utilised to optimise As(III) removal in conventional aeration-filtration processes, where the filter bed is already biologically active for As(III) oxidation. Implementing embedded-FeEC in existing infrastructure eliminates the need for additional construction and allows for efficient As(III) removal without the use of costly chemicals. Adopting a zero-chemical approach resolves issues related to the generation of unwanted by-products, chemical handling and storage, and complex supply chains.

Operating FeEC within a biological bed also enhances As uptake by the released Fe. The As/Fe ratio in the biotic embedded-FeEC column was 0.05 (mol:mol) (considering a theoretical 1.85 mg/L Fe release), while it was 0.04 (mol:mol) (1.73 mg/L Fe release) in the supernatant-FeEC column. This translates to a lower Fe dosage requirement to achieve the desired As removal, leading to reduced operational costs, sludge generation, backwashing frequency, and environmental impact. However, conducting a Life Cycle Assessment (LCA) for the novel system described in this work is essential to thoroughly evaluate its environmental impact throughout its entire life cycle. This evaluation is crucial for making informed decisions regarding sustainable water management. Therefore, it is recommended to undertake a comprehensive LCA of the biotic embedded-FeEC systems and compare the findings with conventional technologies, such as chemical oxidation and chemical coagulation. This comparative analysis will provide valuable insights for assessing the system's environmental sustainability and guiding future decision-making processes. Moreover, while the biotic embedded-FeEC system removed 81% of the influent 150 µg/L As(III) and, the removal was not below the WHO guideline value of 10 µg/L, the embedded-FeEC system can be adjusted based on the required level of As removal. One of the main factors that influences As removal during FeEC is the amount of Fe dosed and as observed from batch experiments (Fig. S3.2), the removal of As can be improved by changing the Fe dosage or CD. Therefore, in

the current study or in situations where the As concentration is higher than 150 µg/L, by applying a higher current (I), the Fe dosage can be increased, thereby improving removal efficacy and enabling the attainment of removal levels below 1 µg/L (Dutch drinking water target), as observed in batch experiments (Fig. S3.2).

It is important to note that embedded-FeEC systems exhibit higher energy consumption compared to operating FeEC in water. This can be considered a drawback since energy consumption significantly impacts operational costs. However, by fine-tuning the operational parameters, the energy consumption of embedded-FeEC systems can be optimised. For example, operating at a relatively higher flow rate (5 m/h) or lower pH (7.0) results in a smaller increase in energy consumption (51% and 57% increase, respectively) compared to the reference condition (82% increase) (Fig. 3.6). This can be attributed to deep-bed infiltration of the Fe(III)-precipitates under higher flow rate and lower pH conditions (Fig. 3.5). The deep-bed infiltration phenomenon minimises the accumulation of Fe(III)-precipitates near the electrodes, thereby reducing the impact on cell resistance and effective electrode surface area.

The findings in this study introduce a promising avenue for water treatment by exploring into the idea of embedding and operating FeEC within a biological As(III) oxidising filter bed. However, the system was operated under controlled laboratory conditions using model water that does not accurately reflect natural groundwater conditions. In reality, natural groundwater exhibits variations in pH, the presence of competing ions (e.g., phosphate and silicate), fluctuating As concentrations, and other factors known to influence As removal by FeEC. Therefore, although the laboratory findings provided proof of concept, demonstrating the feasibility and advantages of biotic embedded-FeEC systems for As(III) removal, it is strongly recommended to conduct further testing by operating the system with natural groundwater under diverse environmental conditions. This will provide additional insights and validation of the novelty of the proposed system. While the biotic and abiotic embedded-FeEC systems developed in this study were operated for 11 and 7 hours, respectively, over three consecutive days, conducting a long-term operational study is crucial to assess their sustained effectiveness, reliability, and environmental impact. This approach ensures informed decision-making for widespread implementation and addresses evolving challenges over time. For example, continuous operation of abiotic embedded-FeEC systems showed an increase in cell resistance and applied voltage (for constant Fe dosage or applied current) over time (Fig. 3.6). This increase in cell potential can reach the limit of the DC current supplier (30 V in our system), beyond which the system cannot supply the required Fe dosage. Consequently, this reduction in efficiency necessitates a backwash to remove the accumulated Fe(III)-precipitates,

thereby reducing the increased cell resistance and restoring the system to its initial performance stage. Moreover, the long-term application of FeEC systems revealed a reduction in the amount of Fe dosage in the bulk solution for an applied current due to the development of passivation layers on the electrode surface, impacting efficiency (van Genuchten et al., 2016). Therefore, it is recommended to conduct a comprehensive long-term study with embedded-FeEC systems before practical implementation to thoroughly investigate and address potential challenges associated with the system. Identifying and mitigating these challenges will be crucial to ensure the effectiveness and sustainability of this innovative strategy in real-world applications.

3.4 Conclusions

This study focused on the implementation of horizontally embedded FeEC within a biologically active filter bed for As(III) removal. The performance of this system was compared to FeEC operated in the supernatant water and FeEC embedded in an abiotic filter bed. The results demonstrated that the biotic embedded-FeEC system, where As(III) was first biologically oxidised and then treated with FeEC, achieved a higher As(III) removal efficacy (81%) compared to operating FeEC in the supernatant water prior to biological oxidation (67%). Moreover, the As(III) removal in the biotic embedded-FeEC system (81%) was similar to the removal observed when embedded-FeEC was operated in an abiotic bed with As(V)-contaminated water (85%). However, it should be noted that the embedded-FeEC systems exhibited higher energy requirements compared to operating FeEC in the supernatant water. The efficacy of As removal and energy consumption in these embedded-FeEC systems was further influenced by the deep-bed infiltration of Fe(III)-precipitates, which can be controlled by adjusting operational parameters such as flow rate and pH. Nevertheless, the novelty of the embedded-FeEC system lies in leveraging biological As(III) oxidation within rapid sand filter beds of conventional aeration-filtration systems to effectively remove oxidised As(V) within the bed, without the need for chemicals or significant additional infrastructure.

References

- Ahmad, A., Cornelissen, E., van de Wetering, S., van Dijk, T., van Genuchten, C., Bundschuh, J., van der Wal, A., & Bhattacharya, P. (2018). Arsenite removal in groundwater treatment plants by sequential Permanganate—Ferric treatment. *Journal of Water Process Engineering*, 26, 221–229. <https://doi.org/10.1016/J.JWPE.2018.10.014>
- Alka, S., Shahir, S., Ibrahim, N., Ndejiko, M. J., Vo, D. V. N., & Manan, F. A. (2021). Arsenic removal technologies and future trends: A mini review. *Journal of Cleaner Production*, 278. <https://doi.org/10.1016/J.JCLEPRO.2020.123805>
- Amrose, S. E., Bandaru, S. R. S., Delaire, C., van Genuchten, C. M., Dutta, A., DebSarkar, A., Orr, C., Roy, J., Das, A., & Gadgil, A. J. (2014). Electro-chemical arsenic remediation: Field trials in West Bengal. *Science of the Total Environment*, 488–489(1), 539–546. <https://doi.org/10.1016/j.scitotenv.2013.11.074>
- Bandaru, S. R. S., Roy, A., Gadgil, A. J., & van Genuchten, C. M. (2020). Long-term electrode behavior during treatment of arsenic contaminated groundwater by a pilot-scale iron electrocoagulation system. *Water Research*, 175, 115668. <https://doi.org/10.1016/j.watres.2020.115668>
- Delaire, C., Amrose, S., Zhang, M., Hake, J., & Gadgil, A. (2017). How do operating conditions affect As(III) removal by iron electrocoagulation? *Water Research*, 112, 185–194. <https://doi.org/10.1016/j.watres.2017.01.030>
- Dixit, S., & Hering, J. G. (2003). Comparison of Arsenic(V) and Arsenic(III) Sorption onto Iron Oxide Minerals: Implications for Arsenic Mobility. *Environmental Science and Technology*, 37(18), 4182–4189. <https://doi.org/10.1021/ES030309T>
- Garg, S., Jiang, C., & Waite, T. D. (2018). Impact of pH on Iron Redox Transformations in Simulated Freshwaters Containing Natural Organic Matter. *Environmental Science and Technology*, 52(22), 13184–13194. https://doi.org/10.1021/ACS.EST.8B03855/ASSET/IMAGES/LARGE/ES-2018-03855R_0006.JPEG
- Gude, J. C. J., Joris, K., Huysman, K., Rietveld, L. C., & van Halem, D. (2018a). Effect of supernatant water level on As removal in biological rapid sand filters. *Water Research X*, 1. <https://doi.org/10.1016/j.wroa.2018.100013>
- Gude, J. C. J., Rietveld, L. C., & van Halem, D. (2018b). As (III) removal in rapid filters: Effect of pH, Fe (II)/Fe (III), filtration velocity and media size. *Water research*, 147, 342–349. <https://doi.org/10.1016/j.watres.2018.10.005>
- Gude, J. C. J., Rietveld, L. C., & van Halem, D. (2016). Fate of low arsenic concentrations during full-scale aeration and rapid filtration. *Water Research*, 88, 566–574. <https://doi.org/10.1016/j.watres.2015.10.034>
- Gude, J. C. J., Rietveld, L. C., & van Halem, D. (2018c). Biological As(III) oxidation in rapid sand filters. *Journal of Water Process Engineering*, 21, 107–115. <https://doi.org/10.1016/j.jwpe.2017.12.003>
- Hug, S. J., & Leupin, O. (2003). Iron-catalysed oxidation of Arsenic(III) by oxygen and by hydrogen peroxide: pH-dependent formation of oxidants in the Fenton reaction. *Environmental Science and Technology*, 37(12), 2734–2742. <https://doi.org/10.1021/es026208x>
- Jackman, T. A., & Hughes, C. L. (2010). Formation of Trihalomethanes in Soil and Groundwater by the Release of Sodium Hypochlorite. *Ground Water Monitoring & Remediation*, 30(1), 74–78. <https://doi.org/10.1111/j.1745-6592.2009.01266.x>
- Kapaj, S., Peterson, H., Liber, K., & Bhattacharya, P. (2006). Human health effects from chronic arsenic poisoning - A review. *Journal of Environmental Science and Health - Part A Toxic/Hazardous Substances and Environmental Engineering*, 41(10), 2399–2428. <https://doi.org/10.1080/10934520600873571>
- Katsoyiannis, I. A., & Zouboulis, A. I. (2004). Application of biological processes for the removal of arsenic from groundwaters. *Water Research*, 38(1), 17–26. <https://doi.org/10.1016/j.watres.2003.09.011>

- King, D. W., Lounsbury, H. A., & Millero, F. J. (1995). Rates and Mechanism of Fe(II) Oxidation at Nanomolar Total Iron Concentrations. *Environmental Science and Technology*, 29(3), 818–824. <https://doi.org/10.1021/ES00003A033>
- Kowalski, K. P. (2014). Advanced Arsenic Removal Technologies Review. *Chemistry of Advanced Environmental Purification Processes of Water: Fundamentals and Applications*, 285–337. <https://doi.org/10.1016/B978-0-444-53178-0.00008-0>
- Kumpiene, J., Engström, K., Pinedo Taquia, A., Carabante, I., & Bjuhr, J. (2023). Arsenic immobilisation in soil using electricity-induced spreading of iron in situ. *Journal of Environmental Management*, 325. <https://doi.org/10.1016/J.JENVMAN.2022.116467>
- Lytle, D. A., Chen, A. S., Sorg, T. J., Phillips, S., & French, K. (2007). Microbial As(III) oxidation in water treatment plant filters. *Journal - American Water Works Association*, 99(12), 72–86. <https://doi.org/10.1002/j.1551-8833.2007.tb08108.x>
- Mollah, M. Y. A., Morkovsky, P., Gomes, J. A. G., Kesmez, M., Parga, J., & Cocke, D. L. (2004). Fundamentals, present and future perspectives of electrocoagulation. *Journal of Hazardous Materials*, 114(1–3), 199–210. <https://doi.org/10.1016/j.jhazmat.2004.08.009>
- Müller, S., Behrends, T., & van Genuchten, C. M. (2019). Sustaining efficient production of aqueous iron during repeated operation of Fe(0)-electrocoagulation. *Water Research*, 155, 455–464. <https://doi.org/10.1016/j.watres.2018.11.060>
- Roberts, L. C., Hug, S. J., Ruettimann, T., Billah, M., Khan, A. W., & Rahman, M. T. (2004). Arsenic Removal with Iron(II) and Iron(III) in Waters with High Silicate and Phosphate Concentrations. *Environmental Science and Technology*, 38(1), 307–315. <https://doi.org/10.1021/es0343205>
- Roy, M., van Genuchten, C. M., Rietveld, L., & van Halem, D. (2020). Integrating biological As(III) oxidation with Fe(0) electrocoagulation for arsenic removal from groundwater. *Water Research*, 188, 116531. <https://doi.org/10.1016/j.watres.2020.116531>
- Sodhi, K. K., Kumar, M., Agrawal, P. K., & Singh, D. K. (2019). Perspectives on arsenic toxicity, carcinogenicity and its systemic remediation strategies. *Environmental Technology and Innovation*, 16. <https://doi.org/10.1016/J.ETI.2019.100462>
- Sorlini, S., & Gialdini, F. (2010). Conventional oxidation treatments for the removal of arsenic with chlorine dioxide, hypochlorite, potassium permanganate and monochloramine. *Water Research*, 44(19), 5653–5659. <https://doi.org/10.1016/j.watres.2010.06.032>
- Steinmaus, C., Ferreccio, C., Acevedo, J., Yuan, Y., Liaw, J., Durán, V., Cuevas, S., García, J., Meza, R., Valdés, R., Valdés, G., Benítez, H., Van Der Linde, V., Villagra, V., Cantor, K. P., Moore, L. E., Perez, S. G., Steinmaus, S., & Smith, A. H. (2014). Increased lung and bladder cancer incidence in adults after in utero and early-life arsenic exposure. *Cancer Epidemiology, Biomarkers & Prevention: A Publication of the American Association for Cancer Research, Cosponsored by the American Society of Preventive Oncology*, 23(8), 1529–1538. <https://doi.org/10.1158/1055-9965.EPI-14-0059>
- van Genuchten, C. M., Bandaru, S. R. S., Surorova, E., Amrose, S. E., Gadgil, A. J., & Peña, J. (2016). Formation of macroscopic surface layers on Fe(0) electrocoagulation electrodes during an extended field trial of arsenic treatment. *Chemosphere*, 153, 270–279. <https://doi.org/10.1016/j.chemosphere.2016.03.027>
- van Genuchten, C. M., Behrends, T., & Dideriksen, K. (2019). Emerging investigator series: Interdependency of green rust transformation and the partitioning and binding mode of arsenic. *Environmental Science: Processes and Impacts*, 21(9), 1459–1476. <https://doi.org/10.1039/C9EM00267G>
- van Genuchten, C. M., Behrends, T., Kraal, P., Stipp, S. L. S., & Dideriksen, K. (2018). Controls on the formation of Fe(II,III) (hydr)oxides by Fe(0) electrolysis. *Electrochimica Acta*, 286, 324–338. <https://doi.org/10.1016/j.electacta.2018.08.031>

- van Genuchten, C. M., Behrends, T., Stipp, S. L. S., & Dideriksen, K. (2020). Achieving arsenic concentrations of $<1 \mu\text{g/L}$ by Fe(0) electrolysis: The exceptional performance of magnetite. *Water Research*, 168, 115170. <https://doi.org/10.1016/j.watres.2019.115170>
- van Genuchten, C. M., Dalby, K. N., Ceccato, M., Stipp, S. L. S., & Dideriksen, K. (2017). Factors affecting the Faradaic efficiency of Fe(0) electrocoagulation. *Journal of Environmental Chemical Engineering*, 5(5), 4958–4968. <https://doi.org/10.1016/J.JECE.2017.09.008>
- van Genuchten, Case M., Addy, S. E. A., Peña, J., & Gadgil, A. J. (2012). Removing arsenic from synthetic groundwater with iron electrocoagulation: An Fe and As K-edge EXAFS study. *Environmental Science and Technology*, 46(2), 986–994. <https://doi.org/10.1021/es201913a>
- van Genuchten, Case M., Peña, J., Amrose, S. E., & Gadgil, A. J. (2014). Structure of Fe(III) precipitates generated by the electrolytic dissolution of Fe(0) in the presence of groundwater ions. *Geochimica et Cosmochimica Acta*, 127, 285–304. <https://doi.org/10.1016/J.GCA.2013.11.044>
- Wan, W., Pepping, T. J., Banerji, T., Chaudhari, S., & Giammar, D. E. (2011). Effects of water chemistry on arsenic removal from drinking water by electrocoagulation. *Water Research*, 45(1), 384–392. <https://doi.org/10.1016/j.watres.2010.08.016>
- World Health Organization. (2004). Guidelines for Drinking-water Quality, vol. 1. Recommendations, 3rd ed. World Health Organization, Geneva, Switzerland.
- Yang, L., Li, X., Chu, Z., Ren, Y., & Zhang, J. (2014). Distribution and genetic diversity of the microorganisms in the biofilter for the simultaneous removal of arsenic, iron and manganese from simulated groundwater. *Bioresource Technology*, 156, 384–388. <https://doi.org/10.1016/J.BIORTECH.2014.01.067>

Appendix

S3.1 Batch FeEC reactor

The batch reactor consisted of a 1 L glass beaker containing 0.9 L tap water spiked with 150 $\mu\text{g/L}$ As(V). The FeEC cell was comprised of two circular perforated Fe electrodes (one anode and one cathode, mild steel) immersed entirely in the solution (Fig. S3.1). The anode and cathode were 75 and 55 mm in diameter, respectively, and were horizontally immersed (cathode above anode) with an inter-electrode gap of 1.5 cm, which was maintained by plastic spacers (Fig. S3.5). Before the start of the experiment, the electrodes were cleaned with sandpaper, immersed in 0.1 M HCl solution for 1 hour and washed with demi-water to remove any scale and Fe precipitates. A direct current (DC) was passed through the electrodes using a DC power supply (TENMA 72–10500 Power Supply, 30V, 3A) to generate the Fe(III)-precipitates. The initial pH (monitored by WTW Sentix 940) and DO (monitored by SI Analytics FDO 1100 IDS) varied between 7.8 to 8.0 and 8.3 to 9.3 mg/L, respectively. A magnetic stirrer was set at 120 to 160 rpm to prevent the settling of the formed Fe(III)-flocs and ensure uniform solution mixing during the experiments and sampling procedures.

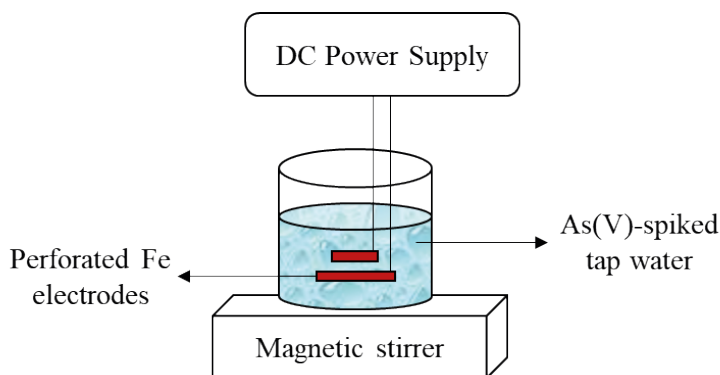


Fig. S3.1. Schematic overview of the batch FeEC reactor.

In FeEC, As removal is dependent on the amount of Fe dosed into the system (Roy et al., 2020). The amount Fe released by the anode during FeEC is defined by the charge dosage (CD) (q in C/L) following Faraday's law (eq. S3.1) (Roy et al., 2020). The batch experiments were performed by applying a CD (or Fe dosage) in the range between 5 to 35 C/L under a constant charge dosage rate (CDR) of 5 C/L/min. The CDR (dq/dt in C/L/min) controls the rate of Fe dosage and can be defined by eq. S3.2 by Faraday's law. The corresponding current (to be applied for the corresponding CD), electrolysis

time, and the theoretical Fe generated from the anode during the batch experiments were calculated from eq. S3.1 and S3.2. To determine the As(V) removal efficacy for an applied CD, water samples (filtered and unfiltered) were collected before and 5 to 10 min after the electrolysis time (to ensure complete oxidation of the released Fe) and analysed for total dissolved As and Fe.

$$W = \frac{qM}{nF} = \frac{ItM}{nFV} \quad (\text{S3.1})$$

$$\frac{dq}{dt} = \frac{I}{V} \quad (\text{S3.2})$$

where, W = Amount of generated Fe (mg/L); I = Applied current (A); t = Electrolysis time (s); M = Molecular weight of Fe (mg/mol) = 55845; F = Faraday's constant (96485 C/mol); n = Number of transferred electrons (2 for Fe); V = Solution volume (L)

S3.2 As removal in batch FeEC

Fig. S3.2 shows the dissolved As(V) concentration after batch FeEC experiments across the different applied CD (between 5 to 35 C/L) with a constant CDR of 5 C/L/min. The results show that with an increase in CD and corresponding increase in the released Fe, the dissolved As(V) concentration decreased, which is consistent with previous FeEC batch studies (Roy et al., 2020; Tong et al., 2014). Measurements of the total Fe released for a given CD revealed a Faradaic efficiency near 1, which is also in line with previous studies (van Genuchten et al., 2018; van Genuchten et al., 2017). Furthermore, all released Fe(II) was oxidised and formed Fe(III)-precipitates, with no residual Fe observed in the filtered samples.

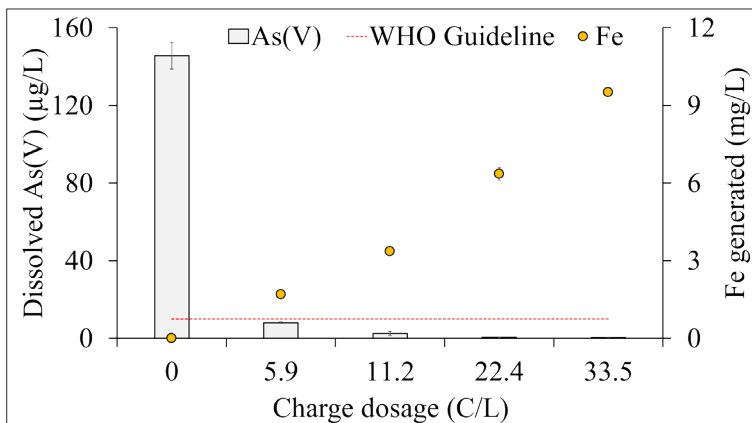


Fig. S3.2. Dissolved As(V) concentration and the corresponding Fe dosed after FeEC batch experiments by applying different CD under 5 C/L/min CDR in tap water containing 145 ± 7 µg/L As(V).

With a CD of 5.9 C/L (1.7 mg/L Fe generated), the initial $145 \pm 7 \mu\text{g/L As(V)}$ was removed below the WHO guideline ($10 \mu\text{g/L}$), and with CD of 22.4 C/L (6.36 mg/L Fe generated), removal below $1 \mu\text{g/L}$ was also achieved, which is the new target for Dutch drinking water companies. The Fe/As ratio (mg:mg) to remove $150 \mu\text{g/L As(V)}$ below $10 \mu\text{g/L}$ and $1 \mu\text{g/L}$ was found out to be approximately 12 and 43 respectively, which is in-line with previous studies (Roy et al., 2020; Tong et al., 2014). From these batch study results, a CD of approximately 6.4 C/L (1.85 mg/L Fe as per eq. S3.1) was selected for the subsequent flow-through embedded-FeEC experiments.

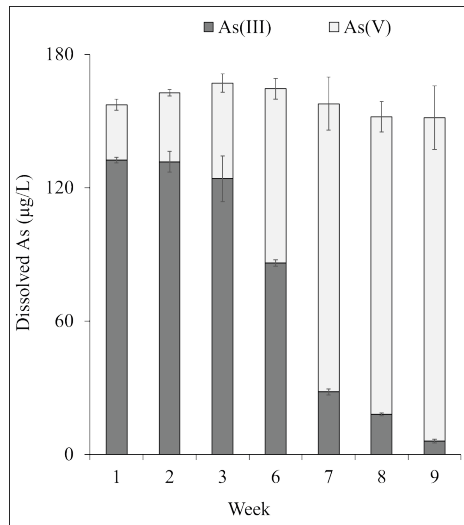


Fig. S3.3. As(III) and As(V) concentration in the effluent of the duplicate biotic columns ripened with $150 \pm 20 \mu\text{g/L As(III)}$ -spiked tap water for nine weeks.

S3.3 Electrode characteristics

Perforated steel electrodes (R: 12 mm, T: 16 mm), with an open area of 51% and a thickness of 2 mm, were used in all FeEC experiments (Fig. S3.4). The electrochemical cell consisted of an anode (diameter = 74 mm) and a cathode (diameter = 55 mm). Characteristics of the used material, including production numbers, chemical composition, and density, can be found in Table S3.1.

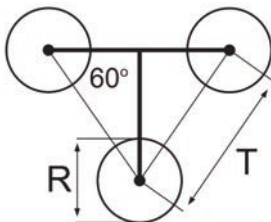


Fig. S3.4. Schematic overview of perforated plate configuration used for FeEC experiments.

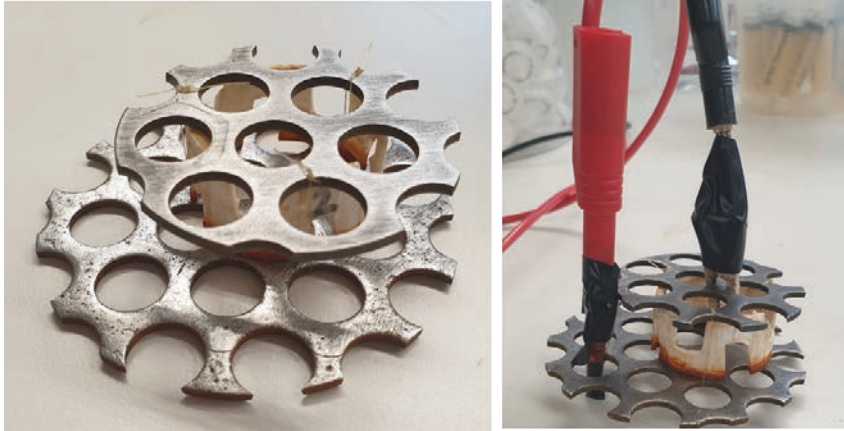


Fig. S3.5. Anode and cathode configuration (left) and connection of the electrodes to the DC power source (right). In this configuration the cathode can be seen on top of the anode, connected by nylon wire and a plastic spacer in between.

Table S3.1. Properties of the electrode materials in FeEC experiments

| Group | Property | Value / description |
|----------------------|------------------------------|---|
| General properties | Material | STW22 (DD11; 1.0332) |
| | Description | Low-carbon, warm rolled non-alloy steel |
| | Density [kg/m ³] | 7850 |
| Chemical composition | C [max %] | 0.10 |
| | Si [max %] | 0.15 |
| | P [max %] | 0.035 |
| | S [max %] | 0.035 |
| | Mn [max %] | 0.037 |
| | N [max %] | 0.007 |

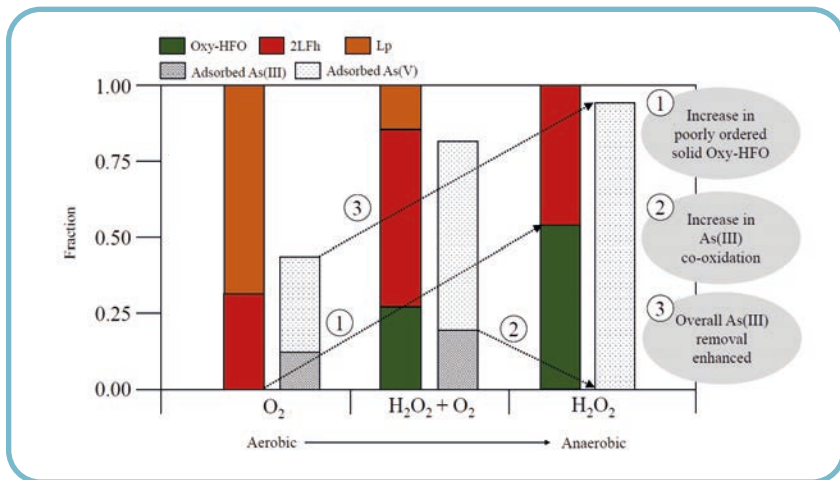
Table S3.2: Tap water composition

| Species | Initial value | Species | Initial value |
|-------------------------------|----------------|------------------|-----------------|
| pH | 7.8-8.0 | Fe | 0 |
| PO ₄ ³⁻ | 0 | As | 0 |
| SO ₄ ²⁻ | 52.1 ± 1 mg/L | Ca ²⁺ | 49.8 ± 0.3 mg/L |
| NO ₂ ⁻ | 0 | Na ⁺ | 41.5 ± 0.4 mg/L |
| NO ₃ ⁻ | 2.4 ± 0.3 mg/L | Si | 2.2 ± 0.1 mg/L |
| NH ₄ ⁺ | 0 | Mg ²⁺ | 7 ± 0.1 mg/L |



Chapter 4

Groundwater native-Fe(II) oxidation prior to aeration with H_2O_2 to enhance As(III) removal



This chapter is based on:

Roy, M., van Genuchten, C. M., Rietveld, L., & van Halem, D. (2022). Groundwater-native Fe (II) oxidation prior to aeration with H_2O_2 to enhance As (III) removal. *Water Research*, 223, 119007.

Abstract

Groundwater contaminated with arsenic (As) must be treated prior to drinking, as human exposure to As at toxic levels can cause various diseases including cancer. Conventional aeration-filtration applied to anaerobic arsenite (As(III))-contaminated groundwater can remove As(III) by co-oxidising native-iron (Fe(II)) and As(III) with dissolved oxygen (DO) inserted during aeration. However, the As(III) removal efficacy of conventional aeration can be low, in part, because of incomplete As(III) oxidation to readily sorbed arsenate (As(V)). In this work, we investigated a new approach to enhance As(III) co-removal with groundwater native-Fe(II) by the anaerobic addition of hydrogen peroxide (H_2O_2) prior to aeration. Experiments were performed to co-oxidise Fe(II) and As(III) with H_2O_2 (anaerobically), DO (referred as O_2 in this chapter) (aerobically), and by sequentially adding of H_2O_2 and O_2 . Aqueous As(III) and As(V) measurements after the reaction were coupled with solid-phase speciation by Fe and As K-edge X-ray absorption spectroscopy (XAS). We found that complete anaerobic oxidation of $100 \mu\text{M}$ Fe(II) with $100 \mu\text{M}$ H_2O_2 resulted in co-removal of 95% of $7 \mu\text{M}$ As(III) compared to 44% with $8.0\text{--}9.0 \text{ mg/L}$ O_2 . Furthermore, we found that with $100 \mu\text{M}$ Fe(II), the initial Fe(II): H_2O_2 ratio was a critical parameter to remove $7 \mu\text{M}$ As(III) to below the $10 \mu\text{g/L}$ ($0.13 \mu\text{M}$) WHO guideline, where ratios of 1:4 (mol:mol) Fe(II): H_2O_2 led to As(III) removal matching that of $7 \mu\text{M}$ As(V). The improved As(III) removal with H_2O_2 was found to occur partly because of the well-established enhanced efficacy of As(III) oxidation in Fe(II)+ H_2O_2 systems relatively to Fe(II)+ O_2 systems. However, the XAS results unambiguously demonstrated that a large factor in the improved As(III) removal was also due to a systematic decrease in crystallinity, and thus increase in specific surface area, of the generated Fe(III) (oxyhydr)oxides from lepidocrocite in the Fe(II)+ O_2 system to poorly-ordered Fe(III)-precipitates in the Fe(II)+ H_2O_2 system. The combined roles of H_2O_2 (enhanced As(III) oxidation and structural modification) can be easily overlooked when only aqueous species are measured, but this dual impact must be considered for accurate predictions of As removal in groundwater treatment.

Keywords: Arsenic, Iron, Hydrogen Peroxide, Groundwater, Drinking water

4.1 Introduction

An estimated 94 to 220 million people are exposed to naturally occurring arsenic (As) in groundwater (mainly as arsenite As(III)) at levels above the World Health Organization (WHO) drinking water guideline of 10 µg/L (0.13 µM) (Podgorski & Berg, 2020). Exposure to As-contaminated water can pose major threats to human health causing diseases such as skin, bladder and lung cancers, reproductive disorders, and neuro-developmental problems in children (Kapaj et al., 2006; Tseng, 1977). Therefore, it is crucial that groundwater contaminated with toxic levels of As be treated prior to drinking.

Conventional aeration-filtration is a common treatment method that involves aerating anaerobic As(III)-rich groundwater that contains co-occurring iron (Fe(II)), followed by filtration of the generated precipitates (Gude et al., 2016; Hug & Leupin, 2003; Roberts et al., 2004). This method relies on As(III) and Fe(II) co-oxidation by dissolved oxygen (DO) (referred as O₂ in this chapter) to form particulate Fe(III) (oxyhydr)oxides (or Fe(III)-precipitates/Fe solids) that can bind As (Bora et al., 2016; Gude et al., 2016). Compared to other techniques, aeration-filtration is advantageous as it is economically attractive, no dosing of chemicals is required, it removes various groundwater contaminants (Fe(II), ammonium, manganese) simultaneously, and it generates biologically stable drinking water (low in nutrients), thereby ensuring microbial safety in distribution networks (Annaduzzaman et al., 2021a; Gude et al., 2017). While conventional aeration-filtration is applied widely in groundwater treatment and Fe(III)-precipitates are very good adsorbents for As, this conventional approach can be ineffective for As(III) removal, which often demands additional dosing of Fe to meet drinking water guidelines (Annaduzzaman et al., 2018; Annaduzzaman et al., 2021b; Sharma et al., 2016). For example, previous studies have shown that co-removal of As(III) with Fe(II) through aeration-filtration only yields between 8 to 50% removal, depending on the initial As concentration, Fe/As ratio, and the presence of other competing ions (i.e. Mn(II), PO₄³⁻) (van Genuchten & Ahmad, 2020; Holm & Wilson, 2006; Li et al., 2016).

The low efficacy of As(III) co-removal with groundwater native-Fe(II) during aeration-filtration can be due to several factors. First, Fe(III)-precipitates generated through aeration (by O₂) can be moderately crystalline (Ahmad et al., 2019) with a lower reactive specific surface area than the poorly-ordered Fe(III)-precipitates generated with stronger oxidants, such as HOCl and KMnO₄ (Ahmad et al., 2019). Second, Fe(III)-precipitates have orders of magnitude lower sorption affinity for As(III) than oxidised arsenate (As(V)) and As(III) oxidation by O₂ is slow and partial (Bissen & Frimmel, 2003; Gude et al., 2017; Roberts et al., 2004). Third, the relatively high pH resulting from

CO₂ degassing during groundwater aeration creates a less favourable environment for As(V) adsorption (Annaduzzaman et al., 2021b; Dixit & Hering, 2003), which can be minimised by avoiding aeration. Thus, the co-removal of groundwater As(III) with native-Fe(II) can be optimised by forming poorly-ordered Fe(III)-precipitates, with high reactive surface area, and by co-oxidising As(III) effectively and rapidly prior to aeration to minimise pH increase induced by CO₂ efflux.

The addition of hydrogen peroxide (H₂O₂) is an attractive option for anaerobic As(III) and Fe(II) co-oxidation because H₂O₂ reacts rapidly with Fe(II), and is relatively inexpensive to generate on- or off-site, and is considered a green alternative to harsher chemical oxidants because of its non-toxic reaction products (Bandaru et al., 2020; Pham et al., 2012a; Pham et al., 2012b). Additionally, H₂O₂ is an intermediate formed during Fe(II) oxidation by O₂ (Hug & Leupin, 2003) and may as such be considered a natural additive in anaerobic groundwater treatment. In principle, the presence of H₂O₂ in As(III) and Fe(II)-rich solutions is beneficial because it oxidises Fe(II) at a rate four orders of magnitude higher than O₂ (Bandaru et al., 2020; King & Farlow, 2000; King, 1998), which can result in the generation of poorly-ordered Fe(III)-precipitates (Bandaru et al., 2020; van Genuchten & Peña, 2017). In addition, while direct As(III) oxidation by H₂O₂ is kinetically limited, the oxidation of Fe(II) by H₂O₂ leads to a high stoichiometric yield of reactive oxygen species (ROS), such as *OH or Fe(IV), that can effectively oxidise As(III) (Hug & Leupin, 2003). The theoretical ROS yield per mol of oxidised Fe(II) is 1:1 for H₂O₂ compared to 1:3 for O₂ (Hug & Leupin, 2003), which would translate to more As(III) co-oxidation per mole of oxidised Fe(II) if H₂O₂ is applied. While Fenton-type systems (i.e., those containing Fe(II)+H₂O₂) have been investigated in the context of As(III) removal previously (Bandaru et al., 2020; Catrouillet et al., 2020), most studies performed, are over-dosing H₂O₂ in solutions open to the atmosphere, initially containing O₂. Careful control of the H₂O₂ input and thus the Fe(II):H₂O₂ ratio, could thus be more effective, particularly in the case of treating anaerobic groundwater, because it can optimise the use of natural Fe(II), minimise the consumption of H₂O₂, and can avoid an increase in pH due to CO₂ efflux.

In this study a novel approach is therefore proposed to enhance As(III) removal in groundwater with the native-Fe(II), through anaerobic oxidation of the native-Fe(II) by H₂O₂ prior to aeration. Moreover, we compared the impact of oxidising Fe(II) with O₂ (aerobically), H₂O₂ (anaerobically), and sequentially with H₂O₂ (anaerobically) followed by O₂ (aerobically) on As(III) removal. The reactions were tracked by aqueous As(III) and As(V) speciation measurements and by characterisation of the solid reaction products by synchrotron-based Fe and As K-edge X-ray absorption spectroscopy (XAS). In addition, we examined the impact of under- and over-dosage of H₂O₂ (anaerobically)

on the extent of Fe(II) and As(III) co-oxidation. Finally, we validated this approach by studying H₂O₂ addition to Fe(II)-containing raw anaerobic groundwater.

4.2 Materials and methods

4.2.1 Chemicals

Ultrapure water (18.2 mΩ.cm) was used to prepare all experimental solutions and was spiked with to 2.5 mM NaHCO₃ and 10 mM NaCl by dissolving 0.32 g of sodium bicarbonate (J.T. Baker™) and 0.88 g of sodium chloride (J.T. Baker™) in 1.5 L. The concentration of NaHCO₃ (2.5 mM) and NaCl (10 mM) were selected to achieve an alkalinity and conductivity (990 μS/cm) similar to previous studies in synthetic groundwater (Ahmad et al., 2019; van Genuchten et al., 2012). As(III), As(V), and Fe(II) were added from stock solutions, which were freshly prepared daily. Stock solutions were generated by dissolving defined amounts of sodium (meta)arsenite (NaAsO₂) or sodium arsenate dibasic heptahydrate (Na₂HAsO₄·7H₂O) (Sigma-Aldrich) to ultrapure water and ferrous sulfate heptahydrate (FeSO₄·7H₂O) (Sigma-Aldrich) to 1 mM HCl respectively. H₂O₂ stock solutions were also freshly diluted with defined volumes of the 30% w/w H₂O₂ solution (Sigma-Aldrich) in ultrapure water. For pH adjustment, 1 M HCl or 1 M NaOH (Merck Millipore) was used.

4.2.2 Experimental setup and procedure

The experiments were conducted at room temperature (20±3°C) in 2 L glass jars with perforated lids (Fig. S4.1). The jars initially contained 1 L of ultrapure water (18.2 mΩ.cm) with 2.5 mM NaHCO₃, 10 mM NaCl, and 7 μM As(III) or As(V). The solution was then purged with N_{2(g)} to obtain O₂ concentrations of <0.1 mg/L and the pH was set to 7.3-7.5. Next, Fe(II) was added to the O₂-purged solution. The oxidation of Fe(II) was initiated by dosing H₂O₂ or O₂ alone or by sequentially dosing H₂O₂ followed by O₂ (H₂O₂+O₂). To dose O₂, an air-pump was used to raise the O₂ level to 8.0-9.0 mg/L (from initial levels of <0.1 mg/L) after adding Fe(II). The solution was mixed with a magnetic stirrer (LABINCO L23) at 150 rpm for 30 min after Fe(II) oxidation began. In H₂O₂ experiments, N_{2(g)} was continuously purged throughout the mixing period to minimise the impact of atmospheric O₂ influx and to maintain O₂ levels <0.1 mg/L. For the sequential H₂O₂+O₂ experiments, partial Fe(II) oxidation was performed first by adding H₂O₂ and mixing for 5 min under continuous N_{2(g)} purging (O₂ <0.1 mg/L), followed by O₂ dosing using the air-pump (O₂ = 8.0-9.0 mg/L) for the remaining 25 min. The pH of all solutions was maintained between 7.3-7.5 during experiments by manual additions of 1 M NaOH or 1 M HCl. The pH and DO were monitored using a multimeter (WTW™ MultiLine™ Multi 3630 IDS).

4.2.3 Experimental conditions

To determine the impact of various Fe(II) oxidant conditions on As(III) co-removal, experiments were performed in the H_2O_2 , O_2 , and sequential $\text{H}_2\text{O}_2+\text{O}_2$ systems by completely oxidising 100 μM Fe(II) with 100 μM H_2O_2 (anaerobically), 8.0–9.0 mg/L O_2 (aerobically), or sequentially by 5, 10, 20, or 40 μM H_2O_2 (anaerobically) followed by O_2 (aerobically). Another set of experiments was performed to examine the effect of H_2O_2 concentration (and thus Fe(II): H_2O_2 ratio) on the co-oxidation and removal of 100 μM Fe(II) and 7 μM As(III). For these experiments, the H_2O_2 concentrations (i.e., 10, 20, 40, 60, 100, 200, 300, and 400 μM) were selected to span the stoichiometric amount required for total Fe(II) oxidation. A set of experiments was also repeated with initial 7 μM As(V) in place of As(III). In addition to laboratory tests, experiments were performed using raw Dutch groundwater, which was obtained directly from the influent of a drinking water treatment plant. For these experiments, the raw anaerobic water (initial composition given in Table S4.1) was spiked with 7 μM As(III). The removal of As(III) was investigated by completely oxidising the groundwater native-Fe(II) with either H_2O_2 or O_2 . In the H_2O_2 experiments with raw groundwater, $\text{N}_{2(\text{g})}$ was not used to decrease the O_2 level to <0.1 mg/L. All experiments were replicated at least twice. A schematic overview of the experimental conditions is shown in Fig. S4.1.

4.2.4 Chemical analysis

During the 30 min reaction time, filtered and unfiltered water samples were collected at 0, 2, 5, 10, 20, and 30 min. Filtration was performed with 0.2 μm polyethersulfone filters (Macherey-Nagel GmbH & Co. KG). Immediately after collection, the samples were acidified with 1% (v/v) ultrapure nitric acid (ROTIPURAN® Ultra 69%) to stop further reactions and dissolve any precipitates. Acidified samples were stored at 4°C until analysis. We refer to Fe measured in the filtered solution as Fe(II), which we verified by measuring Fe(II) in a subset of filtered samples using an Fe cell test kit (Merck Millipore). For dissolved As speciation, we followed the approach described in Gude et al. (2018), which is based on using an anionic exchange resin (Amberlite* IRA-402 chlorite) to separate non-ionic As(III) and negatively-charged As(V). The unfiltered samples were used to determine the total Fe and Fe(III) concentration, where the difference between total Fe and dissolved Fe represented the Fe(III). The samples were analysed for As and Fe (in triplicates) by inductively coupled plasma mass spectrometry (ICP-MS, Analytikal Jena model PlasmaQuant MS).

4.2.5 X-ray absorption spectroscopy

4.2.5.1 Data collection

Fe(III)-precipitates for Fe and As K-edge XAS analysis were collected using filter papers at the end of the oxidation experiments. The filter papers with precipitates attached

were stored at -80°C before affixing the sample (filter and precipitates) to custom sample holders using Kapton tape. Fe and As K-edge XAS data were collected at beam line 2-2 of the Stanford Synchrotron Radiation Lightsource (SSRL, Menlo Park, USA). Fe K-edge XAS data were recorded at room temperature out to $k = 13 \text{ \AA}^{-1}$ and As K-edge XAS data were recorded at liquid nitrogen temperatures ($\approx 80^\circ\text{K}$) in fluorescence mode out to $k = 14 \text{ \AA}^{-1}$. For beam calibration, the maximum of the first derivative of Fe(O) and Au(O) foils was set to 7112 eV and 11919 eV for Fe and As data, respectively. Spectral alignment, averaging and background subtraction of individual spectra were performed using SixPack software (Webb, 2005), following standard procedures described in van Genuchten et al. (2012). Extraction of the Fe K-edge EXAFS spectra was performed using k^3 -weighting and the Fe K-edge EXAFS spectra were Fourier-transformed over the k -range 2 to 11 \AA^{-1} using a Kaiser-Bessel window with dk of 3 \AA^{-1} .

4.2.5.2 Data Analysis

The Fe K-edge EXAFS spectra were analysed by linear combination fits (LCFs) ($k = 2$ to 11 \AA^{-1}) with the SixPack software (Webb, 2005) using the EXAFS spectra of three reference Fe(III) (oxyhydr)oxides: moderately crystalline lepidocrocite (Lp), nanocrystalline 2-line ferrihydrite (2LFh), and highly disordered oxyanion-rich hydrous ferric oxide (oxy-HFO). These three reference Fe(III) (oxyhydr)oxides were selected based on previous studies that report these references reproduced the Fe(III)-precipitates generated by Fe(II) oxidation using a range of chemical oxidants (Ahmad et al., 2019; van Genuchten et al., 2018; van Genuchten et al., 2014). The fraction of the three references in each experimental sample derived from the LCFs was normalised to one.

The As K-edge XANES spectra were analysed by LCFs using SixPack software to determine the fraction of adsorbed As(III) and As(V). The LCFs were performed with a fit range of 11860 to 11880 eV using reference spectra of As(III) and As(V) adsorbed to 2-line ferrihydrite. In the LCFs, negative fractions of the reference spectra were not allowed and the component sum was not constrained to 1. The concentration of adsorbed As(III) and As(V) was calculated by multiplying the LCF-derived fraction of As(III) and As(V) by the concentration of total As removed from solution determined by ICP-MS. We use the As K-edge XAS data primarily to determine the oxidation state of As bound to the solid phase. Shell-by-shell fits of the EXAFS spectra were not performed partly because many of the samples contained multiple As oxidation states, which complicates the interpretation of shell fits (van Genuchten et al., 2012; van Genuchten & Ahmad, 2020). Further details on XAS sample preparation and data collection are given in the appendix (section S4.1).

4.3 Results and discussion

4.3.1 Solid-phase Fe structure and its relation to Fe(II) oxidation kinetics

Fig. 4.1(A) and (B) shows the Fe K-edge EXAFS spectra, and corresponding Fourier transforms, of the three reference Fe(III) (oxyhydr)oxides and the experimental samples generated in the O_2 , H_2O_2 , and sequential $H_2O_2+O_2$ systems. Comparing the EXAFS spectral features of Lp, 2LFh, and oxy-HFO, a peak can be observed in Lp near 7.84 \AA^{-1} , which dampened in 2LFh and disappeared in oxy-HFO. In addition, the first oscillation from $4\text{-}5 \text{ \AA}^{-1}$ is asymmetric in Lp but becomes more symmetric for 2LFh and oxy-HFO, with the oscillations at $k > 8 \text{ \AA}^{-1}$ becoming more broad with lower amplitude from Lp to 2LFh to oxy-HFO. These features are consistent with a progressive decrease in structural order from Lp to 2LFh to oxy-HFO (Toner et al., 2009; van Genuchten et al., 2012). Visual comparison of the EXAFS spectra of the experimental Fe(III)-precipitates indicates that the EXAFS spectrum of the sample generated by O_2 oxidation closely matched the line shape and phase of the Lp EXAFS spectrum. However, a gradual and systematic shift in EXAFS features from Lp to 2LFh and oxy-HFO was observed with an increasing concentration of initial H_2O_2 , and thus increasing fraction of Fe(II) oxidised by H_2O_2 . As shown in the Fourier-transform (Fig. 4.1(B)), these changes in the EXAFS spectra of the samples correspond to a systematic decrease in the amplitude of second-shell peak, which arises from Fe-Fe atomic pairs, suggesting a progressive decrease in structural order with increasing H_2O_2 concentration (Toner et al., 2009; van Genuchten et al., 2012). We assign the second-shell peak with Fe-Fe atomic pairs because no other atoms can be present in the second shell of Fe at high enough concentrations to contribute significantly to this peak (i.e., As can occur in the second shell, but its concentration in the solid phase is too low to be detected in the Fe data).

The LCFs of the EXAFS spectra (Fig. 4.1(C); Table S4.2) confirmed the decrease in Fe(III)-precipitates crystallinity with increasing initial H_2O_2 concentration. The LCFs indicated that the highest fraction of moderately crystalline Lp was present in the sample generated by O_2 oxidation of Fe(II). The fraction of Lp in the precipitates derived by LCFs decreased systematically in favor of poorly-ordered Fe(III)-precipitates (2LFh and oxy-HFO) with increasing Fe(II) oxidation by H_2O_2 . Lp was not detected in the experiments where 100% of Fe(II) was oxidised by H_2O_2 . Instead, the precipitates generated by Fe(II) oxidation with H_2O_2 consisted of 100% poorly-ordered Fe(III)-precipitates (Fig. 4.1(C); Table S4.2). Such formation of a higher fraction of poorly-ordered Fe(III)-precipitates with H_2O_2 compared to O_2 is consistent with the previously reported impact of Fe(II) oxidation rate on Fe(III)-precipitates structure (Ahmad et al., 2019; Bandaru et al., 2020; Catrouillet et al., 2020; van Genuchten & Peña, 2017). The low oxidation rate of Fe(II) with O_2 allows the presence of aqueous Fe(II) to catalyse

the crystallisation of freshly precipitated Fe(III) precursors into Lp (Ahmad et al., 2019; Pedersen et al., 2005). By contrast, H₂O₂ oxidises aqueous Fe(II) too rapidly to permit any Fe(II)-catalysed crystallisation of newly-formed Fe(III)-precipitates (Ahmad et al., 2019; Pedersen et al., 2005).

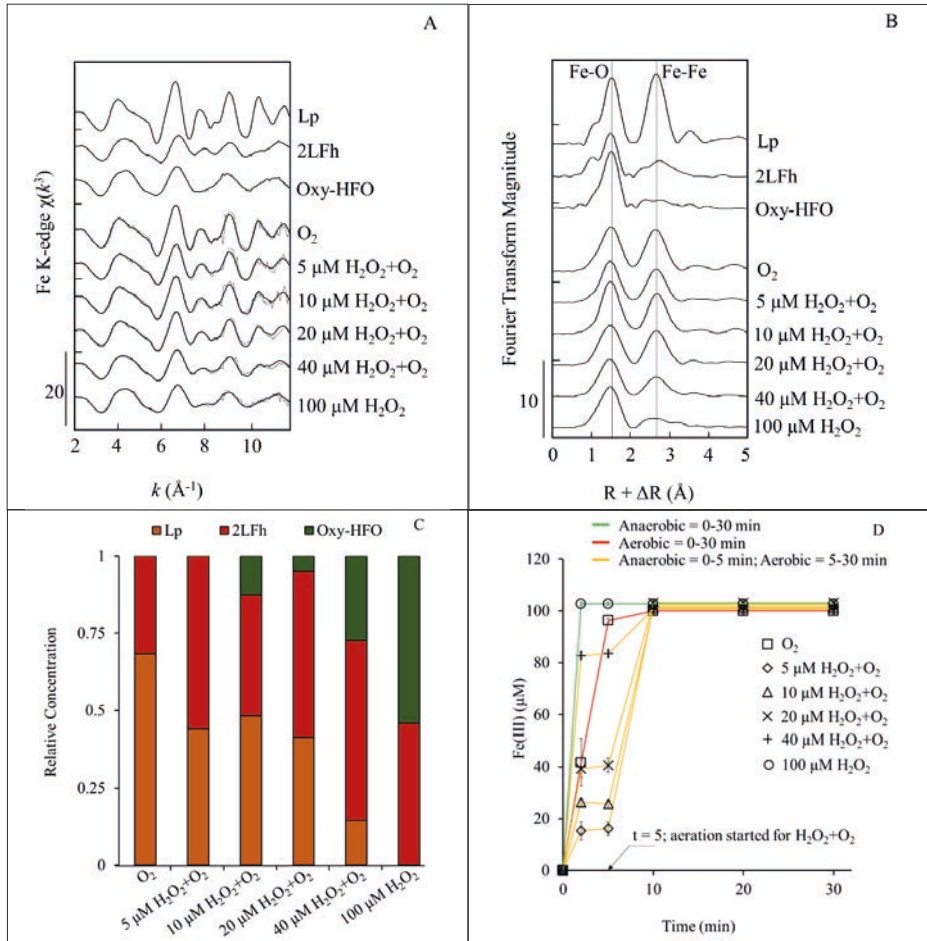


Fig. 4.1. Fe K-edge EXAFS spectra and corresponding Fourier transforms of the Fe(III)-precipitates (**A and B**), relative concentration of lepidocrocite (Lp), 2-line ferrihydrite (2LFh), and oxyanion-rich hydrous ferric oxide (oxy-HFO) in the Fe(III)-precipitates determined from LCFs (**C**), and kinetics of Fe(III) generation over 30 min when $100 \pm 3 \mu\text{M}$ Fe(II) was oxidised by $8.0\text{--}9.0 \text{ mg/L O}_2$ (aerobically; $\tau = 0\text{--}30 \text{ min}$), $100 \mu\text{M H}_2\text{O}_2$ (anaerobically; $\tau = 0\text{--}30 \text{ min}$), or sequentially by 5, 10, 20, or 40 $\mu\text{M H}_2\text{O}_2$ (anaerobically; $\tau = 0\text{--}5 \text{ min}$) followed by $8.0\text{--}9.0 \text{ mg/L O}_2$ (aerobically; $\tau = 5\text{--}30 \text{ min}$). (**D**) The LCF output is overlain on the experimental data in panel A. Solutions initially contained $7 \pm 0.5 \mu\text{M As(III)}$, 2.5 mM NaHCO_3 , and 10 mM NaCl . All Fe(III) formed precipitates and no dissolved Fe(III) was detected (data not shown). Data points and error bars represent the average and standard deviation of the samples obtained from replicate experiments.

To verify rapid Fe(II) oxidation with H_2O_2 , the kinetics of Fe(III) generation was tested over 30 min for the same oxidation conditions (Fig. 4.1(D)) as used to generate the precipitates for XAS analysis (i.e. oxidation of $100\ \mu\text{M}$ Fe(II) in the O_2 , H_2O_2 , and $\text{H}_2\text{O}_2+\text{O}_2$ systems). It was observed that all the Fe(II) was oxidised within 10 min regardless of the oxidant (Fig. 4.1(D)). However, with $100\ \mu\text{M}$ H_2O_2 , complete Fe(II) oxidation was faster (<2 min) than with O_2 (between 5 to 10 min), which is in-line with previous research (Bandaru et al., 2020; King & Farlow, 2000; King, 1998). In the sequential experiments with initial 5, 10, 20 or $40\ \mu\text{M}$ H_2O_2 , Fe(II) oxidation was fast but incomplete, with the expected stoichiometric 2:1 mol:mol ratio of Fe(II) oxidation by H_2O_2 observed for all H_2O_2 experiments. This 2:1 stoichiometry led to residual Fe(II) concentrations of 85, 76, 64, and $17\ \mu\text{M}$ at 5 min using H_2O_2 dosages of 5, 10, 20, and $40\ \mu\text{M}$, respectively, with the remaining Fe(II) oxidised by O_2 added by aeration at $t \times 5$ min. These results show that anaerobic Fe(II) oxidation with H_2O_2 closely followed the expected 2:1 ratio and favoured the formation of poorly-ordered Fe(III)-precipitates, in contrast to O_2 , due to its more rapid oxidation rate with Fe(II).

4.3.2 As(III) removal by Fe(III)-precipitates

Fig. 4.2(A) shows the co-removal of initial $7 \pm 0.5\ \mu\text{M}$ As(III) when oxidising $100 \pm 3\ \mu\text{M}$ Fe(II) in the O_2 , H_2O_2 , and sequential $\text{H}_2\text{O}_2+\text{O}_2$ systems. Comparing the different oxidant conditions, As(III) removal was the lowest in the O_2 system, where the residual dissolved As concentration ($t = 30$ min) was $3.8 \pm 0.2\ \mu\text{M}$ (44% removal). In the sequential $\text{H}_2\text{O}_2+\text{O}_2$ system, As(III) removal was moderate and the residual dissolved As concentration ($t = 30$ min) decreased systematically (3.6 ± 0.2 , 2.9 ± 0.4 , 2.6 ± 0.1 , and $1.3 \pm 0.10\ \mu\text{M}$) with increasing initial H_2O_2 concentration (5, 10, 20, and $40\ \mu\text{M}$ H_2O_2). The most removal of initial As(III) was observed using $100\ \mu\text{M}$ H_2O_2 , with a residual dissolved As concentration ($t = 30$ min) of $0.4 \pm 0.1\ \mu\text{M}$ (95% removal). Thus, the poorest As removal was observed when Fe(II) was oxidised by O_2 alone and removal increased with an increase in the fraction of Fe(II) oxidised by H_2O_2 . This trend is consistent with the increasing fraction of poorly-ordered Fe(III)-precipitates with increasing initial H_2O_2 concentration (Fig. 4.1(C)), as observed in the previous section.

Fig. 4.2(B) shows the As K-edge XANES spectra of samples generated in the O_2 , H_2O_2 , and sequential $\text{H}_2\text{O}_2+\text{O}_2$ systems, with the LCFs of the XANES spectra reported in Table S4.3. The XANES spectra show that As(V) was the dominant species adsorbed on the precipitates, based on the position of the absorption maximum near 11875 eV. The predominance of solid phase As(V) was confirmed by the XANES LCFs (Table S4.3). This suggests effective sorption of As(V) generated via As(III) oxidation by ROS, formed during Fe(II) reactions with both O_2 or H_2O_2 , since direct oxidation of As(III) by O_2 or H_2O_2 in the experimental time frame (30 min) was not feasible (Hug & Leupin, 2003).

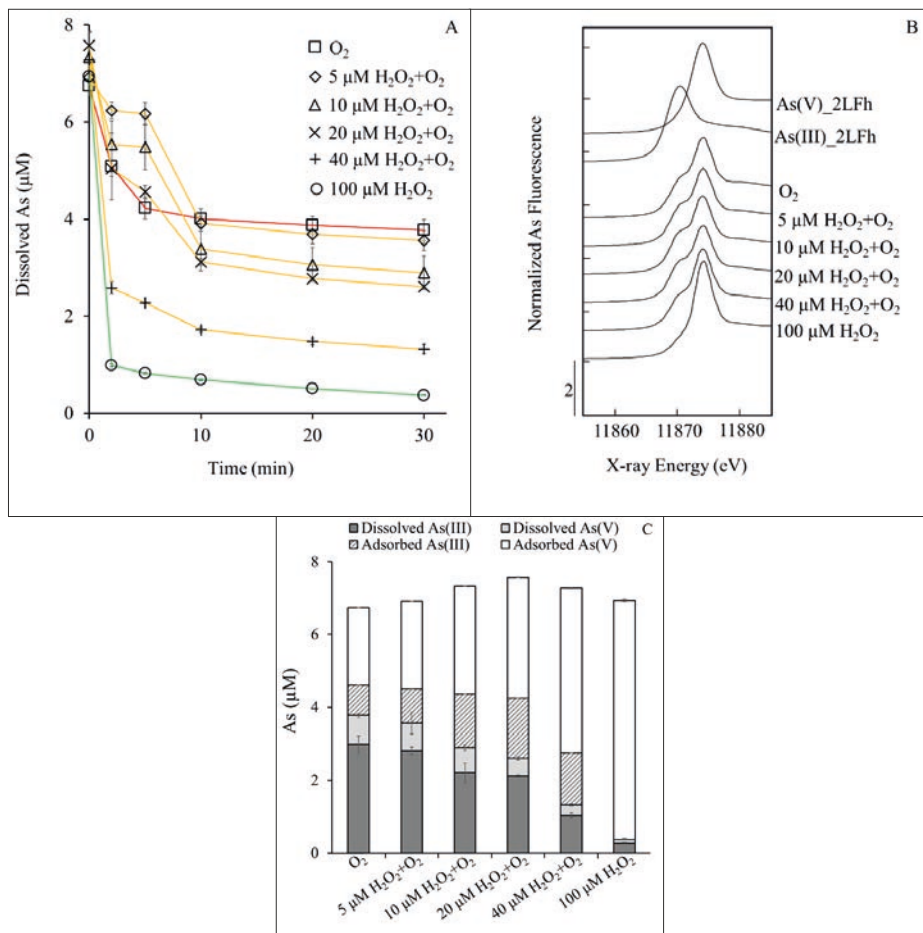


Fig. 4.2. Removal of initial As(III) over 30 min (A), As K-edge XANES spectra of the generated Fe(III)-precipitates (B), and As speciation at the experiment end ($t = 30$ min) when $100 \pm 3 \mu\text{M}$ Fe(II) was oxidised by $8.0\text{--}9.0 \text{ mg/L}$ O₂ (aerobically; $t = 0\text{--}30$ min) (red line), $100 \mu\text{M}$ H₂O₂ (anaerobically; $t = 0\text{--}30$ min) (green line), or sequentially by 5, 10, 20, or 40 μM H₂O₂ (anaerobically; $t = 0\text{--}5$ min) followed by $8.0\text{--}9.0 \text{ mg/L}$ O₂ (aerobically; $t = 5\text{--}30$ min) (yellow line). (C) Solutions initially contained $7 \pm 0.5 \mu\text{M}$ As(III), 2.5 mM NaHCO₃, and 10 mM NaCl. Data points and error bars represent the average and standard deviation of the samples obtained from replicate experiments.

Combining the aqueous As(III) removal results with the measurements of As oxidation state on the precipitates (with XANES LCFs) and in solution (with anionic exchange resins) yields the speciation plot given in Fig. 4.2(C). This plot reveals that, while overall aqueous As(III) removal increased with increasing initial H₂O₂ concentration, the majority of As bound to the precipitates was always As(V) and the majority of residual aqueous As was As(III) for all oxidant conditions. For example, in the O₂ system As(V)

accounted for 2.2 μM of the total adsorbed As content of 3.0 μM (72%), whereas 80% of the 3.8 μM residual As was As(III). Similarly, in the H_2O_2 system, As(V) was 100% of the adsorbed As and As(III) accounted for 72% of the 0.4 μM residual As. These trends were reproduced in the sequential $\text{H}_2\text{O}_2 + \text{O}_2$ system (Fig. 4.2(C)) and are consistent with the orders of magnitude higher sorption affinity of As(V) than As(III) (Roberts et al., 2004). Although the fraction of As(V) and As(III) bound to the precipitates was similar among many of the samples, the total amount of oxidised As(III) increased with increasing H_2O_2 concentration (i.e. total As(V) increased from 2.9 μM in the O_2 system to >6 μM in the H_2O_2 system). The increase in As(III) oxidation with H_2O_2 concentration is consistent with more effective ROS generation when Fe(II) is oxidised by H_2O_2 compared to O_2 (Hug & Leupin, 2003), which is attributed to the 1:1 stoichiometric yield of ROS when Fe(II) reacts with H_2O_2 compared to the 1:3 yield of ROS when Fe(II) reacts with O_2 .

Combining the As speciation plots in Fig. 4.2(C) and the solid-phase Fe speciation plots in Fig. 4.1(C) uncovers a key finding about the anaerobic co-oxidation of As(III) and Fe(II) by H_2O_2 . Comparing the overall As removal between the O_2 experiment and the sequential 40 μM $\text{H}_2\text{O}_2 + \text{O}_2$ experiment showed a decrease in the residual As concentration from 3.8 μM to 1.3 μM , a difference of 2.5 μM As when 40 μM H_2O_2 was applied, whereas for the same samples, the total amount of oxidised As(III) was 2.9 μM for the O_2 experiment and 4.8 μM for the sequential 40 μM $\text{H}_2\text{O}_2 + \text{O}_2$ experiment, a difference of only 1.9 μM As. The higher overall As removal efficacy for the 40 μM $\text{H}_2\text{O}_2 + \text{O}_2$ experiment, cannot be attributed to an increase in As(III) oxidation alone. Therefore, the results indicate that the higher reactive surface area of the poorly-ordered precipitates generated by Fe(II) oxidation with H_2O_2 played a critical role in improving overall As removal efficacy.

4.3.3 Under- and over-dosage of H_2O_2

Experiments were performed to identify any benefit from dosing H_2O_2 below or above the stoichiometric amount required to anaerobically oxidise 100 ± 3 μM Fe(II). Fig. 4.3(A) shows the concentration of oxidised Fe(II) and the corresponding removal of the initial 7 ± 0.2 μM As(III) as a function of different H_2O_2 dosages (10 to 400 μM) at $t = 30$ min. As the H_2O_2 concentration increased, the concentration of oxidised Fe(II) also increased up to the complete oxidation of Fe(II) at H_2O_2 concentrations above 60 μM . For H_2O_2 dosages below 60 μM (i.e., under-dosage; 10 to 40 μM), only partial oxidation of 100 ± 3 μM Fe(II) was observed (20 to 80% oxidation). However, the ratio of generated Fe(III) to dosed H_2O_2 remained around 2:1 mol:mol for all conditions (Fig. 4.3(A)), indicating that the 2:1 stoichiometry of Fe(II) oxidation by H_2O_2 was maintained.

The results from the sequential $\text{H}_2\text{O}_2 + \text{O}_2$ experiments were consistent with the findings mentioned above. Increasing the H_2O_2 concentration from 10 to 40 μM , which is below

the required amount for 100% Fe(II) oxidation, resulted in improved As removal due to the formation of more Fe(III)-precipitates (section 4.3.1 and 4.3.2). For instance, with 10 μM H₂O₂ the residual As concentration ($t = 30$ min) was 4.8 ± 0.2 μM (31% removal), which decreased to 1.7 ± 0.1 μM (76% removal) with 40 μM H₂O₂ (Fig. 4.3(A)). However, we also observed that increasing the H₂O₂ concentration above the amount required to completely oxidise 100 ± 3 μM Fe(II) (i.e., over-dosage) also improved As(III) removal. For example, when the H₂O₂ dosage increased from 60 to 400 μM (i.e., over-dosage), the dissolved As concentration at $t = 30$ min decreased from 0.6 ± 0.1 (92% removal) to 0.1 ± 0.1 μM (98.5% removal), which resulted in As levels below the WHO recommended limit (< 0.13 μM) (Fig. 3.3(A)). This increase in As removal can be explained by the oxidation of As(III) to As(V) via ROS, formed by decomposition of H₂O₂ on the surface of Fe(III)-precipitates (Lin & Gurol, 1998), with subsequent sorption of As(V).

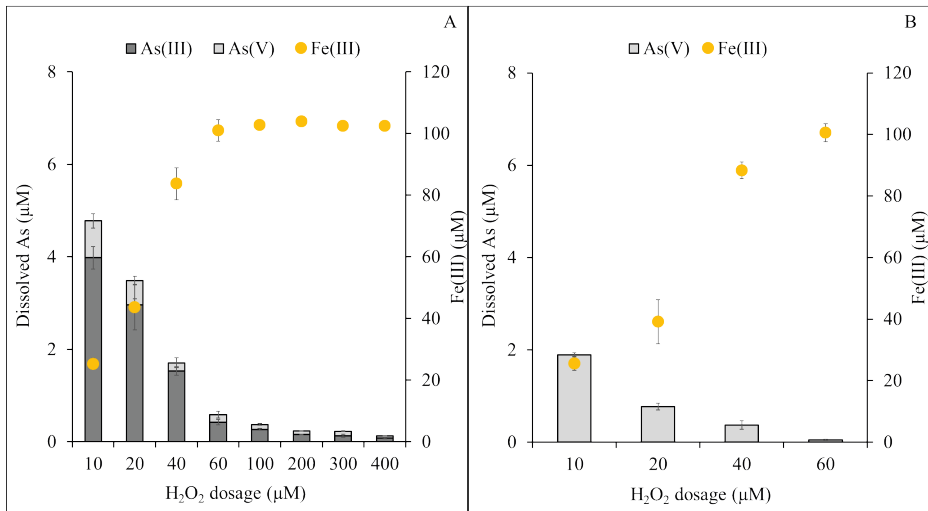


Fig. 4.3. Dissolved As and Fe(III) concentration in solutions at $t = 30$ min plotted as a function of different H₂O₂ dosage when 100 ± 3 μM of Fe(II) was oxidised by 10 to 400 μM H₂O₂ anaerobically. Solutions initially contained 7 ± 0.2 μM As(III) (A) or 7 ± 0.5 μM As(V) (B), 2.5 mM NaHCO₃, and 10 mM NaCl. All Fe(III) formed precipitates and no dissolved Fe(III) was measured (data not shown). Data points and error bars represent the average and standard deviation of the samples obtained from replicate experiments.

Finally, we noted that the removal of the initial 7 ± 0.2 μM As(III) with 400 μM H₂O₂ (98.5% removal) was almost equal to the removal of the initial 7 ± 0.5 μM As(V) (99.3% removal; at 60 μM H₂O₂), when a similar Fe dosage of 100 ± 3 μM was used (Fig. 4.3(B)). This result highlights the advantage of using H₂O₂, because previous Fe(II)-based As removal studies, with only O₂ dosing, have always reported higher removals of initial As(V) compared to As(III) (Kumar et al., 2004; Roberts et al., 2004; Roy et al., 2020; Wan et al., 2011).

4.3.4 Application to raw anaerobic groundwater

To validate that enhanced As(III) co-removal can be achieved by adding H_2O_2 to groundwater containing native-Fe(II), experiments were performed with raw anaerobic groundwater rich in Fe(II), co-occurring As(III), and other native dissolved species (such as phosphorous (total P) and manganese (Mn)). Fig. 4.4 shows the removal of initial As(III), Mn, and total P from raw anaerobic groundwater with Fe(III) generation over 30 min. Consistent with the laboratory experiments (Sections 4.3.1 and 4.3.2), all groundwater native-Fe(II) was oxidised with H_2O_2 and rapidly formed precipitates (within 2 min), whereas O_2 oxidation of Fe(II) required the full 30 min of the experiment. During the H_2O_2 dosing experiment, As(III) was also quickly removed, with 97.6% As(III) removal measured in 2 min. When the native-Fe(II) in groundwater was oxidised by O_2 , As(III) removal continued over the full 30 min reaction duration and at the end of the experiment $1.3 \pm 0.1 \mu\text{M}$ residual As (81% removal) remained in solution.

While the experiments with natural groundwater were consistent with the laboratory experiments (i.e., H_2O_2 addition outperformed aeration), some key differences were observed. First, compared to the laboratory experiments, raw groundwater samples showed a better removal of As(III) for both H_2O_2 and O_2 oxidation. Second, the difference between As(III) removal using H_2O_2 or O_2 was smaller for the raw groundwater experiments. The less distinct As removal of H_2O_2 and O_2 oxidants applied to natural groundwater could be attributed to the four times higher Fe(II) concentration in natural groundwater than in the laboratory experiments, which suggests that optimal conditions for enhancing As removal by H_2O_2 addition occur at lower initial Fe(II) levels.

Additionally, the optimal removal of As(III) with H_2O_2 in groundwater containing low levels of native-Fe(II) can also be impacted by the presence of other native species that can compete for adsorption sites and ROS. For example, phosphorous in groundwater is present mainly as phosphate (PO_4^{3-}) and studies have shown its competition with As(V) for adsorption sites on Fe(III)-precipitates (Roberts et al., 2004). As observed in Fig. 4.4, along with the removal of As(III), total P removal was also observed for both H_2O_2 and O_2 experiments, but the removal of P was different for the different oxidants. In the O_2 experiment, the rate and amount of total P removal was higher than As(III), whereas the H_2O_2 experiment did not display a substantial difference between As(III) and total P removal. This result can be explained by the availability of sufficient sorption sites for both As and P on the Fe(III)-precipitates owing to the formation of poorly-ordered Fe(III)-precipitates during H_2O_2 oxidation, the high Fe(II) concentration ($424 \pm 12 \mu\text{M}$), and to the enhanced oxidation of As(III) using H_2O_2 . However, in situations where groundwater native-Fe(II) is low, a possible lower co-removal of As(III) could be expected due to competition with PO_4^{3-} for adsorption sites.

Apart from PO₄³⁻, groundwater can also contain dissolved Mn, which might impact As(III) co-removal with native-Fe(II). For instance, previous studies have reported that Mn in groundwater, which is present as Mn(II), can compete with As(III) for ROS, yielding oxidised Mn(III) that (partially) incorporates into the co-precipitating Fe(III)-precipitates (Ahmad et al., 2019; Catrouillet et al., 2020; van Genuchten & Peña, 2017). However as shown in Fig. 4.4, Mn removal was relatively low for both H₂O₂ (19% removal) and O₂ (13% removal), suggesting that Mn(III) formation was not substantial. However, since identifying the solid-phase speciation of Mn was beyond the scope of this study, it is not clear whether there was any competition between Mn(II) and As(III) for the generated ROS.

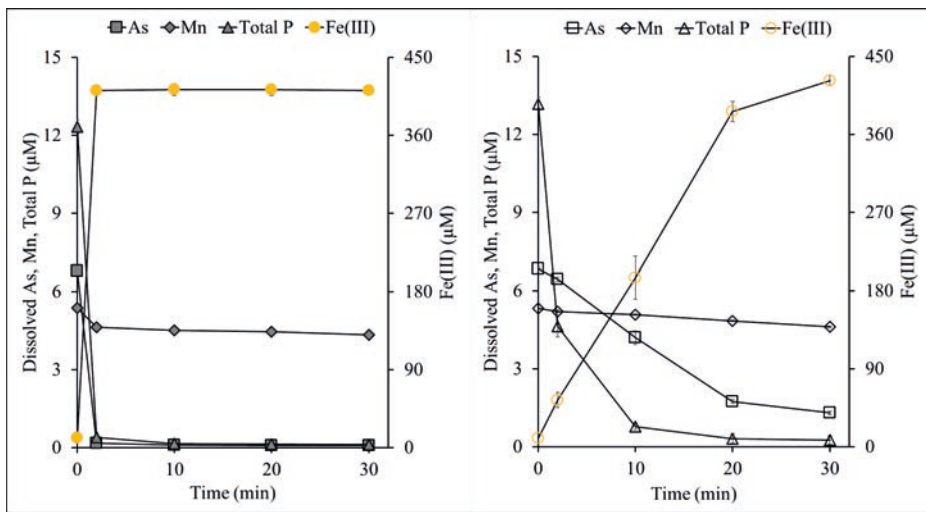


Fig. 4.4. As, Mn, and total P removal from raw anaerobic groundwater as function of time and Fe(III) generation when $424 \pm 12 \mu\text{M}$ groundwater native-Fe(II) was completely oxidised by $800 \mu\text{M}$ H₂O₂ (left) and $8.0\text{--}9.0 \text{ mg/L}$ O₂ (right). Solutions initially contained $6.8 \pm 0.1 \mu\text{M}$ As(III); $5.3 \pm 0.1 \mu\text{M}$ Mn, and $12.7 \pm 0.5 \mu\text{M}$ total P. All Fe(III) formed precipitates and no dissolved Fe(III) was measured (data not shown). Data points and error bars represent the average and standard deviation of the samples obtained from replicate experiments.

4.3.5 Implications for groundwater treatment

We observed improved As(III) removal when co-existing Fe(II) was oxidised by H₂O₂ rather than O₂. The ratio of As(III) removed to Fe(III) generated increased from 0.03 to 0.06 mol:mol when $100 \mu\text{M}$ Fe(II) was completely oxidised with either $8.0\text{--}9.0 \text{ mg/L}$ O₂ or $100 \mu\text{M}$ H₂O₂, respectively, indicating substantially less Fe is required for equivalent As removal with H₂O₂. The application of such Fenton-type systems (i.e., Fe(II)+H₂O₂) to improve As(III) removal from water has been reported previously. For example, Krishna et al. (2001) showed that initial treatment of 2 mg/L As(III) with 100 mg/L

Fe(II) and 100 $\mu\text{L/L}$ of 30% H_2O_2 , followed by passing through zero valent iron columns and a sand bed, achieved As removal to $<10 \mu\text{g/L}$ (WHO guideline). In addition, Wang et al. (2013) observed that oxidising 20 μM Fe(II) with 50 μM H_2O_2 at pH 7.0 resulted in 70% oxidation of 20 μM As(III) compared to just 2.5% while oxidising the Fe(II) with O_2 . While these studies are useful, they interpret their results primarily by improved As(III) co-oxidation by ROS and did not focus on the influence of Fe(III)-precipitates structure. In this study, we also observed that the improved As(III) co-removal by H_2O_2 is partly attributed to the well-established enhanced efficacy of As(III) oxidation in Fe(II)+ H_2O_2 systems due to higher stoichiometric yield of ROS compared to Fe(II)+ O_2 systems (Bandaru et al., 2020; Hug & Leupin, 2003). However, our results explicitly showed that the Fe(III)-precipitates structure played a major role in improving As(III) removal. The Fe K-edge EXAFS analysis performed in this study indicated a systematic decrease in precipitate crystallinity (i.e., increase in reactive specific surface area) from moderately crystalline Lp in the O_2 system to poorly-ordered Fe(III)-precipitates with H_2O_2 (Fig. 4.1(C)). This impact of Fe(III)-precipitates structure is often overlooked in Fe(II)-based As removal techniques, but we show that the type of Fe(III)-precipitates must be considered to accurately predict As removal in groundwater treatment.

Our results also indicated that oxidising the groundwater native-Fe(II) anaerobically with H_2O_2 prior to aeration-filtration can be used to leverage the full potential of native-Fe(II) for As(III) treatment. Depending on the initial Fe/As and Fe: H_2O_2 ratios, this novel approach can remove As(III) to below drinking water standards, achieving a high As(III) removal, which is often difficult with conventional aeration-filtration. The optimal use of groundwater native-Fe(II) via H_2O_2 oxidation can help to avoid the need for additional Fe dosage (as FeCl_3) in situations where oxidising native-Fe(II) by aeration is not sufficient to meet As drinking water limits. This reduction of Fe dosage will also lower the volume of generated Fe sludge and thus lower the frequency of filter backwashing. Additionally, anaerobic oxidation of Fe(II) with H_2O_2 prior to aeration will not result in the same increase in groundwater pH as is observed during aeration due to degassing of CO_2 . As long as Fe(II) is oxidised, maintaining a low pH is advantageous because As(V) adsorption to Fe(III)-precipitates decreases with increasing pH (Annaduzzaman et al., 2021b; Dixit & Hering, 2003).

Usage of other strong oxidants (such as KMnO_4 or NaOCl) during aeration-filtration has been reported previously, effectively oxidising As(III) and also generating poorly-ordered Fe(III)-precipitates (van Genuchten & Ahmad, 2020). However, compared to those oxidants, H_2O_2 is considered a green oxidant, because its by-products, namely H_2O and O_2 , are benign (Goyal et al., 2020; Pham et al., 2012b; Zhao et al., 2019). Recent studies have also shown that H_2O_2 can be electrochemically generated in-situ (Bandaru

et al., 2020), which eliminates the necessity to maintain chemical stocks of H₂O₂ on site, thus decreasing the supply chain for operating groundwater treatment plants.

The results in this work suggest that oxidising groundwater native-Fe(II) with H₂O₂ anaerobically prior to aeration-filtration can be a novel approach to optimise the co-removal of toxic As(III). However, the study did not take into account potentially different environmental scenarios that can impact As(III) removal. For example, the laboratory experiments were performed in controlled conditions with a fixed Fe(II)/As(III) ratio and pH, and without the presence of other competing ions. While a set of experiments with raw anaerobic groundwater was performed, the advantage of oxidising groundwater native-Fe(II) with H₂O₂ over O₂ for As(III) co-removal diminished most likely due to the high concentration of native-Fe(II). In the experiments with real groundwater, although 1 mol of H₂O₂ is sufficient to oxidise 2 mol of Fe(II), an excess H₂O₂ was dosed to minimise the impact of any atmospheric O₂ influx and to ensure complete oxidation of the groundwater native-Fe(II) by H₂O₂ in absence of N_{2(g)} dosage as in laboratory experiments. While our laboratory investigations and tests in real groundwater highlight the potential benefits of H₂O₂ dosing, it is recommended to perform further studies with real anaerobic groundwater under various environmental conditions, with optimisation of the H₂O₂ dosage, to further validate the novelty of the proposed approach. Overall, the advantage of anaerobic H₂O₂ oxidation of groundwater native-Fe(II) for As(III) removal is that it can be easily implemented in conventional or decentralised systems to treat As contaminated groundwater without major changes in infrastructure and without substantial increases in treatment costs.

4.4 Conclusions

In this study, we showed a novel approach where the co-removal of groundwater As(III) with native-Fe(II) can be enhanced by oxidising the Fe(II) anaerobically with H₂O₂ prior to aeration-filtration rather than conventionally by aeration (or O₂) under aerobic conditions. The enhanced As(III) co-removal with H₂O₂ was partly due to generation of a larger fraction of poorly-ordered Fe(III)-precipitates with a higher reactive specific surface area compared to moderately crystalline Fe(III)-precipitates generated by O₂ as well as the generation of more ROS per mole of Fe(II) when dosing H₂O₂ (1:1) compared to O₂ (1:3), thus favouring As(III) oxidation to readily adsorbed As(V). Hence, we propose the application of H₂O₂, a green oxidant, for anaerobic Fe(II) and As(III) co-oxidation in groundwater treatment prior to aeration to optimise groundwater native-Fe(II) usage, which will reduce the volume of generated sludge.

References

- Ahmad, A., van der Wal, A., Bhattacharya, P., & van Genuchten, C. M. (2019). Characteristics of Fe and Mn bearing precipitates generated by Fe(II) and Mn(II) co-oxidation with O₂, MnO₄ and HOCl in the presence of groundwater ions. *Water Research*, 161(June), 505–516. <https://doi.org/10.1016/j.watres.2019.06.036>
- Annaduzzaman, M., Bhattacharya, P., Biswas, A., Hossain, M., Ahmed, K. M., & van Halem, D. (2018). Arsenic and manganese in shallow tubewells: validation of platform color as a screening tool in Bangladesh. *Groundwater for Sustainable Development*, 6, 181–188. <https://doi.org/10.1016/J.GSD.2017.11.008>
- Annaduzzaman, M., Rietveld, L. C., Ghosh, D., Hoque, B. A., & van Halem, D. (2021a). Anoxic storage to promote arsenic removal with groundwater-native iron. *Water Research*, 202. <https://doi.org/10.1016/J.WATRES.2021.117404>
- Annaduzzaman, M., Rietveld, L. C., Hoque, B. A., Bari, M. N., & van Halem, D. (2021b). Arsenic removal from iron-containing groundwater by delayed aeration in dual-media sand filters. *Journal of Hazardous Materials*, 411, 124823. <https://doi.org/10.1016/J.JHAZMAT.2020.124823>
- Bandaru, S. R. S., Van Genuchten, C. M., Kumar, A., Glade, S., Hernandez, D., Nahata, M., & Gadgil, A. (2020). Rapid and Efficient Arsenic Removal by Iron Electrocoagulation Enabled with in Situ Generation of Hydrogen Peroxide. *Environmental Science and Technology*, 54(10), 6094–6103. <https://doi.org/10.1021/acs.est.0c00012>
- Bissen, M., & Frimmel, F. H. (2003). Arsenic — a Review. Part II: Oxidation of Arsenic and its Removal in Water Treatment. *Acta Hydrochimica et Hydrobiologica*, 31(2), 97–107. <https://doi.org/10.1002/AHEH.200300485>
- Bora, A. J., Gogoi, S., Baruah, G., & Dutta, R. K. (2016). Utilization of co-existing iron in arsenic removal from groundwater by oxidation-coagulation at optimized pH. *Journal of Environmental Chemical Engineering*, 4(3), 2683–2691. <https://doi.org/10.1016/J.JECE.2016.05.012>
- Catrouillet, C., Hirose, S., Manetti, N., Boureau, V., & Peña, J. (2020). Coupled As and Mn Redox Transformations in an Fe(0) Electrocoagulation System: Competition for Reactive Oxidants and Sorption Sites. *Environmental Science & Technology*, 54(12), 7165–7174. <https://doi.org/10.1021/acs.est.9b07099>
- Dixit, S., & Hering, J. G. (2003). Comparison of Arsenic(V) and Arsenic(III) Sorption onto Iron Oxide Minerals: Implications for Arsenic Mobility. *Environmental Science and Technology*, 37(18), 4182–4189. <https://doi.org/10.1021/ES030309T>
- Goyal, R., Singh, O., Agrawal, A., Samanta, C., & Sarkar, B. (2020). Advantages and limitations of catalytic oxidation with hydrogen peroxide: from bulk chemicals to lab scale process. *Catalysis Reviews - Science and Engineering*, 64(2), 229–285. <https://doi.org/10.1080/01614940.2020.1796190>/FORMAT/EPUB
- Gude, J. C. J., Rietveld, L. C., & van Halem, D. (2016). Fate of low arsenic concentrations during full-scale aeration and rapid filtration. *Water Research*, 88, 566–574. <https://doi.org/10.1016/j.watres.2015.10.034>
- Gude, J. C. J., Rietveld, L. C., & van Halem, D. (2017). As(III) oxidation by MnO₂ during groundwater treatment. *Water Research*, 111, 41–51. <https://doi.org/10.1016/j.watres.2016.12.041>
- Gude, J. C. J., Rietveld, L. C., & van Halem, D. (2018). Biological As(III) oxidation in rapid sand filters. *Journal of Water Process Engineering*, 21, 107–115. <https://doi.org/10.1016/j.jwpe.2017.12.003>
- Holm, T. R., & Wilson, S. D. (2006). Chemical Oxidation for Arsenic Removal. *MTAC Publication TR06-05*.

- Hug, S. J., & Leupin, O. (2003). Iron-catalyzed oxidation of Arsenic(III) by oxygen and by hydrogen peroxide: pH-dependent formation of oxidants in the Fenton reaction. *Environmental Science and Technology*, 37(12), 2734–2742. <https://doi.org/10.1021/es026208x>
- Kapaj, S., Peterson, H., Liber, K., & Bhattacharya, P. (2006). Human health effects from chronic arsenic poisoning - A review. *Journal of Environmental Science and Health - Part A Toxic/Hazardous Substances and Environmental Engineering*, 41(10), 2399–2428. <https://doi.org/10.1080/10934520600873571>
- King, D. W. (1998). Role of carbonate speciation on the oxidation rate of Fe(II) in aquatic systems. *Environmental Science and Technology*, 32(19), 2997–3003. https://doi.org/10.1021/ES980206O/SUPPL_FILE/ES980206O_S.PDF
- King, D. W., & Farlow, R. (2000). Role of carbonate speciation on the oxidation of Fe(II) by H₂O₂. *Marine Chemistry*, 70(1–3), 201–209. [https://doi.org/10.1016/S0304-4203\(00\)00026-8](https://doi.org/10.1016/S0304-4203(00)00026-8)
- Krishna, M. V. B., Chandrasekaran, K., Karunasagar, D., & Arunachalam, J. (2001). A combined treatment approach using Fenton's reagent and zero valent iron for the removal of arsenic from drinking water. *Journal of Hazardous Materials*, 84(2–3), 229–240. [https://doi.org/10.1016/S0304-3894\(01\)00205-9](https://doi.org/10.1016/S0304-3894(01)00205-9)
- Kumar, P. R., Chaudhari, S., Khilar, K. C., & Mahajan, S. P. (2004). Removal of arsenic from water by electrocoagulation. *Chemosphere*, 55(9), 1245–1252. <https://doi.org/10.1016/j.chemosphere.2003.12.025>
- Li, Y., Bland, G. D., & Yan, W. (2016). Enhanced arsenite removal through surface-catalyzed oxidative coagulation treatment. *Chemosphere*, 150, 650–658. <https://doi.org/10.1016/j.chemosphere.2016.02.006>
- Lin, S. S., & Gurol, M. D. (1998). Catalytic decomposition of hydrogen peroxide on iron oxide: Kinetics, mechanism, and implications. *Environmental Science and Technology*, 32(10), 1417–1423. <https://doi.org/10.1021/es970648k>
- Pedersen, H. D., Postma, D., Jakobsen, R., & Larsen, O. (2005). Fast transformation of iron oxyhydroxides by the catalytic action of aqueous Fe(II). *Geochimica et Cosmochimica Acta*, 69(16), 3967–3977. <https://doi.org/10.1016/J.GCA.2005.03.016>
- Pham, A. L.T., Doyle, F. M., & Sedlak, D. L. (2012a). Inhibitory effect of dissolved silica on H₂O₂ decomposition by iron(III) and manganese(IV) oxides: implications for H₂O₂-based in situ chemical oxidation. *Environmental Science & Technology*, 46(2), 1055–1062. <https://doi.org/10.1021/es203612d>
- Pham, A. L. T., Doyle, F. M., & Sedlak, D. L. (2012b). Kinetics and efficiency of H₂O₂ activation by iron-containing minerals and aquifer materials. *Water Research*, 46(19), 6454–6462. <https://doi.org/10.1016/J.WATRES.2012.09.020>
- Podgorski, J., & Berg, M. (2020). Global threat of arsenic in groundwater. *Science*, 368(6493), 845–850. <https://doi.org/10.1126/science.aba1510>
- Roberts, L. C., Hug, S. J., Ruettimann, T., Billah, M., Khan, A. W., & Rahman, M. T. (2004). Arsenic Removal with Iron(II) and Iron(III) in Waters with High Silicate and Phosphate Concentrations. *Environmental Science and Technology*, 38(1), 307–315. <https://doi.org/10.1021/es0343205>
- Roy, M., van Genuchten, C. M., Rietveld, L., & van Halem, D. (2020). Integrating biological As(III) oxidation with Fe(0) electrocoagulation for arsenic removal from groundwater. *Water Research*, 188, 116531. <https://doi.org/10.1016/j.watres.2020.116531>
- Sharma, A. K., Sorlini, S., Crotti, B. M., Collivignarelli, M. C., Tjell, J. C., & Abbà, A. (2016). Enhancing arsenic removal from groundwater at household level with naturally occurring iron. *Revista Ambiente & Água*, 11(3), 486–498. <https://doi.org/10.4136/AMBI-AGUA.1815>

- Toner, B. M., Santelli, C. M., Marcus, M. A., Wirth, R., Chan, C. S., McCollom, T., Bach, W., & Edwards, K. J. (2009). Biogenic iron oxyhydroxide formation at mid-ocean ridge hydrothermal vents: Juan de Fuca Ridge. *Geochimica et Cosmochimica Acta*, 73(2), 388–403. <https://doi.org/10.1016/j.gca.2008.09.035>
- Tseng, W. P. (1977). Effects and dose response relationships of skin cancer and blackfoot disease with arsenic. *Environmental Health Perspectives*, Vol.19, 109–119. <https://doi.org/10.1289/ehp.7719109>
- van Genuchten, C. M., Behrends, T., Kraal, P., Stipp, S. L. S., & Dideriksen, K. (2018). Controls on the formation of Fe(II,III) (hydr)oxides by Fe(o) electrolysis. *Electrochimica Acta*, 286, 324–338. <https://doi.org/10.1016/j.electacta.2018.08.031>
- van Genuchten, C M, & Pena, J. (2017). Mn(II) Oxidation in Fenton and Fenton Type Systems: Identification of Reaction Efficiency and Reaction Products. *Environmental Science & Technology*, 51(5), 2982–2991. <https://doi.org/10.1021/acs.est.6b05584>
- van Genuchten, Case M., Addy, S. E. A., Peña, J., & Gadgil, A. J. (2012). Removing arsenic from synthetic groundwater with iron electrocoagulation: An Fe and As K-edge EXAFS study. *Environmental Science and Technology*, 46(2), 986–994. <https://doi.org/10.1021/es201913a>
- van Genuchten, Case M., & Ahmad, A. (2020). Groundwater As Removal by As(III), Fe(II), and Mn(II) Co-Oxidation: Contrasting As Removal Pathways with O₂, NaOCl, and KMnO₄. *Environmental Science & Technology*, 54(23), 15454–15464. <https://doi.org/10.1021/acs.est.0c05424>
- van Genuchten, Case M, Gadgil, A. J., & Peña, J. (2014). Fe(III) Nucleation in the Presence of Bivalent Cations and Oxyanions Leads to Subnanoscale 7 Å Polymers. *Environ. Sci. Technol*, 48, 21. <https://doi.org/10.1021/es503281a>
- Wan, W., Pepping, T. J., Banerji, T., Chaudhari, S., & Giammar, D. E. (2011). Effects of water chemistry on arsenic removal from drinking water by electrocoagulation. *Water Research*, 45(1), 384–392. <https://doi.org/10.1016/j.watres.2010.08.016>
- Wang, Z., Bush, R. T., & Liu, J. (2013). Arsenic(III) and iron(II) co-oxidation by oxygen and hydrogen peroxide: Divergent reactions in the presence of organic ligands. *Chemosphere*, 93(9), 1936–1941. <https://doi.org/10.1016/j.chemosphere.2013.06.076>
- Webb, S. M. (2005). SIXpack: A graphical user interface for XAS analysis using IFEFFIT. *Physica Scripta T*, T115(T115), 1011–1014. <https://doi.org/10.1238/Physica.Topical.115a01011>
- Zhao, H., Li, Z., & Jin, J. (2019). Green oxidant H₂O₂ as a hydrogen atom transfer reagent for visible light-mediated Minisci reaction. *New Journal of Chemistry*, 43(32), 12533–12537. <https://doi.org/10.1039/C9NJ03106E>

Appendix

S4.1 X-ray absorption spectroscopy

S4.1.1 Sample preparation

Fe(III)-precipitates for XAS analysis were collected for experiments when 100 ± 3 μM Fe(II) was oxidised completely by 8.0-9.0 mg/L O₂ (aerobically), 100 μM H₂O₂ (anaerobically), or sequentially by 5, 10, 20, or 40 μM H₂O₂ (anaerobically) followed by 8.0-9.0 mg/L O₂ (aerobically). The Fe(III)-precipitates were collected at $t = 30$ min on filter papers using a vacuum filter and immediately stored at -80°C prior to preparation for Fe and As K-edge XAS data collection. Samples were loaded in custom sample holders by first cutting the filter papers containing the precipitates into 3-4 small strips and stacking the strips together to maximise precipitates homogeneity within the X-ray beam path. The stacks were then affixed to custom sample holders with Kapton tape and kept in an air-tight container in a -80°C freezer. Samples were shipped to the beam line using ice packs to maintain low temperatures.

S4.1.2 Data collection

Beam line 2-2 of the Stanford Synchrotron Radiation Lightsource (SSRL, Menlo Park, USA) was used to collect the Fe and As K-edge XAS data. Fe K-edge XAS data were recorded at room temperature out to $k = 13 \text{ \AA}^{-1}$ and As K-edge XAS data were recorded at liquid nitrogen temperatures ($\approx 80^\circ\text{K}$) in fluorescence mode out to $k = 14 \text{ \AA}^{-1}$. All samples were measured concurrently in transmission and fluorescence mode. Ion chambers were employed for transmission mode measurements (I_0 and I_f) and a solid state PIPS detector was used for fluorescence mode measurements. The X-ray beam had dimensions of 1 mm (vertical) \times 6 mm (horizontal). The X-ray beam was detuned 40% to prevent second-order harmonics. For beam calibration, the maximum of the first derivative of Fe(O) and Au(O) foils was set to 7112 eV and 11919 eV for Fe and As K-edge data, respectively. The EXAFS region of the Fe spectra was measured with step sizes of 0.05 \AA^{-1} , whereas the XANES region for As spectra was measured with 0.35 eV steps. Based on data quality, 2 to 6 scans were collected for each sample. No beam damage was observed based on comparison of replicate scans. Spectral alignment, averaging and background subtraction of individual spectra were performed using SixPack software (Webb, 2005), following standard procedures described in van Genuchten et al. (2012). Extraction of the Fe K-edge EXAFS spectra were performed using k^3 -weighting and the EXAFS spectra were Fourier-transformed over the k -range 2 to 11 \AA^{-1} using a Kaiser-Bessel window with dk of 3 \AA^{-1} .

Table S4.1. Groundwater composition

| Ion | Initial value |
|---------|----------------|
| pH | 6.5 to 6.8 |
| DO | 3±1 mg/L |
| Total P | 12.7±0.5 µM |
| Fe(II) | 424±12 µM |
| Mn | 5.3±0.1 µM |
| Ca | 1771±58.6 µM |
| Na | 616.3 ±31.5 µM |
| Si | 315.5±3.8 µM |
| Mg | 171.2±4.1 µM |

Table S4.2. LCFs for Fe K-edge EXAFS spectra using references: lepidocrocite (Lp), 2-line ferrihydrite (2LFh), and oxyanion-rich hydrous ferric oxide (oxy-HFO)

| Sample | Chi-Sq | R factor | Lp fraction | 2LFh fraction | oxy-HFO fraction | Component sum |
|---|--------|----------|-------------|---------------|------------------|---------------|
| O ₂ | 109.91 | 0.054 | 0.68 | 0.32 | 0 | 1.00 |
| 5 µM H ₂ O ₂ +O ₂ | 72.01 | 0.057 | 0.44 | 0.55 | 0 | 0.99 |
| 10 µM H ₂ O ₂ +O ₂ | 89.21 | 0.058 | 0.48 | 0.39 | 0.13 | 1.00 |
| 20 µM H ₂ O ₂ +O ₂ | 54.16 | 0.049 | 0.41 | 0.54 | 0.05 | 1.00 |
| 40 µM H ₂ O ₂ +O ₂ | 41.90 | 0.058 | 0.14 | 0.58 | 0.27 | 0.99 |
| 100 µM H ₂ O ₂ | 41.09 | 0.051 | 0 | 0.46 | 0.54 | 1.00 |

Table S4.3. LCFs for As K-edge XANES spectra using As(III)-Fh and As(V)-Fh

| Sample | Chi-Sq | R factor | Adsorbed As(III) fraction | Adsorbed As(V) fraction | Component Sum |
|---|--------|----------|---------------------------|-------------------------|---------------|
| O ₂ | 1.11 | 0.001 | 0.29 | 0.72 | 1.01 |
| 5 µM H ₂ O ₂ +O ₂ | 1.11 | 0.001 | 0.29 | 0.72 | 1.01 |
| 10 µM H ₂ O ₂ +O ₂ | 1.24 | 0.001 | 0.34 | 0.67 | 1.01 |
| 20 µM H ₂ O ₂ +O ₂ | 1.18 | 0.001 | 0.33 | 0.66 | 0.99 |
| 40 µM H ₂ O ₂ +O ₂ | 1.30 | 0.001 | 0.23 | 0.76 | 0.99 |
| 100 µM H ₂ O ₂ | 3.22 | 0.003 | 0 | 1.01 | 1.01 |

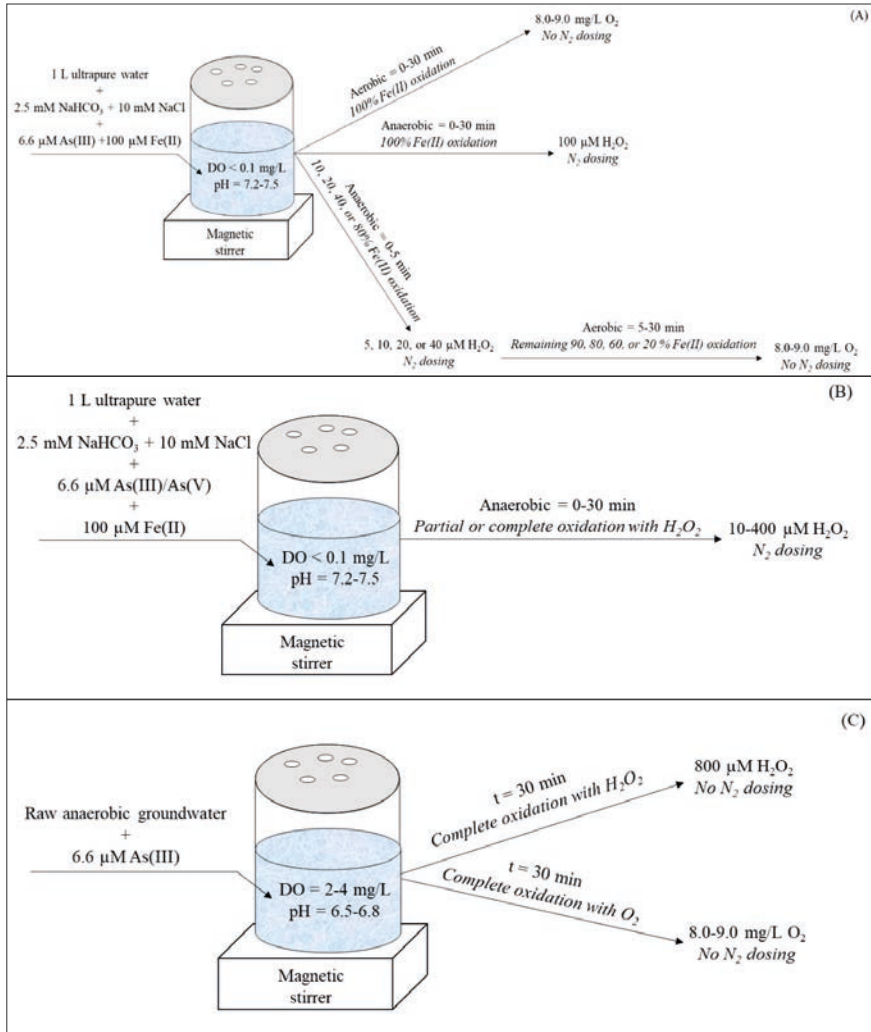


Fig. S4.1. Schematic overview of the different experiments performed

(A) Experiments where 100 μM Fe(II) was oxidised completely 8.0-9.0 mg/L O₂ (aerobically; t = 0-30 min), 100 μM H₂O₂ (anaerobically; t = 0-30 min), or sequentially by 5, 10, 20, or 40 μM H₂O₂ (anaerobically; t = 0-5 min) followed by 8.0-9.0 mg/L O₂ (aerobically; t = 5-30 min).

(B) Experiments where partial or complete oxidation of 100 μM Fe(II) (anaerobically) was performed with a range of 10 to 400 μM H₂O₂ concentrations that were under and over the stoichiometric amount required for total Fe(II) oxidation.

(C) Experiments with raw groundwater where the native-Fe(II) was oxidised by H₂O₂ or O₂.



Chapter 5

Coupling H_2O_2 dosing and $\text{Fe}(0)$ electrocoagulation to enhance $\text{As}(\text{III})$ removal in groundwater – A field study in Assam (India)



This chapter is based on:

Roy, M., Kalamdhad, A., van Genuchten, C. M., Rietveld, L., & van Halem, D. (2024). Coupling hydrogen peroxide dosing and $\text{Fe}(0)$ electrocoagulation to enhance $\text{As}(\text{III})$ removal in groundwater – A field study in Assam (India). *Under preparation*

Abstract

Toxic arsenic (As) has been detected in the groundwaters of Assam (India), requiring treatment before consumption. Meanwhile, household iron (Fe(II)) removal filters, operating on the principle of aeration-filtration, have been documented in Assam, which could also treat arsenite (As(III))-contaminated groundwater by utilising the naturally occurring Fe(II). Unfortunately, As(III) removal during aeration-filtration is often limited due to ineffective oxidation of As(III) to the more readily adsorbable arsenate (As(V)), insufficient native-Fe(II) in groundwater, or an increase in pH during aeration, hindering As(V) adsorption on Fe(III)-precipitates. This study introduces a novel approach that involves the coupling of hydrogen peroxide (H_2O_2) dosing with iron electrocoagulation (FeEC) (Fe dosage technology) before aeration, with the aim to enhance As(III) co-removal during aeration-filtration. Experiments were conducted using groundwater from five different locations within the Kamrup Metropolitan district, where the Fe(II) and As(III) concentrations in raw anaerobic groundwater ranged from 3.7 to 11.7 mg/L and 80 to 462 $\mu\text{g/L}$, respectively. Both the groundwater native-Fe(II) and Fe(II) released by FeEC (6 to 10.8 mg/L) were completely oxidised by 400 μM H_2O_2 or dissolved oxygen (DO) inserted through aeration (8.0-9.0 mg/L DO). As(III) removal in the five locations ranged between 44 to 88% when the groundwater native-Fe(II) was oxidised by H_2O_2 , compared to 26 to 34% when using DO as the oxidant, respectively. The application of FeEC further improved the overall As removal, where with H_2O_2 , the efficacy ranged between 82 to 99%, compared to the 49 to 72% with DO, respectively. Consequently, As(III) co-removal per mass of Fe(II) was higher with H_2O_2 as an oxidant compared to the use of DO. Furthermore, the As(III) removal varied among locations, with those exhibiting a relatively higher Fe/As ratio in the water demonstrating greater co-removal of the initial As(III). However, the amount of As(III) removed per mass of Fe(III)-precipitates generated (i.e., As/Fe uptake ratio) displayed an inverse relationship where locations with a higher Fe/As ratio in the water showed a lower As/Fe uptake ratio. Additionally, oxidising the native-Fe(II) in groundwater at the raw anaerobic groundwater pH level (6.5 to 6.8) in all five locations achieved a higher As/Fe uptake ratio compared to oxidising at pH levels commonly observed after aeration (7.0 to 8.0). This indicates that oxidising Fe(II) anaerobically, before aeration, will take advantage of the lower pH level compared to oxidising after aeration due to CO_2 degassing. In conclusion, this study has demonstrated that coupling anaerobic H_2O_2 dosing with FeEC before aeration promotes As removal and is a promising approach for decentralised application in rural Assam, for example in combination with existing low-cost Fe removal filters.

Keywords: Arsenic, Hydrogen Peroxide, Iron electrocoagulation, Groundwater

5.1 Introduction

Various technologies, such as chemical precipitation, adsorption, ion exchange, and membrane filtration have been reported to effectively remove the toxic arsenic (As) from groundwater (Alka et al., 2021; Annaduzzaman et al., 2021; Kowalski, 2014; Meng et al., 2001; Niazi et al., 2018; Pio et al., 2015; Worou et al., 2021). However, in long-run these technologies are often impractical and unsustainable in rural and semi-urban communities in South Asian countries such as Assam (India), due to their reliance on expensive chemicals, skilled personnel, and energy-intensive operations (Ahamad & Jawed, 2012).

Assam is a northeastern state in India where the groundwater has been reported to contain As at concentrations above the 10 µg/L guideline of the World Health Organization (WHO) for drinking water (Chakraborti et al., 2004; Mahanta et al., 2004; Nickson et al., 2007; WHO, 2004). In the rural and semi-urban areas of Assam, where piped water supply systems are limited, the main source of drinking water is (untreated) groundwater accessed through hand pumps, dug wells, and tube wells (Ahamad & Jawed, 2012). This situation puts people at risk since prolonged ingestion of As-contaminated drinking water has been linked to the development of skin, bladder, and lung cancers, along with reproductive abnormalities and neurodevelopmental disorders in children (Kapaj et al., 2006; Tseng, 1977).

Meanwhile, household iron (Fe) removal filters have been successfully applied in Assam to remove excess native-iron (Fe(II)) from groundwater. These low-cost filters, made with local materials such as charcoal, sand, and gravel, function similarly to the aeration-filtration technology used to remove Fe(II) from raw anaerobic groundwater (Baruah et al., 2011; Kanoo et al., 2020). The process involves oxidation of the groundwater native-Fe(II) via dissolved oxygen (DO) (inserted during aeration) to form Fe(III)-precipitates, which are then filtered out. However, the Fe(III)-precipitates can also adsorb As, which could then be co-removed during this filtration process (Bora et al., 2016; Gude et al., 2016).

Nevertheless, the aeration-filtration process cannot be considered a robust technology for As removal, given the fluctuating efficacies (8 to 50%) in As removal attributed to various factors (Holm & Wilson, 2006; Li et al., 2016; van Genuchten & Ahmad, 2020). Such limited As removal with the groundwater native-Fe(II) during aeration-filtration can be due to the initial ratio of Fe(II) to As, where there might be insufficient native-Fe(II) in groundwater to remove As below the drinking water guidelines (Annaduzzaman et al., 2018; Biswas et al., 2012; Sharma et al., 2016). In such cases,

chemical coagulants dosing such as FeCl_3 are commonly used to improve As removal (Laky & Licskó, 2011), which, though effective, introduces the drawbacks of buying extra chemicals as mentioned earlier. To address the limitations of chemical coagulants dosing, an alternative approach is iron electrocoagulation (FeEC), a low-cost and robust Fe dosage technology (Bandaru et al., 2020a). The method involves generating Fe coagulants in-situ through electrochemical reactions using Fe(O) electrodes. A small electric current is passed through the Fe(O) electrodes, releasing Fe(II) ions from the Fe(O) anode into the bulk solution due to oxidation. These Fe(II) ions are then oxidised by DO to produce Fe(III)-precipitates capable of adsorbing As (van Genuchten et al., 2012; Wan et al., 2011). Compared to other techniques, FeEC is more suitable for long-term sustainable operation and implementation in e.g., low-income and resource-poor rural communities due to its modular design, affordability, adaptability, minimal infrastructure requirements, and potential for automation (Amrose et al., 2014; Bandaru et al., 2020a; Holt et al., 2005; Kumar et al., 2004; Wan et al., 2011).

However, in all Fe(II)-based As removal technologies, the As removal challenges also arise due to the oxidation state of As in the groundwater. In raw anaerobic groundwater, arsenite (As(III)) is the common form of As, which is neutrally charged, and the generated Fe(III)-precipitates have a higher affinity to adsorb the negatively charged oxidised arsenate species (As(V)) (Bissen & Frimmel, 2003; Hering et al., 2017; Manning et al., 2002; Mercer & Tobiason, 2008). While oxidation of As(III) with DO is thermodynamically feasible, the process is slow and partial compared to Fe(II) oxidation (Hug & Leupin, 2003). As a result, a significant portion of the unoxidised As(III) remains in the dissolved phase without adsorbing during aeration-filtration. In such situations, chemical oxidants could be dosed to oxidise As(III), being costly and capable of producing undesirable by-products. The As oxidation state also impacts its removal by FeEC, where As(III) removal requires a relatively higher Fe dosage compared to As(V), thereby increasing the overall sludge production and energy consumption (Roy et al., 2020).

Dosing hydrogen peroxide (H_2O_2) to oxidise groundwater native-Fe(II) and Fe(II) released by FeEC is an alternative approach to improve As(III) co-oxidation with Fe(II). Among other chemical oxidants H_2O_2 is considered as a green oxidant, since its reaction products are only H_2O and O_2 (Goyal et al., 2020; Pham et al., 2012; Zhao et al., 2019). Although As(III) oxidation with H_2O_2 is also slow, Fe(II) oxidation by H_2O_2 leads to higher stoichiometric yield of reactive oxygen species (ROS) (through Fenton reactions), compared to oxidation with DO, accelerating the oxidation of As(III) to As(V) (Hug & Leupin, 2003). In addition, Fe(II) oxidation by H_2O_2 also generates poorly-ordered Fe(III)-precipitates, compared to moderately crystalline with DO,

having a higher adsorption capacity per mass of Fe compared to moderately crystalline Fe(III)-precipitates (Bandaru et al., 2020b; Roy et al., 2022; van Genuchten & Peña, 2017). Moreover, the groundwater native-Fe(II) and Fe(II) generated by FeEC can be oxidised anaerobically with H₂O₂ before aeration, where CO₂ degassing occurs, and generate the Fe(III)-precipitates at a relatively low pH, which benefits As(V) adsorption (Dixit & Hering, 2003; Gude et al., 2016). The advantages of utilising H₂O₂ instead of DO as an oxidant in Fe(II)-based As(III) removal technologies, such as FeEC, have been documented previously while using aerobic synthetic groundwater (Bandaru et al., 2020b). However, the benefits of dosing H₂O₂, while using raw anaerobic groundwater under varying real groundwater conditions, with potential inhibitory effects of co-contaminants, have not been thoroughly studied.

In this study, we coupled H₂O₂ dosing and FeEC in raw anaerobic groundwater. The objective was to anaerobically oxidise the groundwater native-Fe(II) and Fe(II) released by FeEC with H₂O₂ and compare the As(III) removal when DO (introduced through aeration) was used as oxidant. Furthermore, the pH impact on the As/Fe uptake ratio during the oxidation of groundwater native-Fe(II) with H₂O₂ was studied.

5.2 Materials and methods

5.2.1 Experimental setup and procedure

The experiments in this study were conducted in the field, near the source, at five selected locations (named L1-L5) within the Kamrup Metropolitan district (composition in Table S5.1). The setup consisted of glass beakers, each containing 2 L of raw anaerobic groundwater, which was spiked with As(III) using a stock solution. At each of the five locations, the groundwater was spiked to a varying concentration of As(III) within a range of 50 to 500 µg/L, see Table S5.1. Different As(III) concentrations were spiked in the five locations to represent various Fe(II)/As(III) ratios as typically found in groundwaters. Subsequently, after spiking with As(III), the native-Fe(II) in the groundwater was completely oxidised first by introducing either H₂O₂ or DO into the anaerobic water. To introduce H₂O₂, a 30% w/w H₂O₂ solution (Merck Millipore) was used to achieve a H₂O₂ concentration of 400 µM. Alternatively, for the introduction of DO, an air-pump was employed to raise the DO level to 8.0-9.0 mg/L. The solution was mixed at 150 rpm using a magnetic stirrer for a duration of 30 min after initiating the oxidation of native-Fe(II) in the groundwater.

Upon completion of the groundwater native-Fe(II) oxidation experiment (after 30 min), 1 L of the solution was transferred to another glass beaker to apply the FeEC. The

FeEC cell was composed of two Fe(0) electrodes (15 x 5 x 0.2 cm each; one cathode and one anode) with a submerged area of 35 cm² and an inter-electrode gap of 1 cm. The electrodes were cleaned before each experiment using sandpaper to remove any scaling, and they were rinsed with demineralised water. The electrodes were connected to a direct current (DC) power supply (TENMA 72–10500 Power Supply, 30V, 3A). The FeEC process was also conducted under the influence of either H₂O₂ or DO, meaning that the dosed Fe(II) from the anode was completely oxidised by either H₂O₂ or DO (using the air-pump). To facilitate the oxidation of Fe(II) dosed by FeEC using H₂O₂, the addition of 400 µM H₂O₂ prior to the groundwater native-Fe(II) oxidation proved to be adequate across all locations. During the FeEC process, the solution was also mixed using a magnetic stirrer at 150 rpm. FeEC was introduced to dose a theoretical concentration of 10 mg/L Fe, achieved at a rate of 0.024 mg/L/s, corresponding to an applied current of 0.083 A for 415 s, as per Faraday's law (Roy et al., 2020). Throughout the duration of the experiment, water samples were collected at 10 min intervals (0, 10, 20, and 30 min) during the groundwater native-Fe(II) oxidation, as well as immediately after FeEC application. The initial pH of the untreated raw anaerobic groundwater at each location (ranging from 6.5 to 6.8) was maintained throughout the duration of the both H₂O₂ and DO oxidant experiments by adding either 0.1/1 M HCl or 0.1/1 M NaOH.

A separate set of experiments was conducted to explore the influence of groundwater pH on As removal via groundwater native-Fe(II) oxidation. In these experiments, the process of oxidising groundwater native-Fe(II) with H₂O₂ was repeated. However, prior to the dosing of 400 µM H₂O₂, the initial pH of the As(III)-spiked anaerobic groundwater (6.5 to 6.8) was adjusted to either 7.0, 7.5, or 8.0, respectively. The adjusted pH level was maintained throughout the 30 min duration of the experiment, and water samples were collected at 0 and 30 min after the start of the experiment. All experiments were performed in duplicates.

5.2.2 Chemicals, sampling, and analytical methods

Spiking of groundwater with As(III) was performed using As(III) stock solutions, which were prepared by dissolving sodium (meta)arsenite (NaAsO₂) (Sigma-Aldrich) to ultrapure water and acidifying to a pH < 3, using HNO₃, to prevent As(III) oxidation. H₂O₂ was added directly from 30% w/w H₂O₂ solution (Merck Millipore). For pH adjustment, 1/0.1 M HCl or 1/0.1 M NaOH (Merck Millipore) were used.

At all locations, the raw groundwater was collected from deep tube wells (depth >30.48 m or 100 ft) using hand pumps. The groundwater was collected after 5 to 10 min of pumping to minimise O₂ interference and to remove stagnant water. Prior to the experiments, raw groundwater samples were collected at each location in 1 L

cleaned plastic bottles. Two types of water samples were collected during this sampling period, one acidified with 2 ml/L HNO₃ acid to reduce pH<2 and the other without acidification. The acidified samples were used to analyse for metal ions (As, Fe, etc) and the unacidified samples were used for physicochemical parameters analysis. All samples after collection were lightproof to the laboratory, where they were stored at 4°C before analysis.

Water sampling during the As-removal experiments was done: (a) direct, unfiltered, (b) through filtration over a 0.20 µm polystyrene sulfone filter procured from Macherey-Nagel GmbH & Co. KG, and (c) through filtration over a 0.20 µm polystyrene sulfone filter, succeeded by passage through an anion exchange resin. All three resulting types of samples were immediately acidified with 1% (v/v) HNO₃ acid and lightproof transported to the laboratory, where it was stored at 4°C before analysis. The Fe measured after filtration with the 0.20 µm polystyrene sulfone filter is referred to as Fe(II) (or dissolved Fe), while the difference in Fe concentration between the unfiltered and 0.20 µm polystyrene sulfone filtered samples represented Fe(III)-precipitates. The quantification of dissolved As speciation was achieved using an anion exchange resin (Amberlite® IRA-402 chlorite form resin), following the methodology outlined by Gude et al. (2018).

The pH and DO measurements were conducted using a multimeter (WTW™ MultiLine™ Multi 3630 IDS). During the characterisation of the raw groundwater quality at the various locations, pH and DO were immediately measured in the field. Electric conductivity (EC), nitrate, sulphate, chloride, and dissolved organic carbon (DOC) were measured in the laboratory in Assam using the unacidified water samples. EC was determined using a digital conductivity meter (VSI-04-Deluxe), DOC was analysed using a TOC analyser, and nitrate was measured using a spectrophotometer (Cary50UV-Vis Spectrophotometer, Agilent Technologies). Alkalinity and chloride were determined trimetrically. Laboratory analyses in Assam using the unacidified samples followed standard protocols outlined in APHA, (2012). The acidified water samples collected during groundwater characterisation and As-removal experiments were analysed for various elements (As, Fe, Ca, Total P, etc.) by inductively coupled plasma mass spectrometry (ICP-MS) using the Analytik Jena PlasmaQuant MS instrument.

All As-removal experiments were performed in duplicates. The various collected water samples during groundwater characterisation and As-removal experiments were measured in triplicates. The presented data represent the average of the results obtained for each data point, and the error bars indicate the corresponding standard deviation, from replicate experiments.

5.3 Results and discussion

5.3.1 Impact of Fe(II) oxidant type on As(III) removal

Fig. 5.1(A) and (B) illustrates the removal of As(III) from groundwater at the five locations (L1-L5) within the Kamrup Metropolitan district while using H_2O_2 or DO as the oxidant. The pH of the water during the experiments was consistently maintained at the initial pH value of the untreated raw anaerobic groundwater (6.5 to 6.8), even during the DO experiments, wherein the pH was tending to increase due to CO_2 degassing from the aeration process. The results obtained demonstrate that, across all locations, groundwater native-Fe(II) was completely oxidised to Fe(III), leading to the formation of Fe(III)-precipitates, regardless of whether H_2O_2 or DO was used as the oxidising agent (see Fig. 5.1(A) and (B)). However, the removal of As(III) with the groundwater native-Fe(II) was consistently higher at all five locations when H_2O_2 was employed for Fe(II) oxidation.

After 30 minutes, FeEC was applied to remove residual As from the water. The FeEC system was operated to dose an additional 10 mg/L Fe. However, in L2 and L3, 6 and 8.6 mg/L Fe were introduced by FeEC, respectively. This disparity may be attributed to experimental error. The Fe(II) introduced by FeEC also underwent complete oxidation, forming Fe(III)-precipitates, regardless of the oxidant used. After FeEC, the concentrations of dissolved As at the five locations were 1.2 ± 0.3 , 10.8 ± 0.3 , 6 ± 0.4 , 52.1 ± 0.2 , and 71.2 ± 1 $\mu\text{g/L}$ when H_2O_2 was used (Fig. 5.1(A)), and 38.9 ± 5 , 98.6 ± 0.1 , 41.6 ± 1.6 , 162.4 ± 1.1 , and 189.4 ± 2.5 $\mu\text{g/L}$ when DO was employed (Fig. 5.1(B)), respectively. This shows that, even in combination with FeEC, As removal was more effective with H_2O_2 compared to with DO.

These findings are consistent with previous research (Bandaru, et al., 2020b; Roy et al., 2022), where, under controlled laboratory settings, oxidising Fe(II) with H_2O_2 resulted in a higher co-removal of As(III), compared to the oxidation with DO. This improved As(III) co-removal with H_2O_2 could be attributed to the combined effect of generating poorly-ordered Fe(III)-precipitates with H_2O_2 , rather than the moderately crystalline ones formed with DO, as well as a higher co-oxidation of As(III) due to a higher yield of ROS when H_2O_2 was used over oxidation with DO. The present study demonstrated that these effects were also relevant under real groundwater conditions, where co-occurring contaminants (phosphate and silicate) could have influenced the process.

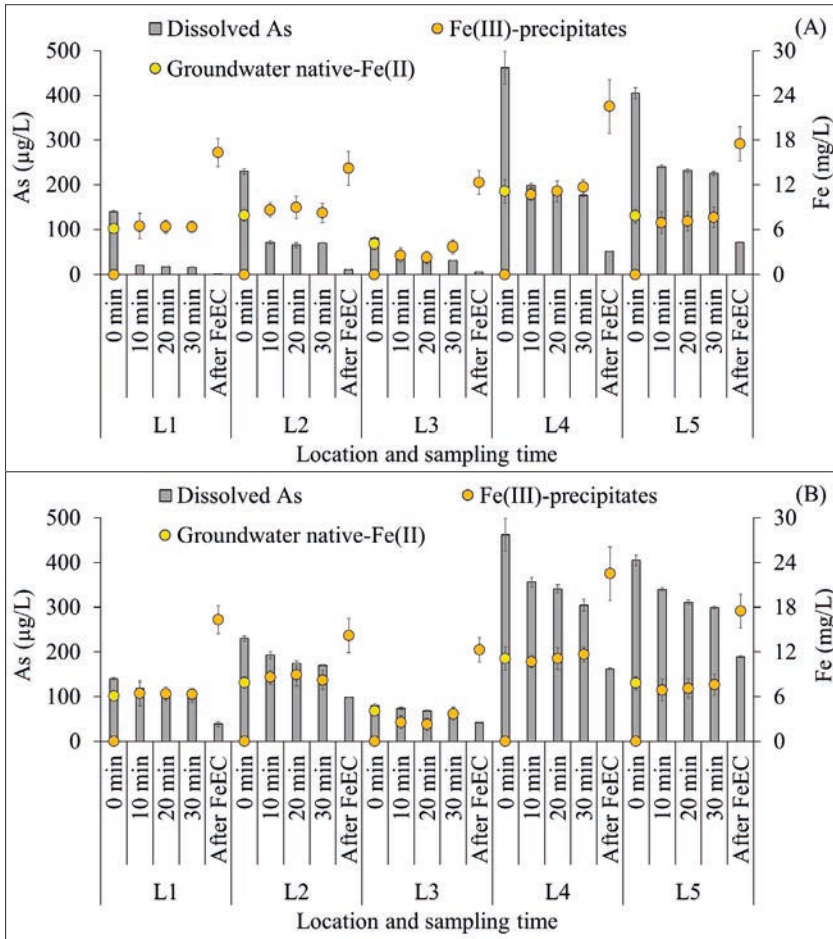


Fig. 5.1. Removal of initial As(III) in the groundwater of the five selected locations (L1-L5) within Kamrup Metropolitan district when the groundwater native-Fe(II) and Fe(II) released by FeEC was completely oxidised by dosing 400 µM H₂O₂ (A) and DO inserted during aeration (B). The pH was maintained at the raw anaerobic groundwater pH level of 6.5 to 6.8.

5.3.2 Impact of Fe/As ratio on As(III) co-removal

Using H₂O₂ as an oxidant, as compared to DO, resulted in a better removal of As(III) at all five locations (Fig. 5.1(A) and (B)). However, the extent of As(III) removal varied across these locations (Fig. 5.2). When considering H₂O₂ as the oxidant and under the pH conditions of raw groundwater (6.5 to 6.8), the removal of As(III) at L1, L2, and L3 was higher than at L4 and L5 (Fig. 5.2). Notably, only at L1, L2, and L3 did the As(III) removal meet the WHO guideline value of 10 µg/L, while this achievement was not observed at locations L4 and L5. This disparity can be attributed to the initially

lower concentration of the As(III) at L1, L2, L3 in comparison to L4, L5 (Table S5.1). Additionally, a higher available Fe to initial As(III) ratios were observed at L1, L2, and L3, with ratios of 58.4, 46, and 68.7 mol:mol (with groundwater native-Fe(II)) and 156, 82.7, and 206 mol:mol (with native-Fe(II)+FeEC), as opposed to 32.2, 25.8 mol:mol (with groundwater native-Fe(II)) and 65.3, 57.9 mol:mol (with native-Fe(II)+FeEC) at L4 and L5, respectively (Fig. 5.2). Gude et al. (2016) and Ahmad et al. (2018) reported an Fe/As ratio of 141.3 to 246.7 mol:mol for achieving As removal (initial As concentration = 10 to 26 $\mu\text{g/L}$) below 10 $\mu\text{g/L}$ during aeration-filtration. Similarly, Roberts et al. (2004) showed a requirement of 146.7 mol:mol Fe/As ratio to reduce the As concentration from 500 $\mu\text{g/L}$ to below 50 $\mu\text{g/L}$ through aeration-filtration. Therefore, theoretically, at an optimum Fe(II)/As(III) ratio in raw groundwater, As(III) removal below a certain standard can be achieved only with the groundwater native-Fe(II) without any additional Fe dosage. In practice, however, Fe(II)/As(III) ratios in groundwater do not suffice, requiring additional dosing of Fe.

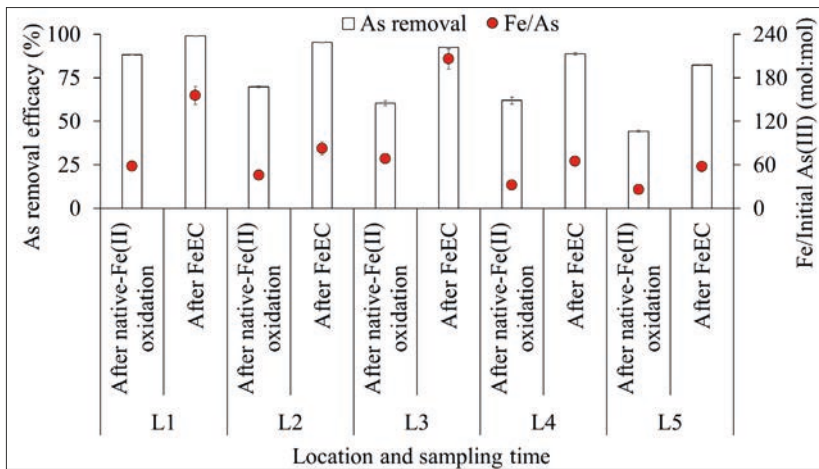


Fig. 5.2. Removal efficacy of the initial As(III) and the corresponding available Fe to initial As(III) ratio in the groundwater of the five selected locations (L1-L5) within Kamrup Metropolitan district when the groundwater native-Fe(II) and Fe(II) released by FeEC was completely oxidised by dosing 400 μM H_2O_2 . The pH was maintained at the raw anaerobic groundwater pH level of 6.5 to 6.8.

With the groundwater native-Fe(II) and under the pH conditions of raw groundwater (6.5 to 6.8), the efficacy of As(III) removal was found to be higher at L1, L2, and L3 in comparison to L4 and L5 (Fig. 5.2). However, when comparing the As(III) removal per unit mass of generated Fe(III)-precipitates, referred to as the As/Fe uptake ratio, an inverse correlation was observed. As illustrated in Fig. 5.3(A) and (B), the As/Fe uptake ratio of L4 and L5 was higher than that of L1, L2, and L3, even though the

initial ratio of available native-Fe(II) to initial As(III) in groundwater was lower in L4 and L5 compared to L1, L2, and L3, respectively. This inverse relationship, wherein a higher As/Fe uptake ratio was observed in locations with lower initial native-Fe(II) to As(III) ratios in groundwater, can be explained by the fact that in locations with higher initial Fe/As ratios, there is relatively less As available for sorption. Consequently, when dosing additional Fe in groundwater, an optimal amount should be chosen to achieve the desired As(III) removal and to optimise the As/Fe uptake ratio, thereby maximising the utilisation of the dosed Fe for As(III) removal.

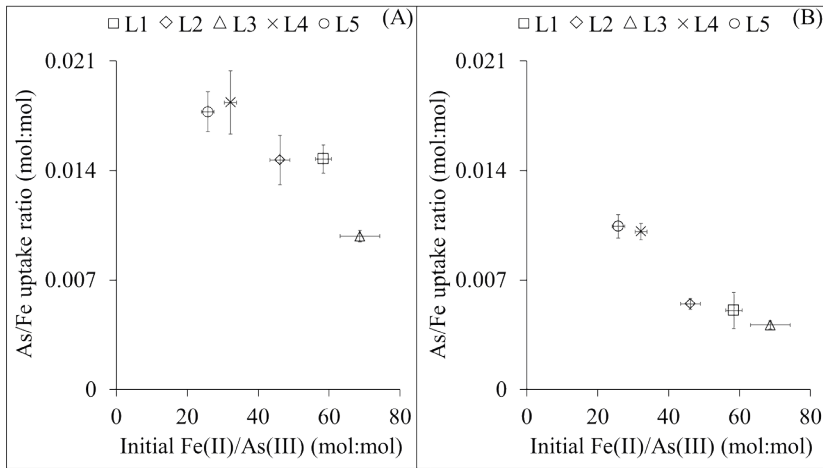


Fig. 5.3. Amount of As(III) removed per mass of Fe(III)-precipitates generated (As/Fe uptake ratio) and the corresponding initial native-Fe(II) to As(III) ratios in the groundwater of the five selected locations (L1-L5) within Kamrup Metropolitan district when the groundwater native-Fe(II) was completely oxidised by dosing 400 μM H₂O₂ (A) and DO inserted during aeration (B). The pH was maintained at the raw anaerobic groundwater pH level of 6.5 to 6.8.

5.3.3 Impact of pH on As/Fe uptake ratio

Fig. 5.4 presents the outcomes of the As/Fe uptake ratio, during the oxidation of groundwater native-Fe(II) using H₂O₂ across varying pH conditions. The graph demonstrates the substantial influence of pH on the As/Fe uptake ratio. Across all test locations (L1-L5), operating within the pH range of raw groundwater (6.5 to 6.8) resulted in the highest As/Fe uptake ratio with the groundwater native-Fe(II). Conversely, experiments conducted at elevated pH levels of 7.0, 7.5, and 8.0 showed a consistent lower As/Fe uptake ratio, with pH 8.0 yielding the lowest As/Fe uptake value. This decline can be attributed to the interaction between As(V) and Fe(III)-precipitates, which forms inner-sphere surface complexes. The intrinsic surface constants of these

complexes exhibit a pH-dependent behaviour. Consequently, increasing the pH leads to a reduction in the adsorption of As(V) onto Fe(III)-precipitates (Dixit & Hering, 2003; Gude et al., 2016). This underscores the advantage of anaerobically oxidising groundwater native-Fe(II) with H_2O_2 before aeration, as aeration tends to elevate the pH due to CO_2 degassing, diminishing the adsorption of As(V), generated through the oxidation of As(III).

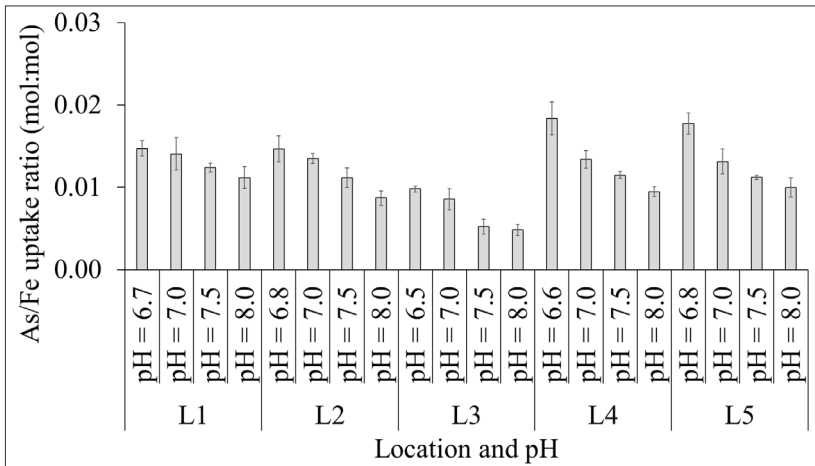


Fig. 5.4. Amount of As(III) removed per mass of Fe(III)-precipitates generated (As/Fe uptake ratio) in the groundwater of the five selected locations (L1-L5) within Kamrup Metropolitan district when the groundwater native-Fe(II) was completely oxidised by dosing $400 \mu\text{M}$ H_2O_2 under varying pH conditions.

5.3.4 Co-removal of other contaminants with As

In addition to As(III), raw groundwater contains other contaminants that could also be co-removed by the Fe(II)-based technologies. These contaminants could potentially compete with As(III) for ROS or for adsorption sites on Fe(III)-precipitates. Manganese (Mn), usually present in groundwater as Mn(II), has been documented to compete with As(III) for ROS, leading to the formation of oxidised Mn(III) (Catrouillet et al., 2020; van Genuchten & Pena, 2017), and subsequently becoming (partially) incorporated into the Fe(III)-precipitates, thereby impacting As adsorption (Ahmad et al., 2019; Catrouillet et al., 2020; van Genuchten & Pena, 2017). Additionally, phosphorus (P), in the form of phosphate (PO_4^{3-}), has been reported to compete with As(V) for adsorption sites on Fe(III)-precipitates (Roberts et al., 2004).

During the course of the experiments at the five different locations, as explained in section 5.3.1, the dissolved Mn concentration was monitored both after the oxidation of groundwater native-Fe(II) (30 min) and after the application of FeEC. Compared

to the initial As(III) concentration at the five locations (after spiking), the Mn concentration in raw groundwater was 2.5 to 55 times lower (in mol/L). The results revealed a relatively low Mn removal (5 to 11 %) (Fig. S1(A) and (B)) when using either H₂O₂ or DO as Fe(II) oxidant. Additionally, there was no impact of the oxidant on the Mn co-removal, as observed for As(III), since the Mn removal under both oxidants was almost similar (Fig. S5.1(A) and (B)).

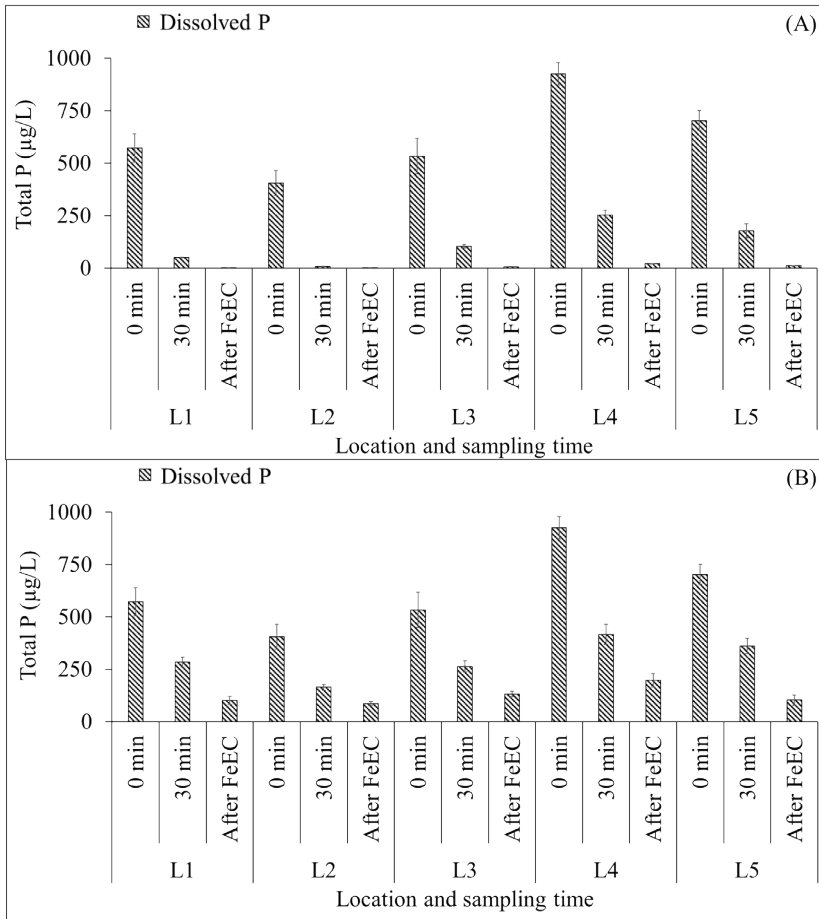


Fig. 5.5. Removal of total P in the groundwater of the five selected locations (L1-L5) within Kamrup Metropolitan district when the groundwater native-Fe(II) and Fe(II) released by FeEC was completely oxidised by dosing 400 µM H₂O₂ (A) and by DO inserted during aeration (B). The pH was maintained at the raw anaerobic groundwater pH level of 6.5 to 6.8.

Fig. 5.5 illustrates the total P concentration at the five selected locations. Similar to As(III) in the raw groundwater, P removal was more effective when H₂O₂ was used as

the oxidant compared to DO (Fig. 5.5(A) and (B)). This enhanced removal of total P with H_2O_2 can be mainly attributed to the increased adsorption capacity of the poorly-ordered Fe(III)-precipitates generated when H_2O_2 is used as the oxidant, since PO_4^{3-} , unlike As(III), does not require oxidation for improved adsorption. Also because the initial total P concentration was 4 to 16 times higher (in mol/L) than that of As(III) at all the locations, total P removal was consistently higher than that of As, whether using groundwater native-Fe(II) or FeEC, regardless of the oxidant used. Therefore, P in the form of PO_4^{3-} can be considered as a potential competitor of As(V) for adsorption sites on the Fe(III)-precipitates, as previously reported by Roberts et al. (2004) and Annaduzzaman et al. (2022).

5.3.5 Implications for groundwater treatment

The study demonstrated the field application of native-Fe(II) oxidation in groundwater using H_2O_2 , along with the application of FeEC before aeration. These two technologies can be synergistically employed to improve As(III) removal in existing household Fe removal filters in Assam (India) or other regions where groundwater, containing native-Fe(II) and As(III), undergoes treatment via aeration-filtration. The study also underscores the advantages of utilising H_2O_2 as a Fe(II) oxidant under natural groundwater conditions. Depending on the initial native-Fe(II) to As(III) ratio in the groundwater, this approach has the potential to achieve As(III) removal below drinking water guidelines with native-Fe(II), eliminating the necessity for additional Fe dosage. For instance, in a scenario like L1, where the initial As(III) (after spiking) and native-Fe(II) concentrations were $140 \pm 2.6 \mu\text{g/L}$ and $6.3 \pm 0.7 \text{ mg/L}$, respectively, the use of $400 \mu\text{M}$ H_2O_2 resulted in the removal of $123.8 \mu\text{g/L}$ As with the groundwater native-Fe(II), achieving a dissolved As concentration of $16.2 \mu\text{g/L}$, close to the WHO guideline of $10 \mu\text{g/L}$. This optimisation of Fe(II) usage will not only reduce the amount of waste sludge but also decrease the backwashing frequency if a subsequent filter is employed.

The attractiveness of these two technologies lies in their ability to work independently or be integrated into conventional and decentralised systems, for removing groundwater As(III). The technologies can be implemented with minimal infrastructural requirements or changes. In addition, FeEC could be operated on-site using solar energy taking out the need for continuous supply of metallic salts, being an advantage in remote locations. The FeEC reactor system (including DC current supplier and Fe electrodes) also requires less space compared to chemical coagulation, which demands chemical's storage and pumps for coagulants dosing (Zhu et al., 2005). Additionally, FeEC systems are amenable to automation (Perren et al., 2018). Moreover, in this study, H_2O_2 was dosed as chemical, however, H_2O_2 can also be

generated electrochemically with FeEC using a carbon-based air-cathode (Bandaru, et al., 2020b), eliminating the need to store H₂O₂ chemical stocks on-site and reducing logistical requirements.

While 1 mol of H₂O₂ theoretically oxidises 2 mol of Fe(II), considering the total Fe concentration across all five locations (min. = 220 µM (L3); max. = 403 µM (L4)), an excess of H₂O₂ (400 µM) was applied during the H₂O₂ oxidant experiments. This was done to minimise the impact of atmospheric O₂ influx into the water, ensuring complete Fe(II) oxidation with H₂O₂. Therefore, it is recommended to conduct further studies with reduced H₂O₂ dosing, while also preventing residual H₂O₂ in the treated water. Additionally, although co-removal of P along with As(III) was observed during the experiments, it remains unclear whether P (as PO₄³⁻) competed with As(V) for adsorption sites, potentially influencing overall As removal. Therefore, further investigations are necessary to understand the impact of other co-contaminants on As removal using the technologies proposed in this study. Finally, before full-scale implementation, it is recommended to explore the long-term application of the combined technologies to assess the consistency of effectiveness, reliability and robustness, maintenance costs and skills requirement, affordability, operation risk and safety to the environment, and cultural acceptance among the targeted end-users.

5.4 Conclusions

In a field study in Assam, India, the combination of H₂O₂ dosing with FeEC before aeration was investigated to enhance the removal of As(III) from groundwater. By employing H₂O₂ to oxidise Fe(II), an overall As removal was achieved ranging from 82 to 99 %, compared to the 49 to 72 % through oxidation with DO by aeration. In addition, with H₂O₂, a pH increase could be avoided, i.e., CO₂ degassing during aeration, providing a pH advantage for As uptake. Oxidising the groundwater native-Fe(II) with H₂O₂ at the natural pH of the studied groundwaters (6.5 to 6.8), yielded a higher As/Fe uptake ratio (range = 0.010-0.020 mol:mol) compared to pH levels of 7.0 (range = 0.008-0.014 mol:mol), 7.5 (0.005-0.012 mol:mol), or 8.0 (0.004-0.010 mol:mol). In conclusion, this study has demonstrated that coupling anaerobic H₂O₂ dosing with FeEC before aeration promotes As removal and is a promising approach for decentralised application in rural Assam, for example in combination with existing low-cost Fe removal filters.

Appendix

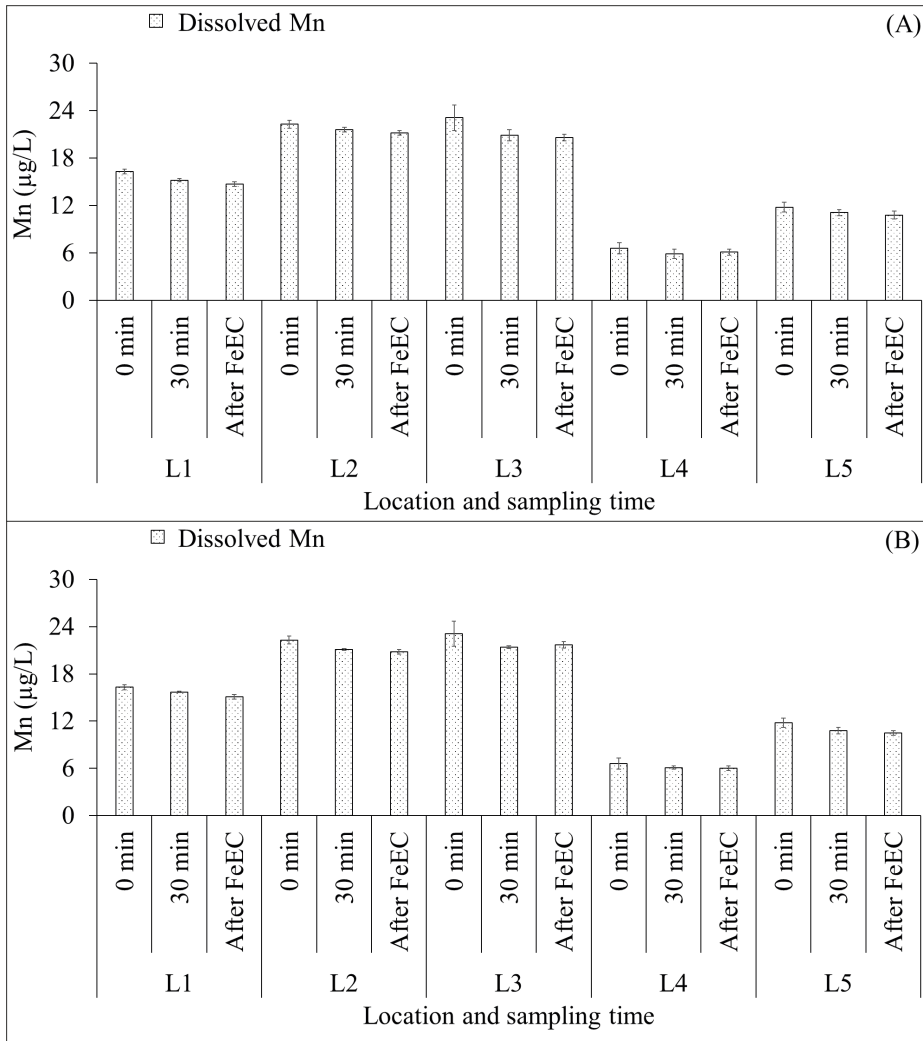


Fig. S5.1. Removal of Mn in the groundwater of the five selected locations (L1-L5) within Kamrup Metropolitan district when the groundwater native-Fe(II) and Fe(II) released by FeEC was completely oxidised by dosing 400 µM H₂O₂ **(A)** and by DO inserted during aeration **(B)**. The pH was maintained at the raw anaerobic groundwater pH level of 6.5 to 6.8.

Table S5.1. Raw groundwater characteristics of the five selected locations (L1-L5) within Kamrup Metropolitan district

| | L1 | L2 | L3 | L4 | L5 |
|--------------------------------------|----------------|----------------|----------------|----------------|----------------|
| pH | 6.7 | 6.8 | 6.5 | 6.6 | 6.6 |
| DO (mg/L) | <1 | <1 | <1 | <1 | <1 |
| EC (µS/cm) | 387.6 | 540 | 290 | 183.5 | 110.7 |
| NO ₃ ⁻ (mg/L) | 1.1±0.1 | 2.8±0.2 | 2.3±0.1 | 0.2±0.1 | 2.5±0.1 |
| SO ₄ ²⁻ (mg/L) | 2.1±0.1 | 17.3±0.5 | 1.4±0.1 | 3.8±0.3 | 10.7±0.2 |
| Cl ⁻ (mg/L) | 5.3±0.6 | 22±1.2 | 8±0.4 | 5.3±1.1 | 5.5±0.8 |
| DOC (mg/L) | 3.6±0.1 | 4.5±0.4 | 3.8±0.2 | 1.2±0.6 | 2.2±0.4 |
| Ca (mg/L) | 39.4±0.4 | 40±0.7 | 32.5±0.1 | 15.9±0.1 | 6±0.5 |
| K (mg/L) | 4.1±0.1 | 3.6±0.03 | 1.8±0.1 | 1.1±0.1 | 1.4±0.3 |
| Si (mg/L) | 21.1±0.9 | 21.3±0.3 | 33.6±0.3 | 26.5±0.2 | 28.9±1.2 |
| Mg (mg/L) | 8.9±0.03 | 11±0.1 | 14.9±0.1 | 5.6±0.1 | 1.6±0.1 |
| As (initial) (µg/L) | Not Detectable | Not Detectable | Not Detectable | Not Detectable | Not Detectable |
| As (after spiking) (µg/L) | 140±2.6 | 230±6.1 | 80±3.7 | 462±36.4 | 405±12.7 |
| Native-Fe(II) (mg/L) | 6.1±0.4 | 7.9±0.8 | 4.1±0.6 | 11.1±1.6 | 7.8±0.9 |
| Total P (µg/L) | 573.1±66.8 | 405.2±60.2 | 533.6±85.1 | 925.7±53.6 | 702.8±47.7 |
| Mn (µg/L) | 16.3±0.3 | 22.3±0.5 | 23.1±1.6 | 6.6±0.7 | 11.8±0.6 |

References

- Ahamad, K. U., & Jawed, M. (2012). Breakthrough studies with mono- and binary-metal ion systems comprising of Fe(II) and As(III) using community prepared wooden charcoal packed columns. *Desalination*, 285, 345–351. <https://doi.org/10.1016/J.DESAL.2011.10.025>
- Ahmad, A., Cornelissen, E., van de Wetering, S., van Dijk, T., van Genuchten, C., Bundschuh, J., van der Wal, A., & Bhattacharya, P. (2018). Arsenite removal in groundwater treatment plants by sequential Permanganate—Ferric treatment. *Journal of Water Process Engineering*, 26, 221–229. <https://doi.org/10.1016/J.JWPE.2018.10.014>
- Ahmad, A., van der Wal, A., Bhattacharya, P., & van Genuchten, C. M. (2019). Characteristics of Fe and Mn bearing precipitates generated by Fe(II) and Mn(II) co-oxidation with O₂, MnO₄ and HOCl in the presence of groundwater ions. *Water Research*, 161, 505–516. <https://doi.org/10.1016/J.WATRES.2019.06.036>
- Alka, S., Shahir, S., Ibrahim, N., Ndejiko, M. J., Vo, D. V. N., & Manan, F. A. (2021). Arsenic removal technologies and future trends: A mini review. *Journal of Cleaner Production*, 278. <https://doi.org/10.1016/J.JCLEPRO.2020.123805>
- Amrose, S. E., Bandaru, S. R. S., Delaire, C., van Genuchten, C. M., Dutta, A., DebSarkar, A., Orr, C., Roy, J., Das, A., & Gadgil, A. J. (2014). Electro-chemical arsenic remediation: Field trials in West Bengal. *Science of the Total Environment*, 488–489(1), 539–546. <https://doi.org/10.1016/j.scitotenv.2013.11.074>
- Annaduzzaman, M., Bhattacharya, P., Biswas, A., Hossain, M., Ahmed, K. M., & van Halem, D. (2018). Arsenic and manganese in shallow tubewells: validation of platform color as a screening tool in Bangladesh. *Groundwater for Sustainable Development*, 6, 181–188. <https://doi.org/10.1016/J.GSD.2017.11.008>
- Annaduzzaman, M., Rietveld, L. C., Hoque, B. A., Bari, M. N., & van Halem, D. (2021). Arsenic removal from iron-containing groundwater by delayed aeration in dual-media sand filters. *Journal of Hazardous Materials*, 411, 124823. <https://doi.org/10.1016/J.JHAZMAT.2020.124823>
- Annaduzzaman, M., Rietveld, L. C., Hoque, B. A., & van Halem, D. (2022). Sequential Fe²⁺ oxidation to mitigate the inhibiting effect of phosphate and silicate on arsenic removal. *Groundwater for Sustainable Development*, 17, 100749. <https://doi.org/10.1016/J.GSD.2022.100749>
- APHA (2012). Standard methods for the examination of water and wastewater, 22nd editi. American Public Health Association (APHA), American Water Works Association (AWWA) and Water Environment Federation (WEF), Washington, D.C., USA
- Bandaru, S. R. S., Roy, A., Gadgil, A. J., & van Genuchten, C. M. (2020a). Long-term electrode behavior during treatment of arsenic contaminated groundwater by a pilot-scale iron electrocoagulation system. *Water Research*, 175, 115668. <https://doi.org/10.1016/j.watres.2020.115668>
- Bandaru, S. R. S., Van Genuchten, C. M., Kumar, A., Glade, S., Hernandez, D., Nahata, M., & Gadgil, A. (2020b). Rapid and Efficient Arsenic Removal by Iron Electrocoagulation Enabled with in Situ Generation of Hydrogen Peroxide. *Environmental Science and Technology*, 54(10), 6094–6103. <https://doi.org/10.1021/acs.est.0c00012>
- Baruah, B. K., Das, B., Haque, A., Misra, K., & Misra, A. K. (2011). Iron removal efficiency of different bamboo charcoals: a study on modified indigenous water filtration technique in rural areas of Assam. *Journal of Chemical and Pharmaceutical Research*, 3(2), 454–459.
- Bissen, M., & Frimmel, F. H. (2003). Arsenic — a Review. Part II: Oxidation of Arsenic and its Removal in Water Treatment. *Acta Hydrochimica et Hydrobiologica*, 31(2), 97–107. <https://doi.org/10.1002/AHEH.200300485>

- Biswas, A., Nath, B., Bhattacharya, P., Halder, D., Kundu, A. K., Mandal, U., Mukherjee, A., Chatterjee, D., & Jacks, G. (2012). Testing tubewell platform color as a rapid screening tool for arsenic and manganese in drinking water wells. *Environmental Science and Technology*, 46(1), 434–440. <https://doi.org/10.1021/ES203058A>
- Bora, A. J., Gogoi, S., Baruah, G., & Dutta, R. K. (2016). Utilization of co-existing iron in arsenic removal from groundwater by oxidation-coagulation at optimized pH. *Journal of Environmental Chemical Engineering*, 4(3), 2683–2691. <https://doi.org/10.1016/J.JECE.2016.05.012>
- Catrouillet, C., Hirose, S., Manetti, N., Boureau, V., & Peña, J. (2020). Coupled As and Mn Redox Transformations in an Fe(0) Electrocoagulation System: Competition for Reactive Oxidants and Sorption Sites. *Environmental Science & Technology*, 54(12), 7165–7174. <https://doi.org/10.1021/acs.est.9b07099>
- Chakraborti, D., Sengupta, M. K., Rahman, M. M., Ahamed, S., Chowdhury, U. K., Hossain, M. A., ... & Quamruzzaman, Q. (2004). Groundwater arsenic contamination and its health effects in the Ganga-Meghna-Brahmaputra plain. *Journal of environmental monitoring: JEM*, 6(6), 74N–83N.
- Dixit, S., & Hering, J. G. (2003). Comparison of Arsenic(V) and Arsenic(III) Sorption onto Iron Oxide Minerals: Implications for Arsenic Mobility. *Environmental Science and Technology*, 37(18), 4182–4189. <https://doi.org/10.1021/ES030309T>
- Goyal, R., Singh, O., Agrawal, A., Samanta, C., & Sarkar, B. (2020). Advantages and limitations of catalytic oxidation with hydrogen peroxide: from bulk chemicals to lab scale process. <https://doi.org/10.1080/01614940.2020.1796190>
- Gude, J. C. J., Rietveld, L. C., & van Halem, D. (2016). Fate of low arsenic concentrations during full-scale aeration and rapid filtration. *Water Research*, 88, 566–574. <https://doi.org/10.1016/j.watres.2015.10.034>
- Gude, J. C. J., Rietveld, L. C., & van Halem, D. (2018). Biological As(III) oxidation in rapid sand filters. *Journal of Water Process Engineering*, 21, 107–115. <https://doi.org/10.1016/j.jwpe.2017.12.003>
- Hering, J. G., Katsoyiannis, I. A., Theoduloz, G. A., Berg, M., & Hug, S. J. (2017). Arsenic Removal from Drinking Water: Experiences with Technologies and Constraints in Practice. *Journal of Environmental Engineering*, 143(5), 03117002. [https://doi.org/10.1061/\(ASCE\)EE.1943-7870.0001225/SUPPL_FILE/SUPPLEMENTAL_DATA_EE.1943-7870.0001225_HERING.PDF](https://doi.org/10.1061/(ASCE)EE.1943-7870.0001225/SUPPL_FILE/SUPPLEMENTAL_DATA_EE.1943-7870.0001225_HERING.PDF)
- Holm, T.R., Wilson, S.D., 2006. Chemical oxidation for arsenic removal. MTAC Publ. TR06. -05.
- Holt, P. K., Barton, G. W., & Mitchell, C. A. (2005). The future for electrocoagulation as a localised water treatment technology. *Chemosphere*, 59(3), 355–367. <https://doi.org/10.1016/j.chemosphere.2004.10.023>
- Hug, S. J., & Leupin, O. (2003). Iron-catalyzed oxidation of Arsenic(III) by oxygen and by hydrogen peroxide: pH-dependent formation of oxidants in the Fenton reaction. *Environmental Science and Technology*, 37(12), 2734–2742. <https://doi.org/10.1021/es026208x>
- Kanoo, B., Soni, A., & Jawed, M. (2020). Performance monitoring of indigenous household groundwater filter for iron and fluoride removal: a case study from Assam, India. *Journal of The Institution of Engineers (India): Series A*, 101, 535–548.
- Kapaj, S., Peterson, H., Liber, K., & Bhattacharya, P. (2006). Human health effects from chronic arsenic poisoning - A review. *Journal of Environmental Science and Health - Part A Toxic/Hazardous Substances and Environmental Engineering*, 41(10), 2399–2428. <https://doi.org/10.1080/10934520600873571>

- Kowalski, K. P. (2014). Advanced Arsenic Removal Technologies Review. *Chemistry of Advanced Environmental Purification Processes of Water: Fundamentals and Applications*, 285–337. <https://doi.org/10.1016/B978-0-444-53178-0.00008-0>
- Kumar, P. R., Chaudhari, S., Khilar, K. C., & Mahajan, S. P. (2004). Removal of arsenic from water by electrocoagulation. *Chemosphere*, 55(9), 1245–1252. <https://doi.org/10.1016/j.chemosphere.2003.12.025>
- Laky, D., & Licskó, I. (2011). Arsenic removal by ferric-chloride coagulation – effect of phosphate, bicarbonate and silicate. *Water Science and Technology*, 64(5), 1046–1055. <https://doi.org/10.2166/WST.2011.419>
- Li, Y., Bland, G. D., & Yan, W. (2016). Enhanced arsenite removal through surface-catalyzed oxidative coagulation treatment. *Chemosphere*, 150, 650–658. <https://doi.org/10.1016/j.chemosphere.2016.02.006>
- Mahanta, D. B., Das, N. N., & Dutta, R. K. (2004). A chemical and bacteriological study of drinking water in tea gardens of central Assam. *Indian J. Environ. Prot.*, 24(5), 654.
- Manning, B. A., Fendorf, S. E., Bostick, B., & Suarez, D. L. (2002). Arsenic(III) oxidation and arsenic(V) adsorption reactions on synthetic birnessite. *Environmental Science and Technology*, 36(5), 976–981. <https://doi.org/10.1021/ES0110170/ASSET/IMAGES/LARGE/ES0110170FO0008.JPG>
- Meng, X., Korfiatis, G. P., Christodoulatos, C., & Bang, S. (2001). Treatment of arsenic in Bangladesh well water using a household co-precipitation and filtration system. *Water Research*, 35(12), 2805–2810. [https://doi.org/10.1016/S0043-1354\(01\)00007-0](https://doi.org/10.1016/S0043-1354(01)00007-0)
- Mercer, K. L., & Tobiason, J. E. (2008). Removal of arsenic from high ionic strength solutions: Effects of ionic strength, pH, and preformed versus in situ formed HFO. *Environmental Science and Technology*, 42(10), 3797–3802. https://doi.org/10.1021/ES702946S/SUPPL_FILE/ES702946S-FILE002.PDF
- Niazi, N. K., Bibi, I., Shahid, M., Ok, Y. S., Burton, E. D., Wang, H., Shaheen, S. M., Rinklebe, J., & Lüttge, A. (2018). Arsenic removal by perilla leaf biochar in aqueous solutions and groundwater: An integrated spectroscopic and microscopic examination. *Environmental Pollution*, 232, 31–41. <https://doi.org/10.1016/J.ENVPOL.2017.09.051>
- Nickson, R., Sengupta, C., Mitra, P., Dave, S. N., Banerjee, A. K., Bhattacharya, A., ... & Deverill, P. (2007). Current knowledge on the distribution of arsenic in groundwater in five states of India. *Journal of Environmental Science and Health, Part A*, 42(12), 1707–1718.
- Perren, W., Wojtasik, A., & Cai, Q. (2018). Removal of Microbeads from Wastewater Using Electrocoagulation. *ACS Omega*, 3(3), 3357–3364. https://doi.org/10.1021/ACSOMEGA.7Bo2037/ASSET/IMAGES/AO-2017-02037A_M013.GIF
- Pham, A. L. T., Doyle, F. M., & Sedlak, D. L. (2012). Kinetics and Efficiency of H₂O₂ Activation by Iron-Containing Minerals and Aquifer Materials. *Water Research*, 46(19), 6454. <https://doi.org/10.1016/J.WATRES.2012.09.020>
- Pio, I., Scarlino, A., Bloise, E., Mele, G., Santoro, O., Pastore, T., & Santoro, D. (2015). Efficient removal of low-arsenic concentrations from drinking water by combined coagulation and adsorption processes. *Separation and Purification Technology*, 147, 284–291. <https://doi.org/10.1016/J.SEPPUR.2015.05.002>
- Roberts, L. C., Hug, S. J., Ruettimann, T., Billah, M., Khan, A. W., & Rahman, M. T. (2004). Arsenic Removal with Iron(II) and Iron(III) in Waters with High Silicate and Phosphate Concentrations. *Environmental Science and Technology*, 38(1), 307–315. <https://doi.org/10.1021/es0343205>
- Roy, M., van Genuchten, C. M., Rietveld, L., & van Halem, D. (2020). Integrating biological As(III) oxidation with Fe(0) electrocoagulation for arsenic removal from groundwater. *Water Research*, 188, 116531. <https://doi.org/10.1016/j.watres.2020.116531>

- Roy, M., van Genuchten, C. M., Rietveld, L., & van Halem, D. (2022). Groundwater-native Fe(II) oxidation prior to aeration with H₂O₂ to enhance As(III) removal. *Water Research*, 223, 119007. <https://doi.org/10.1016/J.WATRES.2022.119007>
- Sharma, A. K., Sorlini, S., Crotti, B. M., Collivignarelli, M. C., Tjell, J. C., & Abbà, A. (2016). Enhancing arsenic removal from groundwater at household level with naturally occurring iron. *Revista Ambiente & Água*, 11(3), 486–498. <https://doi.org/10.4136/AMBI-AGUA.1815>
- Tseng, W. P. (1977). Effects and dose response relationships of skin cancer and blackfoot disease with arsenic. *Environmental Health Perspectives*, Vol.19, 109–119. <https://doi.org/10.1289/ehp.7719109>
- van Genuchten, C M, & Pena, J. (2017). Mn(II) Oxidation in Fenton and Fenton Type Systems: Identification of Reaction Efficiency and Reaction Products. *Environmental Science & Technology*, 51(5), 2982–2991. <https://doi.org/10.1021/acs.est.6b05584>
- van Genuchten, Case M., Addy, S. E. A., Peña, J., & Gadgil, A. J. (2012). Removing arsenic from synthetic groundwater with iron electrocoagulation: An Fe and As K-edge EXAFS study. *Environmental Science and Technology*, 46(2), 986–994. https://doi.org/10.1021/ES201913A/SUPPL_FILE/ES201913A_SI_001.PDF
- van Genuchten, Case M., & Ahmad, A. (2020). Groundwater As Removal by As(III), Fe(II), and Mn(II) Co-Oxidation: Contrasting As Removal Pathways with O₂, NaOCl, and KMnO₄. *Environmental Science & Technology*, 54(23), 15454–15464. <https://doi.org/10.1021/acs.est.0c05424>
- Wan, W., Pepping, T. J., Banerji, T., Chaudhari, S., & Giammar, D. E. (2011). Effects of water chemistry on arsenic removal from drinking water by electrocoagulation. *Water Research*, 45(1), 384–392. <https://doi.org/10.1016/j.watres.2010.08.016>
- World Health Organization, 2004. Guidelines For Drinking-Water Quality, vol. 1. Recommendations, 3rd ed World Health Organization, Geneva, Switzerland .
- Worou, C. N., Chen, Z. L., & Bacharou, T. (2021). Arsenic removal from water by nanofiltration membrane: potentials and limitations. *Water Practice and Technology*, 16(2), 291–319. <https://doi.org/10.2166/WPT.2021.018>
- Zhao, H., Li, Z., & Jin, J. (2019). Green oxidant H₂O₂ as a hydrogen atom transfer reagent for visible light-mediated Minisci reaction. *New Journal of Chemistry*, 43(32), 12533–12537. <https://doi.org/10.1039/C9NJ03106E>
- Zhu, B., Clifford, D. A., & Chellam, S. (2005). Comparison of electrocoagulation and chemical coagulation pretreatment for enhanced virus removal using microfiltration membranes. *Water Research*, 39(13), 3098–3108. <https://doi.org/10.1016/J.WATRES.2005.05.020>



Chapter 6

Conclusions and outlook

6.1 Conclusions

6.1.1 Overall conclusion

Aeration-filtration is a widely applied technology to treat raw groundwater by removing iron (Fe(II)), manganese (Mn(II)), methane (CH₄), hydrogen sulfide (H₂S), and ammonium (NH₄⁺), while also co-removing arsenic (As) from groundwater using the native-Fe(II). However, in most cases, the removal of arsenite (As(III)), the dominant As species in groundwater, is limited. This limitation arises, among others, due to ineffective oxidation of the neutral As(III) to the negatively charged arsenate (As(V)) leading to limited uptake by the precipitating Fe(III) (oxyhydr)oxides, a limited Fe(II)/As(III) ratio in the groundwater, and groundwater pH. An effective and chemical-free pathway to oxidise As(III) during aeration-filtration is by transforming the rapid sand filters into As(III) oxidising biofilters (Crognale et al., 2019; Gude et al., 2018). This thesis presents, amongst others, a new strategy to increase groundwater As(III) removal by coupling novel technologies with the aeration and subsequent (bio)filtration process, thereby utilising the capability of the filters to biologically oxidise As(III) to As(V). The biologically oxidised As(V) can then be removed through iron electrocoagulation (FeEC), a low-cost and robust iron dosing technology. The application of FeEC in the biofilter filtrate, inside the biofilter as well as in the supernatant water, was studied in a continuous-flow mode. When applied in the biofilter filtrate, FeEC reduced As(III) levels from 150 µg/L to below the WHO guideline value of 10 µg/L, requiring ten times less Fe dosage (and energy) than FeEC applied in the supernatant (i.e., FeEC before biological oxidation). Nonetheless, this system needs an additional step to filter the As-laden Fe(III)-precipitates, which would require additional infrastructure. To avoid an extra filtration step, the application of FeEC within the biofilter bed was further demonstrated. Embedding and operating FeEC within a biofilter removed 81% of the initial 150 µg/L As(III) concentration, compared to 67% when FeEC was operated in the supernatant (i.e., FeEC before biological oxidation). However, operating FeEC within the biofilter (sand) was more energy-intensive than in the supernatant (water). The efficacy of As removal and energy consumption in the embedded-FeEC biofilter system was influenced by the deepness of penetration of Fe(III)-precipitates into the bed, a factor that can be controlled by adjusting operational variables such as flow rate and pH levels.

The FeEC technology can also be applied to dose Fe(II) in locations with limited Fe(II)/As(III) ratios in the groundwater. However, to enhance As(III) removal by Fe(II)-based technologies including the groundwater native-Fe(II) and FeEC (in absence of any As(III) pre-oxidation process), the efficacy of As(III) removal was studied while oxidising Fe(II) anaerobically with hydrogen peroxide (H₂O₂), rather than with conventional dissolved oxygen (DO). The laboratory results demonstrated that under

anaerobic conditions, oxidation of 100 μM Fe(II) with 100 μM H_2O_2 led to a 95% removal of 524 $\mu\text{g/L}$ As(III) (or 7 μM), compared to 44% with DO, thus optimising the use of Fe(II) for As(III) removal. Field studies using the groundwaters of Assam (India) further verified these laboratory findings. Additionally, the field study results indicated the benefits of oxidising Fe(II) in raw anaerobic groundwater with H_2O_2 before aeration, capitalising on the low pH levels of the groundwater before aeration that enhances As(V) adsorption to Fe(III)-precipitates.

Overall, it can thus be concluded that As(III) removal during aeration-(bio)filtration can be improved by integrating FeEC and H_2O_2 dosing into groundwater (bio)filters. These technologies do not require major structural changes to existing aeration-filtration systems and can be considered eco-friendly alternatives to conventional oxidants and coagulants. As such, they can offer a viable and low-cost alternative solution for the removal of As(III) from groundwater, particularly in the rural areas of South Asia where As in groundwater poses severe health risks.

6.1.2 Mechanisms for enhanced As(III) removal with anaerobic Fe(II) oxidation by H_2O_2

In any technology, the oxidation of As(III) to As(V) is crucial, and when oxidising Fe(II) with H_2O_2 , a higher co-oxidation of As(III) was observed compared to DO. This increased As(III) co-oxidation with H_2O_2 can be attributed to a higher stoichiometric yield of reactive oxygen species (ROS), produced during Fenton reactions, effectively oxidising As(III) (Bandaru et al., 2020; Hug & Leupin, 2003). For example, while oxidising 100 μM Fe(II) in the presence of 7 μM As(III), only 41% of the initial As(III) was oxidised to As(V) when Fe(II) was oxidised entirely with DO (Chapter 4). However, when the Fe(II) was oxidised entirely with H_2O_2 , the co-oxidation of As(III) increased to 95%. This higher As(III) co-oxidation to As(V) with H_2O_2 can then result in a higher co-removal of As, since Fe(III)-precipitates have a stronger affinity for adsorbing As(V) over As(III).

Previous studies already, consistently, reported that enhanced removal of As(III) in Fe(II)+ H_2O_2 systems is associated with an increased co-oxidation of As(III) (Hug & Leupin, 2003; Krishna et al., 2001; Z. Wang et al., 2013). However, in this thesis it was also explicitly demonstrated that the structure of Fe(III)-precipitates plays an important role in the higher co-removal of As. It was observed that a systematic increase in the fraction of Fe(II) oxidation with H_2O_2 led to a decrease in the fraction of moderately crystalline Fe(III)-precipitates and an increase in the fraction of poorly-ordered precipitates. For instance, when 100 μM Fe(II) was completely oxidised by DO, 69% of the generated precipitates were moderately crystalline, and the rest were poorly-ordered. However, as the fraction of oxidation of 100 μM Fe(II) with H_2O_2 was

increased from 10, 20, 40, 80, to 100%, the fraction of poorly-ordered precipitates generation increased from 56, 52, 59, 86, to 100%, respectively (Chapter 4), positively influencing the adsorption capacity. A comparison of As(III) removal efficacy between two experimental conditions also revealed a clear difference in co-removal of As: one involving the sole use of DO as an oxidant for 100 μM Fe(II), and the other involving a sequential application of 40 μM H_2O_2 (80% oxidation of 100 μM Fe(II)) followed by DO (as discussed in Chapter 4). The experiments resulted in the generation of Fe(III)-precipitates, of which 31% were poorly-ordered for the DO-only experiment, compared to 86 % for the sequential 40 μM H_2O_2 +DO experiment. This led to a decrease of the initial 7 μM As(III) to 3.8 μM with DO-only and to 1.3 μM with 40 μM H_2O_2 +DO, respectively. The addition of 40 μM H_2O_2 led to a reduction of an additional 2.5 μM As compared to the "DO-only" experiment. However, when assessing the total quantity of oxidised As(III) for the same samples, oxidation of 2.9 μM As(III) for the DO-only experiment and 4.8 μM As(III) for the sequential 40 μM H_2O_2 +DO experiment was observed, indicating a difference of only 1.9 μM As. This finding implies that the enhanced As(III) removal observed in the 40 μM H_2O_2 +DO experiment cannot be solely attributed to an increase in As(III) oxidation. It was therefore suggested that an increase in the fraction of the poorly-ordered precipitates, generated through Fe(II) oxidation with H_2O_2 , also played a pivotal role in this improvement.

The presence of CO_2 in raw groundwater results in a relatively low pH compared to during/after aeration. A low pH provides a good environment for enhanced As(V) adsorption on the Fe(III)-precipitates, generated from the groundwater native-Fe(II) or from FeEC. The enhanced As(V) adsorption can be attributed to the greater electrostatic attraction of positively charged Fe(III)-precipitates to the negatively charged As(V) species at lower pH levels. Consequently, oxidation of the Fe(II) in anaerobic groundwater by dosing H_2O_2 before aeration can thus be beneficial, since it ensures that the Fe(III)-precipitates are generated at a lower pH compared to after aeration, resulting in a more effective removal of As. The findings presented in Chapter 5 of this study validate this hypothesis. It was e.g. observed that in groundwaters of Assam (India), the As/Fe uptake ratio was higher when the native-Fe(II) in raw groundwater was oxidised with H_2O_2 at an initial raw groundwater pH of 6.5 to 6.8, than in situations where the native-Fe(II) was oxidised at pH values of 7.0, 7.5, and 8.0. This underscores the importance of anaerobic oxidation of Fe(II) with H_2O_2 before aeration, as the pH of groundwater tends to increase during aeration due to CO_2 degassing. The potential advantage of utilising the naturally occurring groundwater CO_2 for an improved As removal in Fe(II)-based technologies is often overlooked and should be carefully considered to optimise As removal during the aeration-filtration processes.

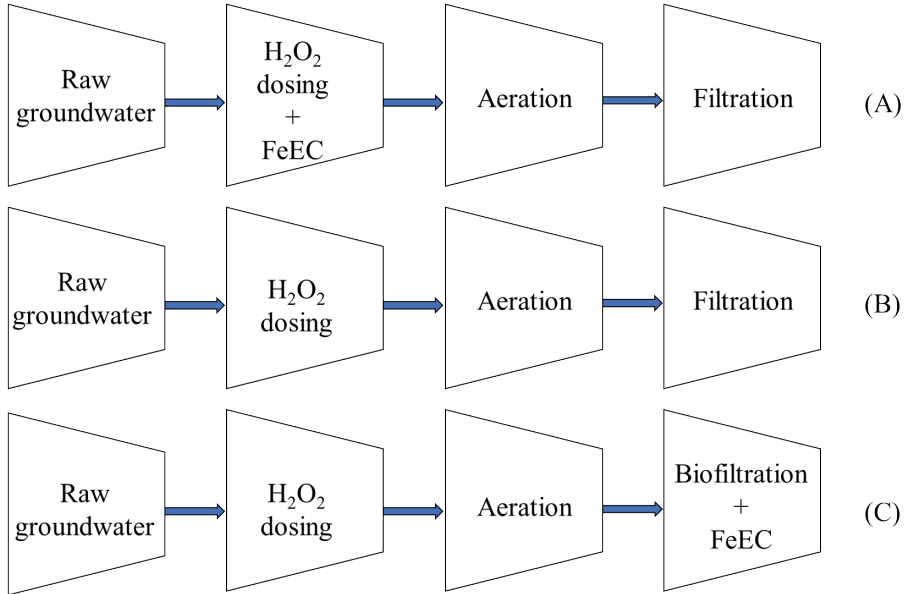


Fig. 6.1. Sequence of technologies integrated to aeration-(bio)filtration under different local conditions. **(A)** In the absence of biofilter and insufficient groundwater native-Fe(II) to co-remove all As(III); **(B)** In the absence of biofilter and sufficient groundwater native-Fe(II) to co-remove all As(III); **(C)** In the presence of biofilter and insufficient groundwater native-Fe(II) to co-remove all As(III).

6.1.3 Technological sequence of the As removal technologies

The integration of three key technologies: biological As(III) oxidation in biofilters, FeEC, and H₂O₂ dosing for Fe(II) oxidation, holds promise for enhancing the removal of As(III) in water treatment processes. However, the sequencing of these technologies should be taken into consideration, depending on local conditions. For instance, in areas where rapid sand filters lack biological activity and groundwater native-Fe(II) concentrations falls short to achieve As(III) removal as per guidelines, a strategic approach involves positioning H₂O₂ dosing and FeEC before aeration (Fig. 6.1(A)). This configuration allows for anaerobic oxidation of groundwater native-Fe(II) and Fe(II) generated by the FeEC process through H₂O₂. This sequence also permits the application of FeEC in the water matrix, instead of within a sand bed, leading to a lower energy consumption during the FeEC process (Chapter 3). In cases where groundwater native-Fe(II) concentrations are adequate to meet As(III) removal criteria, H₂O₂ dosing in the anaerobic groundwater before aeration will be sufficient (Fig. 6.1(B)). When dealing with situations where the filtration beds are biologically active and groundwater native-Fe(II) concentrations are insufficient, H₂O₂ can be dosed before aeration, followed by aeration, biofiltration, and FeEC inside the biofilter (Fig. 6.1 (C)). The concentration of H₂O₂ dosed before aeration should be such that it is sufficient to oxidise the groundwater native-Fe(II) as well the Fe(II)

released by FeEC inside the bed taking into account any quenching reactions, and thereby optimising the As uptake by Fe from both sources. Within the biofilter, the upper section (above FeEC) can eliminate the As-laden Fe(III)-precipitates derived from groundwater native-Fe(II) oxidation and facilitate the oxidation of any remaining dissolved As(III). The bottom portion (below FeEC) can filter out the As-laden Fe(III)-precipitates generated by FeEC. However, care should be taken, while dosing the excess H_2O_2 , to ensure it is sufficient to completely oxidise just the groundwater native-Fe(II) and Fe(II) from FeEC.

6.2 Outlook

6.2.1 Future research

In the presented studies, the interaction of H_2O_2 with Fe(II) and As(III) has been explored. However, further no attention was given to the impact of H_2O_2 on other native groundwater species. For instance, Mn(II), present in groundwater, could compete with As(III) for the ROS and could potentially be co-removed, thereby competing with As (Catrouillet et al., 2020; van Genuchten & Peña, 2017). Although, co-removal of groundwater Mn was not observed, it is still unclear whether Mn(II) competes for ROS, since Mn speciation was not performed. Similarly, natural organic matter, present in groundwater, could also be degraded by the ROS generated in Fe(II)+ H_2O_2 systems (Murray & Parsons, 2004), and thus compete with As(III) for the ROS. Additionally, the effect of H_2O_2 on the microbial community within the biofilters remains unexplored. A study by Wang et al. (2017) showed that H_2O_2 dosing promoted dissolved organic carbon removal and decreased microbial activity in batch scale sand biofilters. Therefore, in locations with active biofilters, an excessive dose of H_2O_2 , used to oxidise the groundwater native-Fe(II), can potentially harm the As(III)-oxidising microbial community, thus affecting the oxidation and removal of As(III) within the biofilters.

In addition, the backwashing process can impact the performance of these biofilters, as evidenced by Li et al. (2012). They observed changes in the microbial community structure and function in a fixed-bed biofilm reactor in response to variations in backwash intensity and frequency. Similarly, Kasuga et al. (2007) noted a 64% reduction in attached bacterial abundance in the top layer of a biological activated carbon filter following backwashing. The growth of biofilm in sand filters can also be impacted by environmental factors such as nutrient levels, temperature, ionic strength, and pH as discussed in Saini et al. (2023). These environmental factors may vary in groundwater from different regions. Therefore, field studies on the development of such biofilters under varying groundwater compositions and conditions that simulate real operational procedures (e.g. backwashing) should be conducted.

The technologies discussed in this thesis provide solutions to remove As from groundwater, but they also generate As-rich Fe sludge. This demands safe handling and proper disposal of the sludge, so that there is no leaching of As into the environment. Therefore, in addition to As removal from groundwater, it is necessary to dive into sustainable waste management strategies for the As sludge. Ideally such research is combined with longer-term, pilot plant research of the proposed technologies to shed light on important practical factors such as performance consistency, reliability, robustness, maintenance costs, skill requirements, affordability, operational risks, safety considerations, and public acceptance (Amrose et al., 2014; Sobsey et al., 2008). Such practical understanding of coupled FeEC and H_2O_2 to aeration-(bio)filtration will be critical for wider scale applicability of these innovative As removal technologies.

References

- Amrose, S. E., Bandaru, S. R. S., Delaire, C., van Genuchten, C. M., Dutta, A., DebSarkar, A., Orr, C., Roy, J., Das, A., & Gadgil, A. J. (2014). Electro-chemical arsenic remediation: Field trials in West Bengal. *Science of the Total Environment*, 488–489(1), 539–546. <https://doi.org/10.1016/j.scitotenv.2013.11.074>
- Bandaru, S. R. S., van Genuchten, C. M., Kumar, A., Glade, S., Hernandez, D., Nahata, M., & Gadgil, A. (2020b). Rapid and Efficient Arsenic Removal by Iron Electrocoagulation Enabled with in Situ Generation of Hydrogen Peroxide. *Environmental Science and Technology*, 54(10), 6094–6103. <https://doi.org/10.1021/acs.est.0c00012>
- Catrouillet, C., Hirose, S., Manetti, N., Boureau, V., & Peña, J. (2020). Coupled As and Mn Redox Transformations in an Fe(0) Electrocoagulation System: Competition for Reactive Oxidants and Sorption Sites. *Environmental Science & Technology*, 54(12), 7165–7174. <https://doi.org/10.1021/acs.est.9b07099>
- Crognale, S., Casentini, B., Amalfitano, S., Fazi, S., Petruccioli, M., & Rossetti, S. (2019). Biological As(III) oxidation in biofilters by using native groundwater microorganisms. *Science of the Total Environment*, 651, 93–102. <https://doi.org/10.1016/j.scitotenv.2018.09.176>
- Gude, J. C. J., Rietveld, L. C., & van Halem, D. (2018). Biological As(III) oxidation in rapid sand filters. *Journal of Water Process Engineering*, 21, 107–115. <https://doi.org/10.1016/j.jwpe.2017.12.003>
- Hug, S. J., & Leupin, O. (2003). Iron-catalyzed oxidation of Arsenic(III) by oxygen and by hydrogen peroxide: pH-dependent formation of oxidants in the Fenton reaction. *Environmental Science and Technology*, 37(12), 2734–2742. <https://doi.org/10.1021/es026208x>
- Kasuga, I., Shimazaki, D., & Kunikane, S. (2007). Influence of backwashing on the microbial community in a biofilm developed on biological activated carbon used in a drinking water treatment plant. *Water Science and Technology*, 55(8–9), 173–180. <https://doi.org/10.2166/WST.2007.256>
- Krishna, M. V. B., Chandrasekaran, K., Karunasagar, D., & Arunachalam, J. (2001). A combined treatment approach using Fenton's reagent and zero valent iron for the removal of arsenic from drinking water. *Journal of Hazardous Materials*, 84(2–3), 229–240. [https://doi.org/10.1016/S0304-3894\(01\)00205-9](https://doi.org/10.1016/S0304-3894(01)00205-9)
- Li, X., Yuen, W., Morgenroth, E., & Raskin, L. (2012). Backwash intensity and frequency impact the microbial community structure and function in a fixed-bed biofilm reactor. *Applied Microbiology and Biotechnology*, 96(3), 815–827. <https://doi.org/10.1007/S00253-011-3838-6>
- Murray, C. A., & Parsons, S. A. (2004). Removal of NOM from drinking water: Fenton's and photo-Fenton's processes. *Chemosphere*, 54(7), 1017–1023. <https://doi.org/10.1016/J.CHEMOSPHERE.2003.08.040>
- Saini, S., Tewari, S., Dwivedi, J., & Sharma, V. (2023). Biofilm-mediated wastewater treatment: a comprehensive review. *Materials Advances*, 4(6), 1415–1443. <https://doi.org/10.1039/D2MA00945E>
- Sobsey, M. D., Stauber, C. E., Casanova, L. M., Brown, J. M., & Elliott, M. A. (2008). Point of Use Household Drinking Water Filtration: A Practical, Effective Solution for Providing Sustained Access to Safe Drinking Water in the Developing World. *Environmental Science and Technology*, 42(12), 4261–4267. <https://doi.org/10.1021/ES702746N>
- van Genuchten, C. M., & Peña, J. (2017). Mn(II) Oxidation in Fenton and Fenton Type Systems: Identification of Reaction Efficiency and Reaction Products. *Environmental Science and Technology*, 51(5), 2982–2991. <https://doi.org/10.1021/acs.est.6b05584>
- Wang, F., van Halem, D., Liu, G., Lekkerkerker-Teunissen, K., & van der Hoek, J. P. (2017). Effect of residual H₂O₂ from advanced oxidation processes on subsequent biological water treatment: A laboratory batch study. *Chemosphere*, 185, 637–646. <https://doi.org/10.1016/j.chemosphere.2017.07.073>

Wang, Z., Bush, R. T., & Liu, J. (2013). Arsenic(III) and iron(II) co-oxidation by oxygen and hydrogen peroxide: Divergent reactions in the presence of organic ligands. *Chemosphere*, 93(9), 1936–1941. <https://doi.org/10.1016/j.chemosphere.2013.06.076>



Curriculum vitae
List of publications

Curriculum vitae

Mrinal Roy was born on 18th March, 1994, in Silchar, India. In 2012, he embarked on his academic journey, pursuing a Bachelor of Engineering in Civil Engineering at Assam Engineering College. After successfully completing his Bachelor's degree in 2016 with First Class Honours, he undertook a 9-month internship at the Waste Management Research Group, IIT Guwahati. Throughout his undergraduate years, Mrinal developed a keen interest in the field of environmental sustainability. Motivated by his passion for the environment, he decided to further his education and enrolled in the Master of Science program in Environmental Engineering at the Delft University of Technology (TU Delft) in 2017. During his master's studies, he specialised in water treatment technologies and completed his thesis on the application of biological and electrochemical pathways to remove arsenic from drinking water.

In 2019, Mrinal commenced his PhD journey in Sanitary Engineering at TU Delft. Under the guidance of Prof. Doris van Halem, Prof. Luuk Rietveld, and Dr. Case van Genuchten, Mrinal delved into researching innovative technologies aimed at removing arsenic from drinking water sourced from groundwater. His doctoral dissertation centered on the application of biological arsenic oxidation, iron electrocoagulation, and hydrogen peroxide (a green oxidant) to enhance the removal of arsenic from groundwater. These approaches were designed for seamless integration with existing treatment infrastructures.

Currently, Mrinal serves as a Process Engineer at Van der Ende Group in The Netherlands. In this role, he leverages his expertise to treat wastewater in greenhouses, aiming to facilitate its reuse as part of a water recirculation strategy.

List of publications

- **Roy, M.**, van Genuchten, C. M., Rietveld, L., & van Halem, D. (2021). Integrating biological As (III) oxidation with Fe (0) electrocoagulation for arsenic removal from groundwater. *Water Research*, 188, 116531.
- **Roy, M.**, van Genuchten, C. M., Rietveld, L., & van Halem, D. (2022). Groundwater-native Fe (II) oxidation prior to aeration with H₂O₂ to enhance As (III) removal. *Water Research*, 223, 119007.
- **Roy, M.**, Kraaijeveld, E., Gude, J. C. J., van Genuchten, C. M., Rietveld, L., & van Halem, D. (2024). Embedding Fe(0) electrocoagulation in a biologically active As(III) oxidising filter bed. *Water Research*, 252, 121233.